THE UNIVERSITY OF CHICAGO

INVESTIGATING CONTACT HYPERSENSITIVITY BY STUDYING BIOCHEMICAL PROPERTIES OF A CONTACT ALLERGEN, 1-CHLORO-2,4-DINITROBENZENE

A DISSERTATION SUBMMITTED TO

THE FACULTY OF THE PRITZKER SCHOOL OF MOLECULAR ENGINEERING

IN CANDIDACY FOR THE DEGREE OF

DOCTOR OF PHILOSOPHY

BY

SEONG-MIN KIM

CHICAGO, ILLINOIS

JUNE 2020

Part of Chapter 2 has been published in the following journal: Kimani, F.*, **Kim, S.*,** Steinhardt, R., Esser-Kahn, A.P. Correlating the Structure and Reactivity of a Contact Allergen, DNCB, and Its Analogs to Their Sensitization Potential. Bioorganic & Medicinal Chemistry. 27. 2985-2990 (2019).

Copyright© 2020 by Seong-Min Kim

All Rights Reserved

For my family and friends who were the greatest support in this journey

TABLE OF CONTENTS

LIST OF TABLES

LIST OF FIGURES

ACKNOWLEDGEMENTS

There are many people whom I would like to express my gratitude for their support and contribution to my time in graduate school. There are many moments that I felt uncertain about my path; however, these following people were always there to support and motivate me.

First of all, I would like to express my deepest, the most sincere gratitude to my thesis advisor, Professor Aaron Esser-Kahn, for his continuous support of my Ph.D. study and research. I would like to thank him for his mentorship, encouragement, and immense knowledge that have helped me reach my goal. He was always patient with me and complimented me on my strengths while refraining to criticize me for my challenges. For the past five years, I have become not only a better scientist but also a better person. Besides my advisor, I would like to express my gratitude to my committee members, Professor Jeffrey Hubbell and Professor Anne Sperling for their insightful comments which incented me to widen my research to various perspectives.

I also would like to thank all members of the Esser-Kahn Group. Special thanks to Dr. Flora Kimani, whom I collaborated with on many parts of my project. I would like to thank Bradley Studnitzer for his insights into the project and wish him the best luck moving forward with the project. Thanks to Dr. Jingjing Shen for helping me with the mice experiments. Your energy and positivity are truly inspiring not only to me but to everyone in lab. I want to express my deepest gratitude to my cohorts, Dr. Brittany Moser and Dr. Tyler Albin. You guys were the best labmates and cohorts I could ever ask for. I will cherish the fun, laughs, conversations, and scientific discussions we had together throughout graduate school. I would like to thank my lab managers, Dr. Troy Moore, Bethany McGonnigal, Yoseline Escalante-Buendia, and Xuewen Gou for their help with ordering and general lab management. Special thanks to Dr. Troy Moore, who taught me the basic lab techniques and cellular assays that helped me start my project. I would like to

thank Tim Steeves for being the most amazing graduating cohort and all his efforts in organizing group fun and group wellness. All of the support he has shown in the past year kept me sane. I will always cherish good laughs and the food adventures I had with Dr. Janine Tom, Dr. Alfred Chon, and Will Howitz. I will never forget my time in Irvine with this amazing group. I also want to thank Nihesh Naorem and Dr. Jun Wang for ensuring that I was physically and mentally healthy in my final two years of graduate school. Thanks to Jainu Ajit and Sophia Huang. I will always remember the good laughs and conversations we had in the lab. Thanks to Dr. Ethan White for the general help in lab and the scientific comments and suggestions. Finally, the rest of the Esser-Kahn group, whenever I was down, you guys were there to encourage and motivate me.

I would like to acknowledge the following core facilities for their contributions to this dissertation. I acknowledge Northwestern Proteomics Core for running the mass spectrometry and proteomics resources to identify modified proteins. I acknowledge Genomics Facility at the University of Chicago for allowing me to use their instruments for qPCR. I also acknowledge the Animal Resources Center for taking care of mice.

In addition to the members of the Esser-Kahn Group, there are many friends from outside the lab that I would like to acknowledge. I would like to thank my cohorts from the University of California, Irvine Department of Chemical Engineering – Dr. Rose Pier, Thao Nguyen, and Tami McTaggart in particular – for sleepless nights we studied together for exams and Trivia nights at the Anteater pub on Tuesdays after the exams. I would like to acknowledge Dr. Sun-Jun Park, a senior student at UCI, for his mentorship that helped me survive graduate school. I would like to thank Dr. Eun-Ah Cho and Dr. Seulgi So, whom I worked together as officers of the Korean Graduate Student Association (KGSA). When I needed somebody to talk to, both of you were

there to chat over a glass of beer. Also, I would like to thank my fellow friends, Mary Hye-Hyun An and Claire Soyeon Kim, for good friendship over the past five years.

In the middle of my Ph.D. career, I had an unexpected transfer to the University of Chicago. Apart from great research opportunities, I have gotten a chance to know a group of amazing people that made my life here remarkable. First of all, I want to thank Siyoung Kim for helping me settle in Chicago and introducing me to the wonderful group of friends that could share unforgettable moments. I would like to thank Dr. Hyeong Min Jin for his advice and mentorship. Thanks to Taehyun Kim, Minju Kim, Jongyoon Baik, and Yeongsu Cho for all the fun we had together. Our trip to Vegas, many K-pop dance sessions we had on weekends, 7 AM cardio kickboxing and Zumba classes, and the weekly mental support/chat-over-coffee-and-sweet, we had so much fun together.

In addition to my friends, I want to acknowledge my family members, mom and dad, my sister Jeongmin Kim, my brother Hanjo Terry Kim, and Bambi for the unconditional love and support for my career goal. Without my family, none of this would have been possible. The love and support from all of you were my motivation for carrying on with my life. Knowing all of you were there for me gave me so much comfort even when I was under the highest pressure. Last but not least, special thanks to my fiancé, Garam Lee for his unconditional love and support. You are the most amazing person I have ever met. Your love means the world to me, and I am very excited about our future together.

Again, the most sincere thanks to everyone and every opportunity I had in the completion of my dissertation. None of this work would have been possible without the mentioned people. Even when I leave the school, and we all go on own ways, I will always pray for the happiness and the well-being of everyone.

ABSTRACT

Contact hypersensitivity is a type IV hypersensitivity reaction that affects about 20 % of the population around the world. It is triggered by a group of chemically-reactive, small molecular-weight compounds called contact allergens. Despite the known dangers of contact allergens and the increase in the number of patients, the pathology at which contact dermatitis develops remains unclear.

This dissertation aims to understand a molecular mechanism of contact dermatitis by investigating contact allergen's interaction with protein targets. Chapter 2 reports a structure-activity relationship of a model contact allergen, 1-chloro-2,4-dinitrobenzene (DNCB). The overall sensitization potential of DNCB and its derivatives, chosen based on DNCB's reaction mechanism, were evaluated by different types of assays that can encompass both physicochemical and biological properties. Peptide reactivity and immune cell-based assays revealed a non-linear correlation that requires a balance of stability and reactivity that dictates a contact allergen's ability to induce the sensitization phase. This also indicates that a non-allergenic compounds can be made to cause sensitization by controlling their rate of reactivity.

In chapter 3, this dissertation shows the identity of protein targets that DNCB reacts to bind during the sensitization phase. Starting with an unbiased sampling, mass spectrometry analysis revealed 9 DNCB-modified proteins. To elucidate the function of the proteins in contact hypersensitivity, cells carrying suppression of the DNCB-modified proteins were cultured with DNCB to evaluate their DNCB-induced response. Real-time PCR revealed that HSP90-knockdown cells reduced DNCB-induced hypersensitivity below the background levels. DNCB's activity was attenuated when it was cultured with geldanamycin, a known inhibitor of HSP90, or anti-CD91, an inhibitor for HSP90 receptor, all of which validate observations from qPCR. As

heat shock proteins are stress-responsive proteins and the molecular chaperones in antigen processing, it is possible that they are the first proteins to respond to DNCB stimulation and the modification somehow signals the activation of the immune cells. These results, altogether, are one of the first evidence and validation of HSP90's involvement in DNCB-induced hypersensitivity and report that the degree of hypersensitivity can be reduced by inhibiting HSP90.

CHAPTER I

INTRODUCTION

1.1 Introduction

Hypersensitivity reaction is an exaggerated immune response that damages the body as opposed to protecting it.[1,2] Examples of hypersensitivity include autoimmune response and allergic response to substances that are foreign to the human body. Contact hypersensitivity is a type IV hypersensitivity mediated by allergen-specific T cells. To date, more than 20 % of the population is affected, and they are still without proper cure and treatment due to its unclear pathology.[3] Elucidation of contact hypersensitivity remains a long-standing goal in the field of contact allergy.

This dissertation aims to elucidate a molecular mechanism of early immune response in contact hypersensitivity by understanding the interaction between contact allergens and their protein targets. Contact allergens are a set of small molecular-weight compounds that induce contact hypersensitivity. Using a well-established contact allergen, 1-chloro-2,4-dinitrobenzene (DNCB), as a model, this work first investigates how overall sensitization potential of contact allergens alters by changing chemical reactivity. Then, this work identifies functionally relevant protein target of DNCB using proteomics, gene-suppression, and inhibition assays.

In this chapter, I will discuss key research topics, project aims, and general background information of contact allergens and allergic contact dermatitis.

1.2 The Pathology of Allergic Contact Dermatitis (ACD)

Allergic contact dermatitis (ACD), or contact dermatitis, is a chronic skin disorder accompanied by clinical symptoms of rashes, itchiness, and inflammation in the lesion area.[4–6] The major cause of ACD is xenobiotics, the substances that are foreign to the body. Through research advances in immunology and allergy, a rough understanding of the mechanism of allergic contact dermatitis has been established (**Figure 1.1**).[7] ACD is comprised of two distinct phases: the sensitization phase and the elicitation phase. During the sensitization phase, the activated Langerhans cells or dermal dendritic cells migrate to the nearest lymph node to present self-antigens. This process ultimately results in the clonal expansion and development of allergen-specific T cells that play major roles in the clinically apparent symptoms of rashes, flare-ups, skin inflammation, etc. The manifestation of symptoms is called the elicitation phase.[8] In regards to terminology, contact dermatitis and contact hypersensitivity are also used to refer to ACD.

A common cause of contact dermatitis is a group of small molecular weight compounds called contact allergens.[9–13] The nature and the properties of contact allergens will be discussed later in the chapter. Another term that describes contact allergens is "haptens," or the active forms of contact allergen. During the sensitization phase, hapten binding, the process in which contact allergens bind to the side chains of target proteins, activates Langerhans cells to generate hapten-specific T cells in the regional lymph node. After repeated exposures to the same allergen, the elicitation phase results in the manifestation of clinical symptoms of contact dermatitis. In brief, contact allergens activate Langerhans cells via a process of hapten-binding, the initial process in the induction of contact dermatitis, though the exact pathology of it is still unclear. This dissertation aims to elucidate hapten-binding in greater detail.

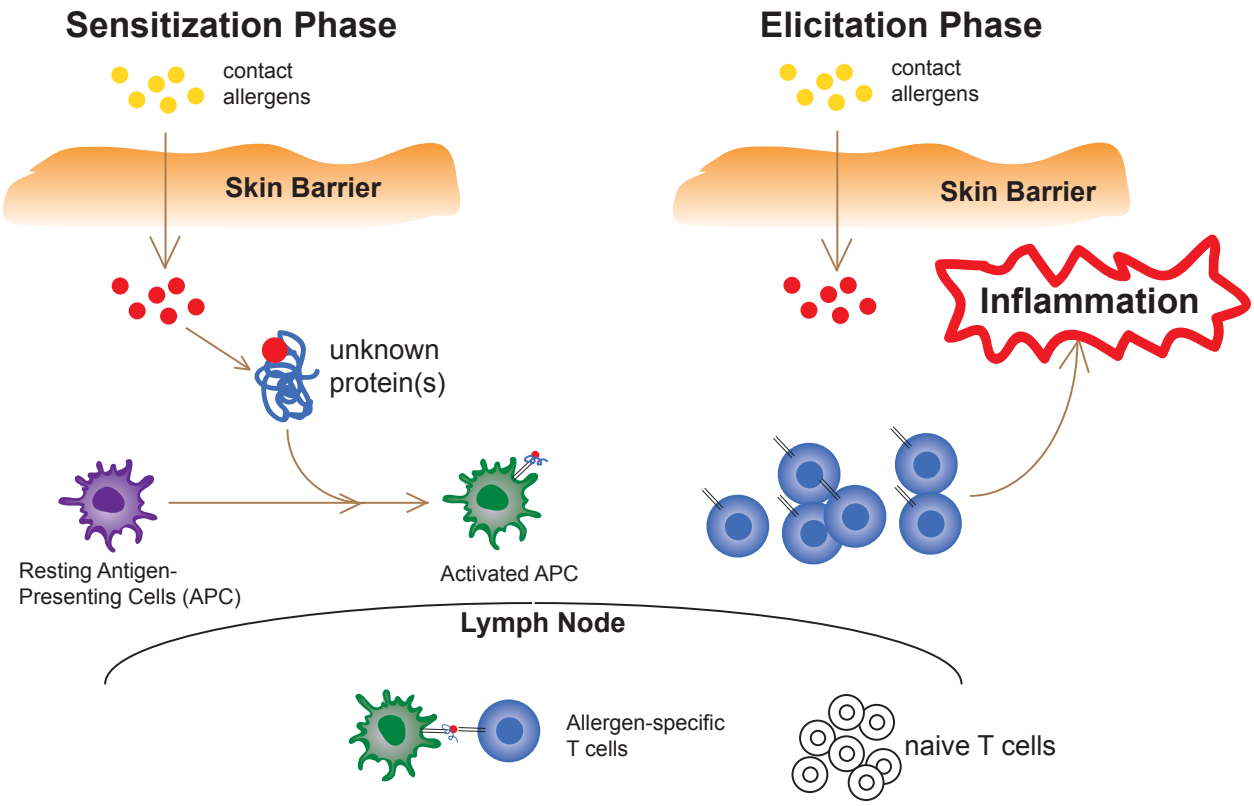

Figure 1.1 Overview of ACD. The left side shows the sensitization phase that is induced by first time exposure of haptens. Repeated exposure of the same hapten leads to clinically apparent elicitation phase, which is shown on the right side.

The exact pathogenesis of allergic contact dermatitis has been controversial. Thus, I want to clarify the differences between ACD and atopic dermatitis (AD) or irritant contact dermatitis (ICD). For a long time, ACD was considered to driven by an IgE response because patients with allergic skin conditions demonstrate specific IgE antibody response to allergens. As an example, skin prick testing (SPT) shows a specific IgE response to allergens. While a positive SPT indicates sensitization to a particular allergen, this does not prove clinical hypersensitivity. Atopic skin conditions fall into this category. AD is a skin disease characterized by immune abnormalities and disrupted skin barrier function due to exposure to chemical substances, environmental factors, and

microbes. It manifests as dry and scaly lesions with a proclivity toward IgE-mediated sensitization.[8,14–17] On the other hand, irritant dermatitis is an immediate effect on toxic substances rather than immune response. As an example, redness in the skin after being splashed with solvents in a laboratory setting is usually a result of irritation.[18–20] In contrast, ACD is a chronic skin condition mediated by allergen-specific T cells. The following table summarizes the differences among these skin conditions.

Table 1.1 Common Skin Conditions (ACD, AD, ICD comparisons)

	Allergic contact dermatitis (ACD)	Atopic Dermatitis (AD)	Irritant Contact Dermatitis (ICD)
Characteristics	Type IV hypersensitivity	Type I hypersensitivity	Toxicological effect, no immune mediators
Mediators	Allergen-specific T cells	Allergen-specific IgE	-
Symptoms	Rashes, dry lesion, inflammation	Dry and scaly lesions	Red, itchy
Manifestation of symptoms	Takes 24-72 hrs	immediate	immediate

To summarize, ACD is a result of a complex immune mechanism. Generally, the above terms are used interchangeably. But it is important to note that they are skin conditions elicited by different immune and cellular responses.

1.3 Clinical Implications and Current State-of-Art Treatment of Allergic Contact Dermatitis

The prevalence of contact dermatitis has increased over the past few decades. It is one of the common occupational health concerns that accounts for more than 20 % of work-related health complaints and a large amount of economic loss.[21–24] Besides, skin allergy is estimated to affect approximately 9.2 million (12.6 %) children under the age of 18 in the United States alone.[25]

Comparing to that of other types of allergies, the number of cases for skin allergy grows at a much faster rate, suggesting that it imposes a higher risk in children (**Table 1.2**).

Table 1.2 Reported Cases of Allergies and Hay Fever in the United States

	Reported Cases in 2018		Reported Cases in 2014	
Disease	Number (millions)	Percentage (%)	Number (millions)	Percentage (%)
Hay Fever	5.2	7.2	6.1	8.4
Respiratory Allergy	7.1	9.6	7.4	10.1
Food Allergy	4.8	6.5	3.9	5.4
Skin Allergy	9.2	12.6	8.6	11.7

Despite this fact, the diagnosis and treatment of contact dermatitis are not well-established. While patch testing is a typical diagnostic test of skin allergies, its clinical significance remains in ACD remains unclear. Thus, currently, the diagnosis of contact dermatitis relies heavily on the severity of clinical symptoms and the patient's medical history, which are qualitative evaluations.[26] Treatment of contact dermatitis is directed at restoring the skin barrier function, which is mostly about limiting itching, hydrating and repairing the skin. Patients often receive topical steroids corticosteroids or topical calcineurin inhibitors (TCIs),[27–30] and education on the chronic nature of the disease and the importance of adherence to the treatment.[31–33] All these measures, however, are focused only on successfully "managing" the onset symptoms of contact dermatitis, not on curing or treating the disorder. Even after patients recover from the symptoms, the condition is likely to return when they are exposed to the same environmental triggers.

To summarize, there are no diagnostic tests or treatments for contact dermatitis. One possible reason is that the pathology of this disorder is not entirely known. To improve treatment, we need to understand this disorder in greater detail.

1.4 Hypersensitivity Reactions

Hypersensitivity is defined as a condition when the immune system gets activated in a way that damages the body rather than protecting the body. There are four broad categories of hypersensitivity reactions.[1,34] Type I hypersensitivity is the most common type of allergic response. It occurs by the interaction between an allergen and the allergen-specific IgE antibodies on the FcεRI receptor of mast cells. Upon stimulation by allergens, these mast cells degranulate to release granules that contain inflammatory mediators such as histamine. Symptoms of type I hypersensitivity can be as mild as runny nose, sneezing, but patients can show breathlessness and asphyxiation that can cause death. Dust mites feces or plant pollen are examples that can cause type I hypersensitivity reaction. Because the reaction occurs immediately upon exposure to the allergen, type I hypersensitivity is also called immediate hypersensitivity.[35,36]

Type II hypersensitivity is caused by antibody response, such as IgG or rarely IgM, by chemically reactive small molecules that become covalently bound to the surface of cells. A typical example of type II hypersensitivity is an allergic response to medication like penicillin.[37] For example, penicillin can bind a red blood cell to form an antigen-cell complex, which stimulates B cells to produce IgG or IgM antibodies against the new antigen. If severe, this antibody response can activate the complement system, or an enzymatic cascade to fight off bacterial infections and thus ultimately killing the host's red blood cells. Type II hypersensitivity is cytotoxic and can result in damage in local tissue.[38,39] Type III hypersensitivity is similar to type II hypersensitivity, considering that they are both mediated by antibodies that recognize self-antigens. In contrast, type III hypersensitivity occurs when chemically-reactive small molecules covalently bind soluble proteins as opposed to the surface of the cells. As a consequence, the antibodies bind these antigen-protein complexes to form immune complexes that can activate the complement system.[40–42]

Unlike type I, II, or III hypersensitivity reactions that are mediated by antibodies, type IV hypersensitivity is mediated by allergen-specific T cells. ACD falls into this category.[2] Type IV hypersensitivity is induced when an allergen or a chemically reactive compound penetrates the skin and reacts with human proteins to generate haptens. Although the exact process of hapten recognition is still unclear, activated dendritic cells migrate to the lymph node to stimulate cytotoxic CD8+ T-cell response.[43] Type IV hypersensitivity is also called delayed-type hypersensitivity, as it takes repeated exposure to the same allergen over time, and the symptoms become apparent 1-3 days after exposure to the allergen. Type IV hypersensitivity can also occur in inflammatory and autoimmune disease as well as in tissues and/or organ transplantation.[44]

Table 1.3 Hypersensitivity Reactions

Hypersensitivity Reactions	Type I	Type II	Type III	Type IV
Triggers	Dust mite feces, Pollen	Antibiotics (ex. Penicillin)	Soluble proteins (ex. Insulin)	Poison oak
Mediators	Allergen-specific IgE antibodies	IgG	IgG	Allergen-specific effector T cells
Pathway	IgE antibodies attached to FcεRI of mast cells degranulate upon activation	Molecules deposited on cells are recognized as xenobiotics	Chemically reactive compounds bind soluble proteins and deposited on the blood wall	Allergen-specific effector T cells react

1.5 The Innate and Adaptive immunity in Allergic Contact Dermatitis

The immune system reacts to organisms and viral particles that are foreign to the human body to protect against a variety of pathogens. The activation of the immune system ultimately results in the development of either a cellular response by antigen-specific T cells or a humoral response mediated by antibody-producing B cells that provide long-lasting protection against the same

pathogen. The development of T cells and B cells in response to a pathogen is part of the adaptive immunity. Adaptive immunity is highly specific to a particular pathogen. The type of adaptive immune response elicited is directed by the innate immune response. In contrast to the adaptive immune response, the innate immune response is non-specific and more general reaction to an infection. The innate immune system includes antigen-presenting cells, such as macrophages and dendritic cells, that reside in local tissues of the body. When pathogens enter the body, innate immune cells recognize molecular patterns that are commonly shared by pathogens but not present in the human body. The molecular patterns, also called pathogen-associated molecular patterns (PAMPs), bind pattern recognition receptors (PRRs) on antigen-presenting cells, which process pathogens and release cytokines that direct priming of adaptive immune response. Thus, the immune system is comprised of two mechanisms: the innate immunity and the adaptive immunity (**Figure 1.2**).[34,45–48]

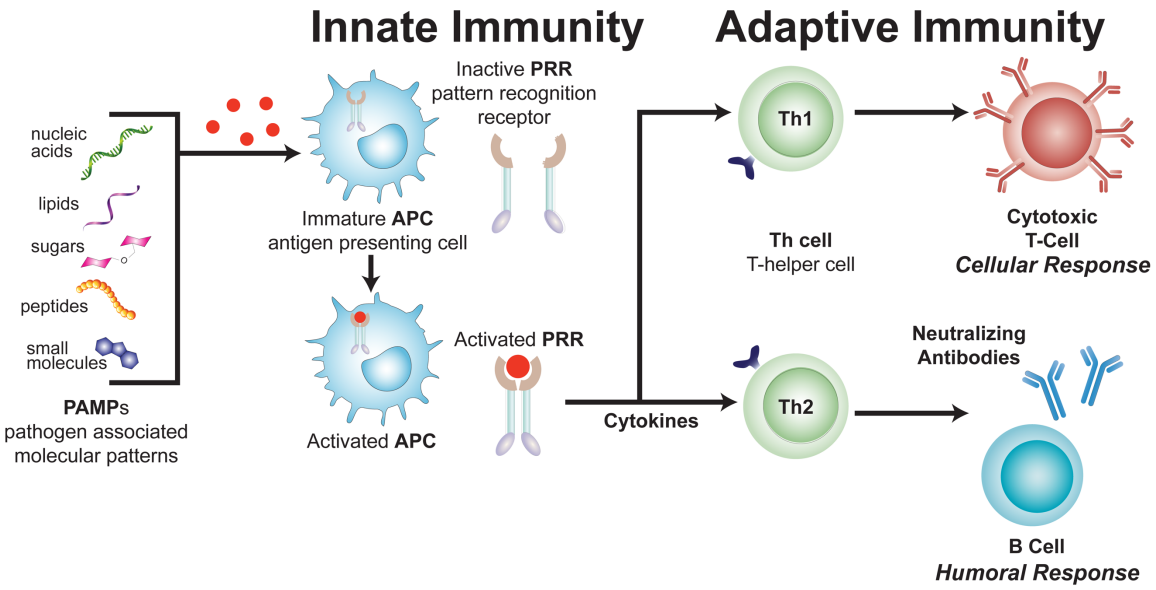

Figure 1.2 General overview of the immune system. Microbes, bacteria, and viruses are pathogens that express pathogen-associated molecular patterns (PAMPs), such as lipopolysaccharides, CpG-DNA, or peptides that are not found associated with mammalian cells. Antigen-presenting cells (APCs) express pattern recognition receptors (PRRs) that are activated when they are bound by PAMPs. Activated APCs release cytokines and migrate to the nearest lymph node to direct the priming of the adaptive immune response.

The pathology of ACD is somewhat similar to the way the immune system activates in response to the invasion of a pathogen. ACD is a T cell-mediated response, meaning that it relies on adaptive immunity developed through the activation of the innate immunity. For instance, the sensitization phase leads to the generation of skin-homing effector CD8+ type 1 cytotoxic (Tc1)/ type 17 cytotoxic (Tc17) and CD4+ T-helper (Th) 1/Th17 T cells that enter the bloodstream. Repeated exposure to the same allergen triggers a cascade of events leading to the infiltration of neutrophils, monocytes, and effector T cells. This leads to clinically apparent elicitation phase.[49–52] This is the reason that the sensitization phase must be studied. The sensitization phase is

triggered by skin dendritic cells that are activated by the penetration of chemically reactive compounds. However, the field is limited by the lack of sufficient knowledge on the activation of Langerhans cells and dermal dendritic cells by the environmental triggers, such as allergens. This process is still not as clear as the interaction of PAMPs and PRRs. The innate immune response of ACD holds a key to understanding the entire process and discovering new diagnostic tests, treatments, and cures for individuals suffering from this skin disorder.

1.6 Characteristics of Contact Allergens

The group of chemical sensitizers that can cause ACD is called contact allergens. There are three characteristics that distinguish contact allergens from other toxic compounds.[3] First, contact allergens are small-molecular-weight organic compounds. Although unclear, small size seems to allow contact allergens to easily penetrate the epidermis and react to form allergen-protein complex.[49] To form an allergen-protein complex, contact allergens must be chemically reactive. The early stage of skin sensitization is the process at which contact allergens covalently bind proteins. This makes sense because contact allergens are too small to be immunogenic. Additionally, contact allergens are almost always strong electrophiles, such as aldehydes, epoxides, or aromatic compounds (**Figure 1.3**), and react with nucleophiles at lysine and cysteine side chains of the proteins.[53] Whereas most of the contact allergens are reactive by themselves, some may become reactive through exposure to UV light, air oxidation, or cutaneous metabolism. Last and most importantly, contact allergens must have the ability to elicit an innate immune response. The adjuvanticity of contact allergens clearly distinguishes them from other common toxic chemicals. Sometimes, chemical triggers that are neither small organic compounds nor chemically reactive can still induce clinical symptoms that seem similar to ACD. In such cases, the chemical triggers

are considered to be irritants. Skin irritation is the result of the direct toxic effects of irritants, therefore, its implication in immune response is minimal.[54] The substances that elicit type I hypersensitivity can also cause an allergic response on the skin. These compounds manifest an antibody-mediated allergic response. Thus, the sensitization phase of contact dermatitis is induced by a set of small-molecular-weight compounds that reacts with proteins in the skin and cause skin inflammatory response.

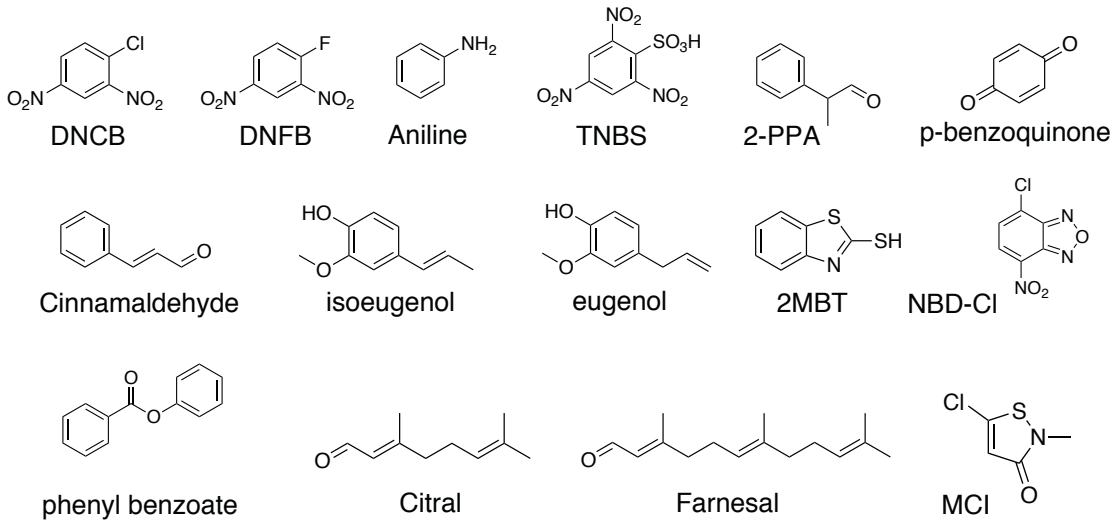

Figure 1.3 Examples of contact allergen. Contact allergens are small molecules that are chemically reactive. The chemical structures of contact allergens vary from aldehydes, ketones, aromatic rings, aromatic amines, and thiols. They bind proteins by different reaction mechanisms.

Thousands of contact allergens have been identified through animal testing or clinical evaluation.[55,56] They are prevalent in many products that individuals encounter in daily life. Examples include citral, which has a strong lemon scent and often used in air refreshers,[57] urushiol, which can be found in poison oak,[58] and phenylenediamine, which is a main ingredient of the hair dye.[59] As seen in the examples, contact allergens are both naturally occurring and essential ingredients in household products.

Contact allergens can contact the skin via several routes including occupational, habitual, regional, and genetic factors. Occupational exposure to contact allergens frequently results in ACD and is a major cause of occupational illness. Aromatic amines and DNCB are good examples of occupational contact allergens.[60] DNCB, in particular, is easy to come across, as they are commonly found as an intermediate for many industrial processes.[61] Nickel (Ni^{2+}) is present in jewelry, and the survey revealed that people who wore jewelry more frequently had a higher risk of ACD than those who did not wear jewelry.[62,63] This demonstrates the influence of personal habits on ACD. On the other hand, the geographical setting also contributes to the likelihood of developing ACD. Plants can also increase the risk of contact dermatitis. The genus *Toxicodendron* includes ivy, poison oak, and the lacquer trees, which are also well-known causes of contact dermatitis. Thus, plant-induced contact dermatitis is predominant among people who live in such habitats compared to people who do not.[64–66] Despite exposure to contact allergens is common, only a minority of exposed individuals develop ACD, suggesting a genetic predisposition. Although the genetics of contact allergy is still not fully understood, polymorphism and mutations could affect functions or conformations of the target proteins, increasing the risk of ACD.[67]

1.7 DNCB as a Model Contact Allergen

Among thousands of known contact allergens, DNCB is the most studied contact allergen. Many of contact allergen studies are based on DNCB-induced contact dermatitis. The skin sensitization potential of DNCB has been known for decades. In the 1930s, Landsteiner and Jacobs published a series of work on sensitization potential of 2,4-dinitrohalobenzene molecules.[68–74] Their findings led to the hypothesis that contact allergens by themselves are not immunogenic; they need to be covalently attached to a large carrier protein to elicit an immune response. Since then, many studies

have used DNCB as a model contact allergen to study the immunology of contact dermatitis for a variety of purposes: to develop in vitro testing methods and to investigate a signal transduction pathway of skin sensitization. Preliminary studies of DNCB have shown that sensitization occurs in proportion to the dose of sensitizer and the area of skin treated.[75,76] This work suggests that haptenation may increase as the concentration of DNCB increases and thus increase the number of activated dendritic cells available for presentation of allergen-specific antigens. The skin sensitization potential of a compound is often quantified using animal testing, and DNCB has also been used as a control contact allergen.[77] Murine contact hypersensitivity is an *in vivo* assay model of cell-mediated immune function in which exposure to a contact allergen elicits ACD and adequately reflect human disease as well. To demonstrate delayed-type hypersensitivity, this assay exposes mice to test compounds applied to the shaven abdomen for 2 days and to the dorsum of the ears for 4 consecutive days, followed by 3 days of rest. A study published in 2011 showed inflammation in the mice ears caused by the recruitment of CD4+ T cells. In addition, DNCB-induced contact hypersensitivity was shown to produce high levels of proinflammatory cytokines such as TNF-α, interleukin (IL)-6, and IL-12.[78] Other assays that assess skin sensitization potential include peptide reactivity assays and cell-based assays, which will be discussed in the next session.

Signal transduction induced by contact allergens has also been investigated using DNCB. Langerhans cells usually show upregulation of CD86, CD54, and HLA-DR expression upon activation and initiate a common signal transduction pathway with major roles for mitogen-activated protein kinases (MAPKs) and nuclear factor kappa B (NF-κB).[79,80] However, according to previous studies, the effect of DNCB was limited to inducing the expression of CD83 and CD86, and the production of IL-8 and TNF-α.[81,82] Nevertheless, DNCB fully activated p38 MAPK and NF-κB pathway, observed by western blot of p65 and translocation to the nucleus.[83]

1.8 Reaction Mechanisms of Contact Allergens

As the chemical reactivity of contact allergens is a determinant feature, this section will discuss different types of reaction mechanisms of contact allergens. Contact allergens are almost always strong electrophiles, and thus, most of them bind proteins through nucleophilic substitution (S_N2) reaction. This reaction occurs when a nucleophile donates an electron pair to an electrophile to displace a chemical group, such as leaving group or saturated or unsaturated carbons.[84] Lysine and cysteine residues of the protein serves as a nucleophile that attacks electrophilic contact allergens.[85–87] Therefore, this study primarily focused on the modification of lysine and cysteine residues when identifying protein targets.

When S_N2 reaction occurs in an aromatic ring, aryl halides, or DNCB, as examples, it is called nucleophilic aromatic substitution (S_NAr) reaction. The nucleophile reacts at the halide-bearing carbon of the aromatic ring to yield a resonance-stabilized ion called Meisenheimer complex. This intermediate is stabilized by electron-withdrawing groups that are on ortho and para to the leaving group and the electronegative leaving group (**Figure 1.4A**).[88] On the other hand, contact allergens that are aldehydes and ketones, citral or cinnamaldehyde as examples, can react with primary amines (ex. lysine), through a process known as imine or Schiff base formation. Imine formation begins as a nucleophilic addition to the carbonyl group. The primary amine reacts with an aldehyde or ketone to form an unstable product called carbinolamine, which undergoes dehydration to form imines (**Figure 1.4B**).[88,89] The formation of imines is a reversible process, which could explain why many aldehydes and ketones are usually moderate to weak sensitizers. Another type of reaction mechanism that commonly occurs with contact allergens is Michael addition, which can be described as conjugate addition of carbanions to α,β-unsaturated carbonyl compounds. In this reaction, a carbon-carbon π bond in the starting compound is replaced with a

carbon-carbon σ bond. Michael addition can occur when a nucleophile with thiols, like cysteine, reacts to a contact allergen with alkene groups (**Figure 1.4C**).[88,90,91] This reaction is called the thiol-ene reaction, yet it is known to proceed through a Michael addition pathway.[92]

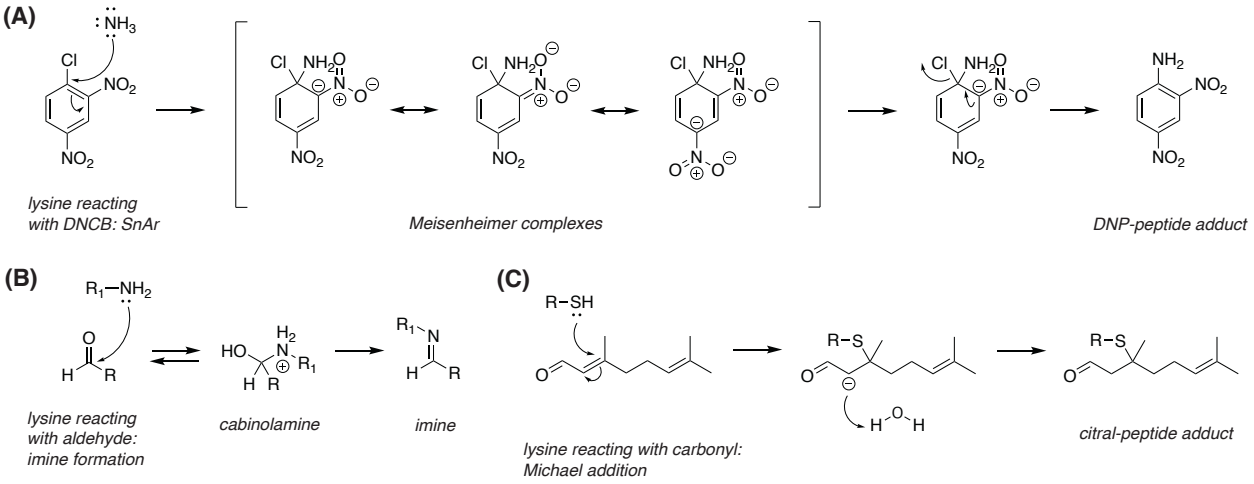

Figure 1.4 Reaction mechanisms of the mentioned reactions. **(A)** S_NAr reaction mechanism with DNCB and the lysine side chain (NH_3) of a protein. They form a resonance stabilized Meisenheimer complex before the chlorine is displaced. **(B)** Imine or Schiff base formation of lysine and aldehydes or ketones. Formation of the unstable product carbinolamine is a reversible process but completed by β-elimination **(C)** Michael addition that occurs when cysteine reacts with the α,β-unsaturated carbonyl of citral.

1.9 Evaluating Skin Sensitization Potential Using *In Vitro* Methods

Contact allergen research was begun by manufacturing industries to identify contact allergens before using them in their products. This research involved the development of predictive tests to both correctly identify and evaluate the relative potency of chemical sensitizers. The original method of evaluation was guinea pig testing.[93,94] While this testing answered the "yes or no" question of whether a compound is capable of sensitization, it failed to provide more quantitative

data, such as the degree of inflammation and relative sensitizing potency. Such limitations were overcome with the development of a new animal testing, the local lymph node assay (LLNA).[95,96] Unlike guinea pig testing, LLNA is based on the evaluation of events induced during the induction phase of skin sensitization. After sensitizing the mice with test compounds, the draining lymph nodes are excised, counted, pooled, and processed into a single-cell suspension. Results are calculated based on the ratio of disintegration per node of the experimental group to that of the control group. Thus, the LLNA not only provides a more accurate prediction of sensitization but also allows assessment of relative skin sensitizing potency for risk assessment.[97–100] Despite these advantages, the use of the LLNA is discouraged because it still uses animal models. With a significant emphasis on animal welfare, there has been an interest in the development of non-animal testing methods to evaluate the skin sensitization potency of chemical compounds.[101]

The direct peptide reactivity assay (DPRA) is a way to predict skin sensitization without using animals. The DPRA examines the reactivity of a compound with peptides, which is based on the characteristics of contact allergens. The test compounds are incubated with seven-residue peptides with either a lysine or cysteine residue, and the presence of peptide adduct is detected using liquid chromatography-mass spectrometry (LC-MS). The compound is classified as a contact allergen if the adduct is present.[85,86,102] However, the DPRA fails to reproduce the physiological condition of the skin, the place where the reaction actually takes place. As an example, lysine is most reactive at pH 10.53. Thus, the DPRA of lysine-containing peptides uses a buffer with pH 10.7, which is not a physiological pH. This might explain why the accuracy of DPRA is 53.8 % for lysine-containing peptides.[56]

As an improvement, cell-based assays have been established. These methods rely on the phenotypic changes of mammalian antigen-presenting cells as markers of skin sensitization

potential. A cell-based assay measuring the changes in human monocyte cell line THP-1 is the most commonly used in replacement for dendritic cells, as monocytes are easier to work with in terms of culturing and cryopreservation. They also exhibit less cell-to-cell variability but display a phenotype similar to that of dendritic cells.[103] The human cell-line activation test (h-CLAT) uses upregulation of CD54 and CD86 as markers for skin sensitization.[104–107] Compared to LLNA data, h-CLAT data are reported to have a sensitivity of 72-75 %, a specificity of 76-77 %, and an overall accuracy of 74-76 %.[56,108]

A refinement from h-CLAT testing is the use of IL-8 as a marker of skin sensitization. This test measures the amount of IL-8 secreted from THP-1 cells stimulated with test compounds. In a study, 13 out of 16 tested contact allergens induced statistically significant augmentation of IL-8 production. Additionally, extreme and strong contact allergens produced higher IL-8 secretion than moderate and weak contact allergens. This trend seemed to be dose-dependent and thus was proposed as an alternative method to animal testing.[109,110] IL-8 is a proinflammatory cytokine and is chemoattractant cytokine, or chemokine, produced following the activation of macrophages during infection. The main job of IL-8 is to attract neutrophils that circulate in the bloodstream to the site of infection. Recruited neutrophils provide aid as the first line of defense against pathogens.[111] In line with the dosage-dependent IL-8 production observed, recent findings have reported an increased number of neutrophils in the inflammatory skin lesions of patients with ACD and have shown that neutrophils are required for both the sensitization and elicitation phase of contact hypersensitivity.[112,113] All of these evidences indicate that IL-8 screening is a relatively robust assay for measuring the skin sensitization potential of chemical sensitizers.

Altogether, the efforts to develop an assay to accurately measure skin sensitization potential have built a foundation for studying the mechanism of skin sensitization, which this thesis

aims to do. Here, for almost all of the results I present in Chapter 2 and 3, I report the level of IL-8 as a measurement of skin sensitization.

1.10 Project Aims

This work aims to elucidate a mechanistic pathway of skin sensitization using DNCB as a model contact allergen. The primary aim of this project is to identify functionally relevant protein targets to which a contact allergen, DNCB, binds. The specific aims are as follows:

1.10.1 Structure-Activity Relationship (SAR) of DNCB

The concept of a structure-activity relationship (SAR) will be discussed in the next section. Though thousands of contact allergens and their sensitization potentials have been known for a long time, a fundamental study that encompasses multiple aspects of contact allergen's properties is still not readily available. Numerous studies have evaluated SARs based on only one aspect of contact allergen's characteristics, mainly evaluating the reactivity to peptides.[114–117] Thus, a study with a rational design for test compounds and performing characterization is needed. For this work, the test compounds were chosen after considering the DNCB's reaction mechanism. The skin sensitization potential of the derivatives were characterized by the following 4 methods: (i) the rate of reactivity to cysteine, (ii) the ability to induce an immune response in human monocyte cell line THP-1, (iii) protein modification trends probed by western blotting, and (iv) ear inflammation tested with a murine model of contact hypersensitivity. Hopefully, this work will contribute to the understanding of the relationship between the physicochemical properties of contact allergens and their skin sensitization potential. This work will be discussed in Chapter 2.

1.10.2 Identification and Validation of Functionally Relevant Protein Targets of DNCB

Despite the known dangers of contact allergens, the molecular mechanism at which they cause contact dermatitis is still unclear. Contact allergens bind protein to become immunogenic, and this work hypothesized that there are target proteins that work like receptors of contact allergens. Here, the goal is not only to identify DNCB-modified proteins but also to validate their functional relevance to skin sensitization in cell and animal models. For this work, DNCB-modified proteins were first probed and enriched using an antibody-based affinity purification technique. After identifying DNCB-modified proteins, this dissertation validates of functional-relevance of the identified proteins by testing DNCB-induced hypersensitivity response (i) in protein knockdown cells, and (ii) suppressing protein activity with chemical inhibitors. As protein modification by a contact allergen is the initial step toward skin sensitization, I hope that this work would contribute to elucidating the overall pathway underlying contact hypersensitivity. This work will be discussed in Chapter 3.

1.11 Background and Concepts I: Structure-Activity Relationship

SAR is a study that aims to understand how changes in the chemical or molecular structure of a compound alter the overall biological response. A typical SAR study begins by understanding the reaction mechanism of the target compound, which will be the basis for derivative designs, and characterizing the derivatives to identify their physicochemical properties pertinent to the biological activity. SAR is especially useful in understanding the properties of immunostimulatory molecules.[118] For example, SAR studies of toll-like receptor (TLR)-7 agonists have helped in refining and improving the immune potency of these molecules. This work not only led to the proposal of alternatives for TLR-7 agonists but also provided more detailed information on TLR

specificity and innate immune function.[119] This example shows that if SAR studies can be applied to contact allergens, our understanding of the properties of protein targets and the skin sensitization pathway would benefit tremendously from the increased level of detail.

Indeed, the SAR is an important tool that predicts skin sensitization potential. The quantitative SAR (QSAR) method is an *in silico* model developed for prediction of skin sensitization potential. Currently, *in silico* tools are available to predict sensitization potential based on the electrophilic functional groups of compounds, such as halogenated carbons, epoxides, aldehydes, ketones, and amines.[120–122] Although it seems to be an ideal method of prediction, its accuracy is limited by several factors. First, *in silico* models can create false predictions due to the inability to calculate the chemical-chemical interaction of contact allergens that can occur *in vivo*. To elaborate, contact allergens can sometimes become reactive upon oxidation, UV activation, or reduction, all of which occur through a contact allergen's interactions with other chemical compounds in the skin. Alternatively, contact allergens can also interact with themselves due to inherent intermolecular forces. These interactions may interfere with a compound's sensitization potential but are challenging to integrate into QSAR models without SAR results from carefully-conducted experiments.[56,123]

In Chapter 2, I propose and report the SAR study of DNCB. By exploring the SAR of DNCB, I aim to establish the SAR result that encompasses multiple physicochemical and biochemical properties that could potentially help establish a more accurate QSAR model and understand DNCB-protein interaction in greater detail.

1.12 Background and Concepts II: Post-Translational Modification

Contact allergens bind proteins in a manner similar to the post-translational modification (PTM). Thus, this section will discuss the importance of PTM and protein modification by DNCB. PTM is a biochemical process that involves covalent and enzymatic modification of proteins, typically after biosynthesis. Three common types of PTM are methylation, acetylation, and phosphorylation. Each type of modification is defined as the addition of methyl, acetyl, and phosphate groups, respectively, to the compounds and biomolecules.[124,125] Whereas methylation usually occurs in DNA to regulate gene expression, acetylation and phosphorylation take place on proteins.[126] N-terminal acetylation is the most common covalent modification of proteins in eukaryotes, and it can affect protein stability, localization, metabolism, and protein synthesis.[127–129] Phosphorylation is critical for many cellular processes in biology. The synthesis of adenosine triphosphate (ATP) from adenosine diphosphate (ADP) by the addition of a third phosphate is a common example of the phosphorylation of a molecular compound.[130] Protein phosphorylation can occur at multiple sites through different reversible mechanisms of bond formation that can alter protein structure. Ultimately, it affects cellular functions including biological thermodynamics, enzyme inhibition and regulation, protein degradation, and protein-protein interactions. Altogether, these modifications to proteins and biomolecules result in activation of cellular processes, including innate immune responses and skin sensitization process.[131–133] Protein modification with DNCB is not very different from PTM (**Figure 1.5**). DNCB modification results in the formation of covalent bonds between DNCB and a protein, producing DNCB-modified proteins. Similar to PTM, DNCB modification initiates cellular responses, but in contrast, through unclear mechanisms.

1.13 Background and Concepts III: Mass Spectrometry

Mass spectrometry is a useful approach for analyzing molecular samples by first converting them into gaseous ions under the influence of an electronic gradient and then characterizing them by mass-to-charge (m/z) ratio and relative abundance. Mass spectrometers consist of three major components: (i) an ionization source that produces gaseous ions from samples, (ii) an analyzer that resolves the ions into their m/z ratio and relative abundance, and (iii) a detector that detects the ions.[134] Because mass spectrometers can be used as a tool for the identification of proteins and sites of PTM, proteomics research increasingly depends on this technology. Thus, this section will discuss the different types of mass spectrometers that are used for proteomics research.

Electronspray ionization-mass spectrometry (ESI-MS) uses an electronspray to ionize samples. The samples are prepared by dissolution in a polar solvent, like methanol. Then, the samples are sprayed to the mass spectrometer via a thin needle that is held at a high electrical potential. This process introduces charged droplets of samples into the instrument.[135,136] ESI-MS is usually coupled with a quadrupole analyzer, which consists of four metal rods with opposite electronic pairs connected. The voltage applied to the rods creates electronic fields that allow the charged droplets to pass through and reach detectors. The main advantage of the quadrupole analyzer in proteomics research is that the electronic fields can be tuned to allow only peptide fragments with a certain range of molecular weights to pass through at a given moment.[137]

In contrast, matrix-assisted laser desorption/ionization (MALDI) requires dried samples. Samples for MALDI are mixed with a UV-absorbing compound, called matrix, and mounted on a plate to form crystals. When a laser is fired at the samples, the energy from the laser is absorbed by the matrix and passed on to the samples, which are then ionized into the gaseous phase.[135] ESI-MS is usually coupled with a quadrupole analyzer, which consists of four metal rods with opposite

electronic pairs connected. The voltage applied to the rods creates electronic fields that can allow the ionized samples to pass through and reach detectors. On the other hand, MALDI-MS is usually coupled with time-of-flight (TOF) mass analyzer. Samples that are ionized enter a vacuum tube, which is sometimes equipped with electrostatic mirrors called reflectrons. Thus, m/z ratio is determined by the speed at which fragments travel through the vacuum tube. The main advantage of TOF is that it allows separation of ions of the same charge by the mass.[138]

Mass spectrometers can be connected in a series of ion sources, called tandem mass spectrometry (MS/MS), to provide relatively valuable information about the sequence of peptides and molecular structures of proteins. A specific ion is selected in the first analyzer and then subjected to collision in the collision cell. The product ions are separated in the second mass analyzer based on their m/z ratio before they reach the detector. Applying this technique to proteomics research, a particular trypsinized peptide ion is selected in the first analyzer, and then subjected to collision. Supposedly, this peptide is fragmented at each amide bond to produce the single amino acid residues from the full-length peptide, and the individual residues can be observed and used to elucidate the peptide sequence.[137,139–144]

1.14 References

1. Justiz Vaillant, A. A. & Zito, P. M. Immediate Hypersensitivity Reactions. in *StatPearls* (StatPearls Publishing, 2020).

2. Justiz Vaillant, A. A., Zulfiqar, H. & Ramphul, K. Delayed Hypersensitivity Reactions. in *StatPearls* (StatPearls Publishing, 2020).

3. Kaplan, D. H., Igyártó, B. Z. & Gaspari, A. A. Early immune events in the induction of allergic contact dermatitis. *Nat. Rev. Immunol.* **12**, 114–124 (2012).

4. Martin, S. F. *et al.* Mechanisms of chemical-induced innate immunity in allergic contact dermatitis. *Allergy* **66**, 1152–1163 (2011).

5. McFadden, J. P., Puangpet, P., Basketter, D. A., Dearman, R. J. & Kimber, I. Why does allergic contact dermatitis exist? *British Journal of Dermatology* **168**, 692–699 (2013).

6. Roberts, D. W. & Aptula, A. O. Allergic contact dermatitis caused by a skin-lightening agent, 5,5′-dipropylbiphenyl-2,2′-diol. A comment. *Contact Dermatitis* **66**, 357–359 (2012).

7. Chulalongkorn Allergy and Clinical Immunology Research Group. Contact dermatitis. (01:55:55 UTC).

8. Gittler, J. K., Krueger, J. G. & Guttman-Yassky, E. Atopic dermatitis results in intrinsic barrier and immune abnormalities: Implications for contact dermatitis. *J Allergy Clin Immunol* **131**, 300–313 (2013).

9. Straube, F., Grenet, O., Bruegger, P. & Ulrich, P. Contact allergens and irritants show discrete differences in the activation of human monocyte-derived dendritic cells: consequences for in vitro detection of contact allergens. *Arch. Toxicol.* **79**, 37–46 (2005).

10. Ryan, C. A. *et al.* Interactions of Contact Allergens with Dendritic Cells: Opportunities and Challenges for the Development of Novel Approaches to Hazard Assessment. *Toxicol. Sci.* **88**, 4–11 (2005).

11. Katz, S. I., Tamaki, K. & Sachs, D. H. Epidermal Langerhans cells are derived from cells originating in bone marrow. *Nature* **282**, 324–326 (1979).

12. Basketter, D., Dooms-Goossens, A., Karlberg, A.-T. & Lepoittevin, J.-P. The chemistry of contact allergy: why is a molecule allergenic? *Contact Dermatitis* **32**, 65–73 (1995).

13. Aptula, A. O., Roberts, D. W. & Pease, C. K. Haptens, prohaptens and prehaptens, or electrophiles and proelectrophiles. *Contact Dermatitis* **56**, 54-U14 (2007).

14. Kapur, S., Watson, W. & Carr, S. Atopic dermatitis. *Allergy, Asthma & Clinical Immunology* **14**, 52 (2018).

15. Akdis, C. A. *et al.* Diagnosis and treatment of atopic dermatitis in children and adults: European Academy of Allergology and Clinical Immunology/American Academy of Allergy, Asthma and Immunology/PRACTALL Consensus Report. *Journal of Allergy and Clinical Immunology* **118**, 152–169 (2006).

16. Gür Çetinkaya, P. & Şahiner, Ü. M. Childhood atopic dermatitis: current developments, treatment approaches, and future expectations. *Turk J Med Sci* **49**, 963–984 (2019).

17. Kim, J. S. Pediatric atopic dermatitis: the importance of food allergens. *Semin Cutan Med Surg* **27**, 156–160 (2008).

18. Nosbaum, A., Vocanson, M., Rozieres, A., Hennino, A. & Nicolas, J.-F. Allergic and irritant contact dermatitis. *Eur J Dermatol* **19**, 325–332 (2009).

19. Freudenberg, M. A., Esser, P. R., Jakob, T., Galanos, C. & Martin, S. F. Innate and adaptive immune responses in contact dermatitis: analogy with infections. *G Ital Dermatol Venereol* **144**, 173–185 (2009).

20. Vocanson, M., Hennino, A., Rozières, A., Poyet, G. & Nicolas, J.-F. Effector and regulatory mechanisms in allergic contact dermatitis. *Allergy* **64**, 1699–1714 (2009).

21. Diepgen, T. L. & Coenraads, P. J. The epidemiology of occupational contact dermatitis. *International Archives of Occupational and Environmental Health* **72**, 496–506 (1999).

22. Thyssen, J. P., Linneberg, A., Menné, T. & Johansen, J. D. The epidemiology of contact allergy in the general population--prevalence and main findings. *Contact Derm.* **57**, 287–299 (2007).

23. Alinaghi, F., Bennike, N. H., Egeberg, A., Thyssen, J. P. & Johansen, J. D. Prevalence of contact allergy in the general population: A systematic review and meta-analysis. *Contact Derm.* **80**, 77–85 (2019).

24. Diepgen, T. L. Occupational skin-disease data in Europe. *Int Arch Occup Environ Health* **76**, 331–338 (2003).

25. FastStats. https://www.cdc.gov/nchs/fastats/allergies.htm (2019).

26. Weidinger, S. & Novak, N. Atopic dermatitis. *Lancet* **387**, 1109–1122 (2016).

27. Schmitt, J., von Kobyletzki, L., Svensson, A. & Apfelbacher, C. Efficacy and tolerability of proactive treatment with topical corticosteroids and calcineurin inhibitors for atopic eczema: systematic review and meta-analysis of randomized controlled trials. *Br. J. Dermatol.* **164**, 415–428 (2011).

28. Broeders, J. A., Ahmed Ali, U. & Fischer, G. Systematic review and meta-analysis of randomized clinical trials (RCTs) comparing topical calcineurin inhibitors with topical corticosteroids for atopic dermatitis: A 15-year experience. *J. Am. Acad. Dermatol.* **75**, 410-419 (2016).

29. Siegfried, E. C., Jaworski, J. C., Kaiser, J. D. & Hebert, A. A. Systematic review of published trials: long-term safety of topical corticosteroids and topical calcineurin inhibitors in pediatric patients with atopic dermatitis. *BMC Pediatr* **16**, 75 (2016).

30. Segal, A. O., Ellis, A. K. & Kim, H. L. CSACI position statement: safety of topical calcineurin inhibitors in the management of atopic dermatitis in children and adults. *Allergy Asthma Clin Immunol* **9**, 24 (2013).

31. Krakowski, A. C., Eichenfield, L. F. & Dohil, M. A. Management of atopic dermatitis in the pediatric population. *Pediatrics* **122**, 812–824 (2008).

32. Lee, J. H., Son, S. W. & Cho, S. H. A Comprehensive Review of the Treatment of Atopic Eczema. *Allergy Asthma Immunol Res* **8**, 181–190 (2016).

33. Gittler, J. K., Wang, J. F. & Orlow, S. J. Bathing and Associated Treatments in Atopic Dermatitis. *Am J Clin Dermatol* **18**, 45–57 (2017).

34. Immunobiologia janeway download. *Google Docs* https://docs.google.com/document/u/2/d/17O1_Ide6EU4df3mEL4e4XOBiHarvEPyg9_zxNoA0wb8/edit?usp=embed_facebook.

35. Son, J. H. *et al.* Immediate Hypersensitivity Reactions Induced by Triamcinolone in a Patient with Atopic Dermatitis. *J Korean Med Sci* **33**, (2018).

36. Koike, Y. *et al.* Predictors of Persistent Milk Allergy in Children: A Retrospective Cohort Study. *Int. Arch. Allergy Immunol.* **175**, 177–180 (2018).

37. Bhattacharya, S. THE FACTS ABOUT PENICILLIN ALLERGY: A REVIEW. *J Adv Pharm Technol Res* **1**, 11–17 (2010).

38. Blumenthal, K. G., Peter, J. G., Trubiano, J. A. & Phillips, E. J. Antibiotic allergy. *Lancet* **393**, 183–198 (2019).

39. King, T. C. Inflammation, Inflammatory Mediators, and Immune-Mediated Disease. in *Elsevier's Integrated Pathology* 21–57 (Elsevier, 2007). doi:10.1016/B978-0-323-04328-1.50008-5.

40. Owczarczyk-Saczonek, A., Wygonowska, E., Budkiewicz, M. & Placek, W. Serum sickness disease in a patient with alopecia areata and Meniere' disease after PRP procedure. *Dermatol Ther* **32**, e12798 (2019).

41. Gershwin, L. J. Adverse Reactions to Vaccination: From Anaphylaxis to Autoimmunity. *Vet. Clin. North Am. Small Anim. Pract.* **48**, 279–290 (2018).

42. Ghazavi, M. K. & Johnston, G. A. Insulin allergy. *Clin. Dermatol.* **29**, 300–305 (2011).

43. Bennett, C. L. *et al.* Inducible ablation of mouse Langerhans cells diminishes but fails to abrogate contact hypersensitivity. *J. Cell Biol.* **169**, 569–576 (2005).

44. Li, N. & Shi, R.-H. Updated review on immune factors in pathogenesis of Crohn's disease. *World J. Gastroenterol.* **24**, 15–22 (2018).

45. Poland, G. A., Quill, H. & Togias, A. Understanding the human immune system in the 21st century: The Human Immunology Project Consortium. *Vaccine* doi:10.1016/j.vaccine.2013.04.043.

46. Medzhitov, R. & Janeway Jr, C. A. Innate immunity: impact on the adaptive immune response. *Current Opinion in Immunology* **9**, 4–9 (1997).

47. Lu, Y.-C., Yeh, W.-C. & Ohashi, P. S. LPS/TLR4 signal transduction pathway. *Cytokine* **42**, 145–151 (2008).

48. Chen, K. *et al.* Toll-like receptors in inflammation, infection and cancer. *International Immunopharmacology* **7**, 1271–1285 (2007).

49. Martin, S. F. T lymphocyte-mediated immune responses to chemical haptens and metal ions: implications for allergic and autoimmune disease. *Int. Arch. Allergy Immunol.* **134**, 186–198 (2004).

50. Kaufmann, S. H. E. The contribution of immunology to the rational design of novel antibacterial vaccines. *Nat Rev Micro* **5**, 491–504 (2007).

51. Martin, S. F. *et al.* Fas-mediated inhibition of CD4+ T cell priming results in dominance of type 1 CD8+ T cells in the immune response to the contact sensitizer trinitrophenyl. *J. Immunol.* **173**, 3178–3185 (2004).

52. Watanabe, H., Unger, M., Tuvel, B., Wang, B. & Sauder, D. N. Contact hypersensitivity: the mechanism of immune responses and T cell balance. *J. Interferon Cytokine Res.* **22**, 407–412 (2002).

53. Basketter, D. A. Chemistry of contact allergens and irritants. *Am. J. Contact Dermatitis* **9**, 119–124 (1998).

54. Dahl, M. V. Chronic, irritant contact dermatitis: mechanisms, variables, and differentiation from other forms of contact dermatitis. *Adv Dermatol* **3**, 261–275 (1988).

55. Groot, A. C. D. & Frosch, P. J. Patch Test Concentrations and Vehicles for Testing Contact Allergens. 22.

56. Bauch, C. *et al.* Putting the parts together: Combining in vitro methods to test for skin sensitizing potentials. *Regulatory Toxicology and Pharmacology* **63**, 489–504 (2012).

57. Heydorn, S. *et al.* Citral a fragrance allergen and irritant. *Contact Derm.* **49**, 32–36 (2003).

58. Bonnekoh, H., Poch, G. & Metz, M. Severe contact dermatitis caused by urushiol in Japanese lacquer. *Contact Dermatitis* **80**, 55–56 (2019).

59. Mukkanna, K. S., Stone, N. M. & Ingram, J. R. Para-phenylenediamine allergy: current perspectives on diagnosis and management. *J Asthma Allergy* **10**, 9–15 (2017).

60. J, G., A, K. & H, L. [Allergological diagnostics and current allergens in occupational dermatology]. *Hautarzt* **60**, 708–717 (2009).

61. Friedmann, P. S. The immunology of allergic contact dermatitis: the DNCB story. *Adv Dermatol* **5**, 175-195;discussion 196 (1990).

62. Uter, W., Pfahlberg, A., Gefeller, O., Geier, J. & Schnuch, A. Risk factors for contact allergy to nickel - results of a multifactorial analysis. *Contact Derm.* **48**, 33–38 (2003).

63. Thyssen, J. P., Ross-Hansen, K., Menné, T. & Johansen, J. D. Patch test reactivity to metal allergens following regulatory interventions: a 33-year retrospective study. *Contact Derm.* **63**, 102–106 (2010).

64. Fisher, A. A. Esoteric contact dermatitis. Part IV: Devastating contact dermatitis in India produced by American parthenium weed (the scourge of India). *Cutis* **57**, 297–298 (1996).

65. Sareen, R. & Shah, A. Hypersensitivity manifestations to the fruit mango. *Asia Pac Allergy* **1**, 43–49 (2011).

66. Cohen, L. M. & Cohen, J. L. Erythema multiforme associated with contact dermatitis to poison ivy: three cases and a review of the literature. *Cutis* **62**, 139–142 (1998).

67. Schnuch, A., Westphal, G., Mössner, R., Uter, W. & Reich, K. Genetic factors in contact allergy--review and future goals. *Contact Derm.* **64**, 2–23 (2011).

68. Landsteiner, K. & Chase, M. W. STUDIES ON THE SENSITIZATION OF ANIMALS WITH SIMPLE CHEMICAL COMPOUNDS. *J Exp Med* **73**, 431–438 (1941).

69. Landsteiner, K. & Jacobs, J. STUDIES ON THE SENSITIZATION OF ANIMALS WITH SIMPLE CHEMICAL COMPOUNDS. *J Exp Med* **61**, 643–656 (1935).

70. Landsteiner, K. & Jacobs, J. STUDIES ON THE SENSITIZATION OF ANIMALS WITH SIMPLE CHEMICAL COMPOUNDS. II. *J Exp Med* **64**, 625–639 (1936).

71. Landsteiner, K. & Jacobs, J. STUDIES ON THE SENSITIZATION OF ANIMALS WITH SIMPLE CHEMICAL COMPOUNDS III. ANAPHYLAXIS INDUCED BY ARSPHENAMINE. *J Exp Med* **64**, 717–721 (1936).

72. STUDIES ON THE SENSITIZATION OF ANIMALS WITH SIMPLE CHEMICAL COMPOUNDS | Journal of Experimental Medicine | Rockefeller University Press. https://rupress.org/jem/article/61/5/643/4009/STUDIES-ON-THE-SENSITIZATION-OF-ANIMALS-WITH.

73. Studies on the sensitization of animals with simple chemical compounds: Landsteiner, K., and Chase, M. D.: J. Exper. Med. 66: 337, 1937. *Journal of Allergy* **9**, 204 (1938).

74. Studies on the sensitization of animals with simple chemical compounds. VII. Skin sensitization by intraperitoneal injections: Landsteiner, K., and Chase, M. W.: J. Exper. Med. 71: 237, 1940. *Journal of Allergy* **11**, 430 (1940).

75. White, S. I., Friedmann, P. S., Moss, C. & Simpson, J. M. The effect of altering area of application and dose per unit area on sensitization by DNCB. *Br. J. Dermatol.* **115**, 663–668 (1986).

76. Rees, J. L., Friedmann, P. S. & Matthews, J. N. The influence of area of application on sensitization by dinitrochlorobenzene. *Br. J. Dermatol.* **122**, 29–31 (1990).

77. Noonan, F. P. & Halliday, W. J. Studies of Contact Hypersensitivity and Tolerance in vivo and in vitro. *IAA* **56**, 523–532 (1978).

78. Röse, L., Schneider, C., Stock, C., Zollner, T. M. & Döcke, W.-D. Extended DNFB-induced contact hypersensitivity models display characteristics of chronic inflammatory dermatoses. *Exp. Dermatol.* **21**, 25–31 (2012).

79. Tuschl, H. & Kovac, R. Langerhans cells and immature dendritic cells as model systems for screening of skin sensitizers. *Toxicol In Vitro* **15**, 327–331 (2001).

80. Tuschl, H., Kovac, R. & Weber, E. The expression of surface markers on dendritic cells as indicators for the sensitizing potential of chemicals. *Toxicology in Vitro* **14**, 541–549 (2000).

81. Ade, N. *et al.* NF-κB Plays a Major Role in the Maturation of Human Dendritic Cells Induced by NiSO4 but not by DNCB. *Toxicol Sci* **99**, 488–501 (2007).

82. Miyazawa, M. *et al.* Role of MAPK signaling pathway in the activation of dendritic type cell line, THP-1, induced by DNCB and $NiSO_4$. *The Journal of Toxicological Sciences* **33**, 51–59 (2008).

83. Kavasi, R.-M. *et al.* Contact allergen (PPD and DNCB)-induced keratinocyte sensitization is partly mediated through a low molecular weight hyaluronan (LMWHA)/TLR4/NF-κB signaling axis. *Toxicology and Applied Pharmacology* **377**, 114632 (2019).

84. McMurry, J. E. *Organic Chemistry*. (Cengage Learning, 2011).

85. Gerberick, G. F. *et al.* Development of a peptide reactivity assay for screening contact allergens. *Toxicol. Sci.* **81**, 332–343 (2004).

86. Gerberick, G. F. *et al.* Quantification of chemical peptide reactivity for screening contact allergens: a classification tree model approach. *Toxicol. Sci.* **97**, 417–427 (2007).

87. Divkovic, M., Pease, C. K., Gerberick, G. F. & Basketter, D. A. Hapten-protein binding: from theory to practical application in the in vitro prediction of skin sensitization. *Contact Derm.* **53**, 189–200 (2005).

88. Loudon, G. M. *Organic Chemistry*. (Roberts and Company, 2009).

89. Stork, Gilbert., Brizzolara, A., Landesman, H., Szmuszkovicz, J. & Terrell, R. The Enamine Alkylation and Acylation of Carbonyl Compounds. *J. Am. Chem. Soc.* **85**, 207–222 (1963).

90. Smith, M. B. *March's Advanced Organic Chemistry: Reactions, Mechanisms, and Structure*. (John Wiley & Sons, 2020).

91. Mather, B. D., Viswanathan, K., Miller, K. M. & Long, T. E. Michael addition reactions in macromolecular design for emerging technologies. *Progress in Polymer Science* **31**, 487–531 (2006).

92. Sinha, A. K. & Equbal, D. Thiol−Ene Reaction: Synthetic Aspects and Mechanistic Studies of an Anti-Markovnikov-Selective Hydrothiolation of Olefins. *Asian Journal of Organic Chemistry* **8**, 32–47 (2019).

93. Magnusson, B. & Kligman, A. M. The identification of contact allergens by animal assay. The guinea pig maximization test. *J. Invest. Dermatol.* **52**, 268–276 (1969).

94. Feinberg, J. G. Allergic Contact Dermatitis in the Guinea Pig. *Immunology* **22**, 511 (1972).

95. Basketter, D. A. & Scholes, E. W. Comparison of the local lymph node assay with the guinea-pig maximization test for the detection of a range of contact allergens. *Food and Chemical Toxicology* **30**, 65–69 (1992).

96. von Blomberg, M., Rijlaarsdam, U. & Scheper, R. J. Direct Macrophage Migration Inhibition Test in DNCB Contact Sensitized Guinea Pigs. *International Archives of Allergy and Immunology* **50**, 503–512 (1976).

97. Kimber, I., Dearman, R. J., Scholes, E. W. & Basketter, D. A. The local lymph node assay: developments and applications. *Toxicology* **93**, 13–31 (1994).

98. Dearman, R. J., Basketter, D. A. & Kimber, I. Local lymph node assay: use in hazard and risk assessment. *J Appl Toxicol* **19**, 299–306 (1999).

99. Gerberick, G. F. *et al.* Local lymph node assay: validation assessment for regulatory purposes. *Am. J. Contact Dermatitis* **11**, 3–18 (2000).

100. Basketter, D. A. *et al.* Local lymph node assay - validation, conduct and use in practice. *Food Chem. Toxicol.* **40**, 593–598 (2002).

101. Kimber, I., Dearman, R. J., Basketter, D. A., Ryan, C. A. & Gerberick, G. F. The local lymph node assay: past, present and future. *Contact Derm.* **47**, 315–328 (2002).

102. Ahlfors, S. R., Sterner, O. & Hansson, C. Reactivity of Contact Allergenic Haptens to Amino Acid Residues in a Model Carrier Peptide, and Characterization of Formed Peptide-Hapten Adducts¹ *Skin Pharmacology and Physiology* **16**, 59–68 (2003).

103. Ashikaga, T., Hoya, M., Itagaki, H., Katsumura, Y. & Aiba, S. Evaluation of CD86 expression and MHC class II molecule internalization in THP-1 human monocyte cells as predictive endpoints for contact sensitizers. *Toxicology in Vitro* **16**, 711–716 (2002).

104. Yoshida, Y., Sakaguchi, H., Ito, Y., Okuda, M. & Suzuki, H. Evaluation of the skin sensitization potential of chemicals using expression of co-stimulatory molecules, CD54 and CD86, on the naive THP-1 cell line. *Toxicol In Vitro* **17**, 221–228 (2003).

105. Ashikaga, T. *et al.* Development of an in vitro skin sensitization test using human cell lines: The human Cell Line Activation Test (h-CLAT): I. Optimization of the h-CLAT protocol. *Toxicology in Vitro* **20**, 767–773 (2006).

106. Sakaguchi, H. *et al.* Development of an in vitro skin sensitization test using human cell lines; human Cell Line Activation Test (h-CLAT) II. An inter-laboratory study of the h-CLAT. *Toxicology in Vitro* **20**, 774–784 (2006).

107. Sakaguchi, H., Miyazawa, M., Yoshida, Y., Ito, Y. & Suzuki, H. Prediction of preservative sensitization potential using surface marker CD86 and/or CD54 expression on human cell line, THP-1. *Arch. Dermatol. Res.* **298**, 427–437 (2007).

108. Ashikaga, T. *et al.* A comparative evaluation of in vitro skin sensitisation tests: the human cell-line activation test (h-CLAT) versus the local lymph node assay (LLNA). *Altern Lab Anim* **38**, 275–284 (2010).

109. Mitjans, M. *et al.* Use of IL-8 release and p38 MAPK activation in THP-1 cells to identify allergens and to assess their potency in vitro. *Toxicol In Vitro* **24**, 1803–1809 (2010).

110. Mitjans, M. *et al.* Role of p38 MAPK in the selective release of IL-8 induced by chemical allergen in naive THp-1 cells. *Toxicol In Vitro* **22**, 386–395 (2008).

111. Mukaida, N., Okamoto, S., Ishikawa, Y. & Matsushima, K. Molecular mechanism of interleukin-8 gene expression. *Journal of Leukocyte Biology* **56**, 554–558 (1994).

112. Goebeler, M. *et al.* Differential and sequential expression of multiple chemokines during elicitation of allergic contact hypersensitivity. *Am. J. Pathol.* **158**, 431–440 (2001).

113. Weber, F. C. *et al.* Neutrophils are required for both the sensitization and elicitation phase of contact hypersensitivity. *J Exp Med* **212**, 15–22 (2015).

114. Delaine, T., Hagvall, L., Rudbäck, J., Luthman, K. & Karlberg, A.-T. Skin Sensitization of Epoxyaldehydes: Importance of Conjugation. *Chem. Res. Toxicol.* **26**, 674–684 (2013).

115. Chipinda, I. *et al.* Rapid and simple kinetics screening assay for electrophilic dermal sensitizers using nitrobenzenethiol. *Chem. Res. Toxicol.* **23**, 918–925 (2010).

116. Mbiya, W., Chipinda, I., Siegel, P. D., Mhike, M. & Simoyi, R. H. Substituent Effects on the Reactivity of Benzoquinone Derivatives with Thiols. *Chem. Res. Toxicol.* **26**, 112–123 (2013).

117. Chipinda, I. *et al.* Pyridoxylamine reactivity kinetics as an amine based nucleophile for screening electrophilic dermal sensitizers. *Toxicology* **315**, 102–109 (2014).

118. McKinney, J. D., Richard, A., Waller, C., Newman, M. C. & Gerberick, F. The Practice of Structure Activity Relationships (SAR) in Toxicology. *Toxicol Sci* **56**, 8–17 (2000).

119. Yoo, E. *et al.* Structure–activity relationships in Toll-like receptor 7 agonistic 1 H - imidazo[4,5- c]pyridines. *Organic & Biomolecular Chemistry* **11**, 6526–6545 (2013).

120. Gholivand, K., Ebrahimi Valmoozi, A. A., Mahzouni, H. R., Ghadimi, S. & Rahimi, R. Molecular Docking and QSAR Studies: Noncovalent Interaction between Acephate Analogous and the Receptor Site of Human Acetylcholinesterase. *Journal of Agricultural and Food Chemistry* **61**, 6776–6785 (2013).

121. Ashby, J., Basketter, D. A., Paton, D. & Kimber, I. Structure activity relationships in skin sensitization using the murine local lymph node assay. *Toxicology* **103**, 177–194 (1995).

122. Larsen, S. T. & Nielsen, G. D. Structure-activity relationship of immunostimulatory effects of phthalates. *BMC Immunology* **9**, 61 (2008).

123. Braeuning, C., Braeuning, A., Mielke, H., Holzwarth, A. & Peiser, M. Evaluation and improvement of QSAR predictions of skin sensitization for pesticides. *SAR and QSAR in Environmental Research* **29**, 823–846 (2018).

124. Walsh, C. T., Garneau-Tsodikova, S. & Gatto, G. J. Protein posttranslational modifications: the chemistry of proteome diversifications. *Angew. Chem. Int. Ed. Engl.* **44**, 7342–7372 (2005).

125. Donald Voet. *Fundamentals of biochemistry*. (Wiley, 2006).

126. Rana, A. K. & Ankri, S. Reviving the RNA World: An Insight into the Appearance of RNA Methyltransferases. *Front Genet* **7**, (2016).

127. Glozak, M. A., Sengupta, N., Zhang, X. & Seto, E. Acetylation and deacetylation of non-histone proteins. *Gene* **363**, 15–23 (2005).

128. Wang, C. *et al.* Direct acetylation of the estrogen receptor alpha hinge region by p300 regulates transactivation and hormone sensitivity. *J. Biol. Chem.* **276**, 18375–18383 (2001).

129. Krauss, G. *Biochemistry of Signal Transduction and Regulation*. (John Wiley & Sons, 2014).

130. Bonora, M. *et al.* ATP synthesis and storage. *Purinergic Signal* **8**, 343–357 (2012).

131. Cohen, P. The origins of protein phosphorylation. *Nat Cell Biol* **4**, E127–E130 (2002).

132. Suet Ting Tan, R. *et al.* The synergy in cytokine production through MyD88-TRIF pathways is co-ordinated with ERK phosphorylation in macrophages. *Immunol. Cell Biol.* **91**, 377–387 (2013).

133. Bode, A. M. & Dong, Z. Post-translational modification of p53 in tumorigenesis. *Nat Rev Cancer* **4**, 793–805 (2004).

134. Robinson, J. W., Frame, E. S., Ii, G. M. F., Frame, E. S. & Ii, G. M. F. *Undergraduate Instrumental Analysis*. (CRC Press, 2014). doi:10.1201/b15921.

135. El-Aneed, A., Cohen, A. & Banoub, J. Mass Spectrometry, Review of the Basics: Electrospray, MALDI, and Commonly Used Mass Analyzers. *Applied Spectroscopy Reviews* **44**, 210–230 (2009).

136. Gross, J. H. *Mass Spectrometry: A Textbook*. (Springer, 2017).

137. Chen, G., Pramanik, B. N., Bartner, P. L., Saksena, A. K. & Gross, M. L. Multiple-stage mass spectrometric analysis of complex oligosaccharide antibiotics (everninomicins) in a quadrupole ion trap. *J. Am. Soc. Spectrom.* **13**, 1313–1321 (2002).

138. Singhal, N., Kumar, M., Kanaujia, P. K. & Virdi, J. S. MALDI-TOF mass spectrometry: an emerging technology for microbial identification and diagnosis. *Front Microbiol* **6**, (2015).

139. Domon, B. & Aebersold, R. Mass spectrometry and protein analysis. *Science* **312**, 212–217 (2006).

140. Han, X., Aslanian, A. & Yates, J. R. Mass Spectrometry for Proteomics. *Curr Opin Chem Biol* **12**, 483–490 (2008).

141. Shi, S. D. *et al.* Phosphopeptide/phosphoprotein mapping by electron capture dissociation mass spectrometry. *Anal. Chem.* **73**, 19–22 (2001).

142. Shukla, null & Futrell, null. Tandem mass spectrometry: dissociation of ions by collisional activation. *J Mass Spectrom* **35**, 1069–1090 (2000).

143. Issaq, H. J., Chan, K. C., Janini, G. M., Conrads, T. P. & Veenstra, T. D. Multidimensional separation of peptides for effective proteomic analysis. *J. Chromatogr. B Analyt. Technol. Biomed. Life Sci.* **817**, 35–47 (2005).

144. Yates, J. R. Mass spectral analysis in proteomics. *Annu Rev Biophys Biomol Struct* **33**, 297–316 (2004).

CHAPTER II

REVEALING A CORRELATION BETWEEN SENSITIZATION POTENTIAL AND REACTIVITY OF DNCB AND ITS ANALOGS

2.1 Summary

Elucidation of contact hypersensitivity reaction has been a long-standing goal; nevertheless, the physicochemical properties of contact allergens have been overlooked. This chapter reports a study that seeks to find a correlation between the overall sensitization potential and the chemical structure of a contact allergen, 1-chloro-2,4-dinitrobenzene (DNCB). Based on DNCB's reaction mechanism (Section 1.8), we chose a set of test compounds with variation in leaving groups and the electron-withdrawing groups. The DNCB derivatives were characterized with the following assays: (i) cell-based assay screening their potential to induce IL-8 response, (ii) the rate of reactivity to cysteine, (iii) murine model of contact hypersensitivity testing induction of subsequent inflammation in vivo, and (iv) western blotting for protein binding in cells. These experiments showed a non-linear correlation between the rate of reaction and biological activity. These results indicate that there is a balance of stability and reactivity that dictates a contact allergen's ability to induce the sensitization phase.

2.2 Introduction

As mentioned in Chapter 1 (Section 1.6-1.8), contact allergens can contact skin and induce contact hypersensitivity. The pathology of contact hypersensitivity still lacks details as to the reactivity of contact allergens with self-proteins.[1,2] The physicochemical properties of the contact

allergens that dictate protein binding include reactivity, spatial geometry, and steric restraints.[3,4] There have been multiple studies highlighting the relationship between chemical reactivity and an external sensitization index such as local lymph node assay (LLNA).[5–8] However, limited studies encompass both the structural and electronic requirements of reactivity, with a direct comparison to *in vivo* and *in vitro* activity. DNCB is a widely-used reference molecule in sensitization models probing pathways and cell types involved in the sensitization pathway.[9–11] Here, I am to investigate the specific structural requirements for the high sensitization potential of DNCB using a two-prolonged strategy encompassing a cell-based assay and examination of parameters defining chemical reactivity (**Figure 2.1**).

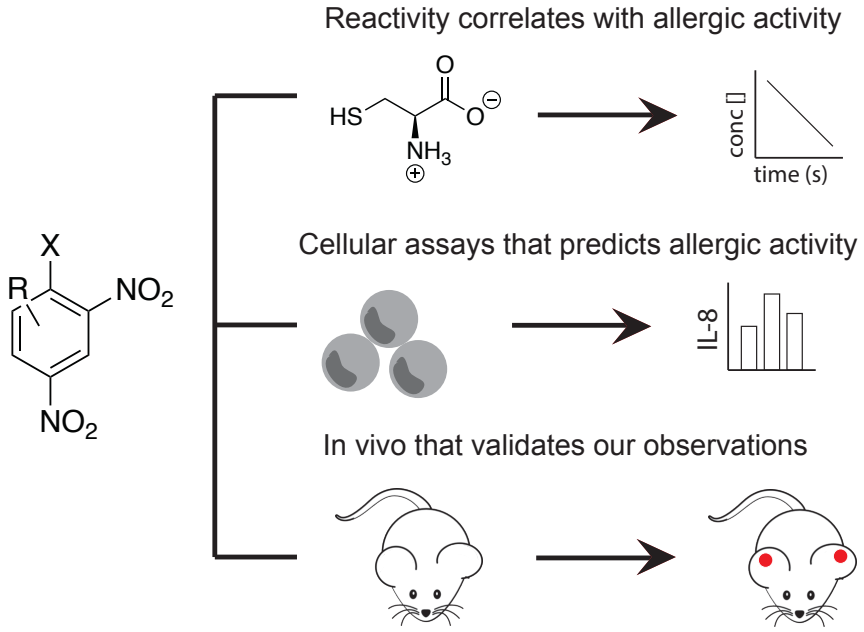

Figure 2.1 Schematics describing the workflow. Derivatives of DNCB varying in leaving group and electron-withdrawing groups were selected. The sensitization potential of DNCB's derivatives was measured following three methods above: (i) rate of reactivity to cysteine, (ii) potency to induce IL-8 response in THP-1 monocytes, and (iii) potency to induce ear inflammation in an animal model.

DNCB is hypothesized to form covalent bonds through a nucleophilic substitution mechanism with nucleophilic residues of proteins. What intrigued us was that despite the widespread use of DNCB both in cell and in animals as a model of hypersensitivity, very little work examines the mechanism of DNCB and its analogs. Thus, this work sought to establish a work that correlates the reactivity of DNCB and its analogs and the allergic response in biological models such as human cell and murine models. Historically, identification of contact allergens was done by guinea pig testing.[12–15] However, in the past decades, the field has moved to LLNA[16–18] and the cell-based assays.[19–21] These cell-based assays, notably the activation of cultured THP-1 cells, minimize animal usage and are translatable to humans.[19]

This chapter report that the rate of reactivity as well as steric elements contribute to a contact allergen's ability to stimulate IL-8 production in target human THP-1 cells and ultimately elicit hypersensitivity *in vivo*. However, this relationship is not linear. The experiments reported in this chapter also demonstrate that non-allergenic compounds can be made to elicit contact hypersensitivity by controlling their rate of reaction.

2.3 Material and Methods

2.3.1 Cell culture

Human monocyte cell line THP-1 was obtained from American Type Culture Collection (ATCC, Manassas, VA) and grown in Roswell Park Memorial Institute (RPMI) 1640 medium (Life Technologies, Carlsbad, CA) supplemented 10 % with Fetal Bovine Serum (FBS, Thermo Fisher Scientific, Waltham, MA) and 1 % antibiotic-antimycotic (Thermo Fisher Scientific) at 37 ^{O}C in 5 % CO_2 incubator. Cells were passed every 3-4 days and plated at a density of 5 x 10^5 cells/mL.

2.3.2 Assessment of Released IL-8 level

The release of IL-8 level was measured by two methods: intracellular cytokine staining and ELISA. They are both commonly used methods for analyzing released cytokine, thus most studies use only one of the two. However, both methods were used in this study to quantitative and qualitative measure the release of cytokine by DNCB and its structural derivatives. For both methods, THP-1 cells were used. The concentration of test compounds and the cell types remained the same. To briefly summarize, test compounds were first dissolved in DMSO (Molecular Biology Grade, Sigma Aldrich, St. Louis, MO) to make 0.5 M or 1 M stock solution and sterile-filtered using 0.22 µm syringe filters. The stock solutions were diluted to 50 µM in regular cell culture medium (10 % FBS in RPMI). Approximately 10^6 THP-1 cells were seeded in a 24-well plate at the concentration of 10^6 cells/ml with diluted compounds. As a positive control for immune response, 200 ng/ml lipopolysaccharide (LPS) diluted in the cell culture medium was used. All experiments were done in triplicate and repeated three times.

Intracellular Cytokine Staining:

Cytofix/Cytoperm™ kit with GolgiPlug™ was purchased from BD Biosciences (San Jose, CA). The experiment was performed according to the manufacturer's recommended protocol with minor changes. First, THP-1 cells were incubated with 1 µl of GolgiPlug™ (containing Brefeldin A). After incubation in 37 ^{O}C with 5 % CO_2 for 10 h, the cells were harvested, washed with 3 x 300 µl FACS Buffer (5 % FBS, 1 mM EDTA in PBS). Cell pellets were resuspended in 200 µl of fixing buffer (Cytofix/Cytoperm™ solution containing 4 % para-formaldehyde, BD Biosciences) and incubated in ice for 20 min. After washing with 3 x 300 µl of washing buffer (1X Perm/Wash™ Buffer, BD Biosciences), the cells were resuspended in 50 µl of 10X BD Perm/Wash™ Buffer. For antibody staining, 5 µl of FITC anti-human IL-8 antibody (BioLegend, San Diego, CA) was

added to each sample and vortexed. After 30 min incubation in ice with rigorous vortexing at the halfway mark, the samples were analyzed using the BD Accuri C6 cytometer and BD Accuri C6 software.

ELISA:

Human IL-8 ELISA MAX™ Deluxe was purchased from BioLegend and performed according to the recommended protocol. Cells were incubated with 50 μM test compounds for 20 h. Supernatant was collected for analysis and cell pellets were subjected to MTT assays.

2.3.3 MTT Assay

To ensure that test compounds were not cytotoxic to the cells, MTT assay was performed. I followed a previously published protocol.[22] After THP-1 cells were incubated with test compounds for ELISA, collected cell pellets were resuspended in 1 ml of RPMI medium without phenol red supplemented 10 % with FBS. Using a micropipette, 100 μl of cell suspension was plated in 96-well plate in triplicate. MTT reagent (Invitrogen) was dissolved in PBS to make 5 mg/ml solution, sterile filtered, and 10 μl was added to each well. The plate was incubated at 37 ^{O}C for 1 h or until purple crystals were visible. The supernatant was removed, purple crystals were dissolved in DMSO, then absorbance was measured at 580 nm.

2.3.4 General Protocol for Rate Analysis

The compounds of interest were dissolved in 10 % CH_3CN in PBS (1 mM, 1 mL). The reaction was initiated by adding 100 μl of cysteine (10 equiv., 10 mM) in PBS to the fully dissolved compounds. At each time point, 10 μl aliquots of solution were quenched with 0.1 % trifluoroacetic acid (TFA) and the content was analyzed by high-performance liquid chromatography (HPLC).

The area under the curves, the compound curve, and compound-cysteine curve, were calculated and used to generate pseudo first-order rate.

2.3.5 Murine Model of Contact Hypersensitivity

This experiment was performed according to literature protocols with minor modifications.[23] For this experiment, male Balb/c mice aged 6-8 weeks old were obtained from Jackson Laboratory. DNCB and its derivatives were dissolved in 4:1 acetone/olive oil mixture to make a 0.5 % w/v solution. The mice were sensitized with 25 µl of test compounds in the shaven abdomen for the first two days (day 0 and 1). On days 5, 6, 7, and 8, the mice were challenged on the dorsum of both ears with 10 µl of 0.3 % (w/v) solutions of test compounds. Ear thickness was measured 24 h after the last compound exposure using a digital micrometer. For negative control, a group of mice was sensitized and challenged with solvent only. All animal studies and mice maintenance were approved by the Institutional of Animal Care and Use (IACUC #2012-3048).

2.3.6 Compound-BSA Conjugation and Western Blot Analysis

First, we confirmed that the anti-DNP antibody can detect DNP-modified proteins with bovine serum albumin (BSA, Millipore Sigma). BSA and test proteins were dissolved in 17:3 (v/v) 1X PBS: CH_3CN (HPLC grade) mixture and incubated at 37 ^{O}C for 7 days. To ensure conjugation, 10 µl of the sample was desalted and subjected to MALDI-TOF. Conjugated samples were then analyzed by western blotting with anti-DNP antibody to confirm its performance.

Western blotting was performed according to previously published protocol with minor changes.[24–26] THP-1 monocytes were incubated in RPMI supplemented 10 % FBS and 50 µM of test compounds. After 30 min incubation at 37 ^{O}C, cells were lysed with 1X cell lysis buffer (50

mM Tris-HCl pH 8.0, 150 mM NaCl, 1 % Triton X-100) with 1 tablet of protease inhibitor cocktail. Cell lysates were quantified using BCA protein assay kit. For western blotting, cell lysates were first separated by 4-15 % Mini-Protean® TGX^{TM} Precast Protein Gels. Then, separated proteins were tank-transferred to PVDF membrane overnight at 4 ^{O}C, primarily stained with mouse DNP antibody (Millipore) 1 h rt, and secondary stained with goat anti-mouse IgG (H+L) Secondary Antibody, DyLight 650. The membrane was imaged using Azure c600 Imaging System (Azure Biosystem).

To ensure that an equal amount of protein was loaded in each lane, another gel was run using the same amount of cell lysates used for western blotting. Separated gel was fixed in gel-fixing solution (50 % ethanol, 10 % acetic acid in water) for 1 h, washed in gel-washing solution (50 % methanol, 10 % acetic acid in water) overnight, stained in Coomassie solution (0.1 % Coomassie blue R350, 20 % methanol, 10 % acetic acid in water) for 3 h, and de-stained with gel-washing solution until the desired color and band intensity appeared. Band intensity was calculated using ImageJ and normalized to the band intensity of the DNCB-treated sample.

2.4 Results

The sensitization potential of DNCB has been known since the 1930s, with the series of papers detailing sensitization potential of DNCB and structurally-similar compounds measured by guinea pig testing.[15,27–29] Since then, there have been many reports studying the effects of electrophilicity of contact allergens on sensitization potential.[30–35] Based on these earlier reports, I designed a series of derivatives of DNCB to investigate the relationships encompassing immunological activity to chemical reactivity and electrophilicity. DNCB is known to undergo an S_NAr reaction, which involves the addition of a nucleophilic functional group to an aromatic ring. For this reaction

to occur successfully, the quality of electronegative leaving groups, as well as the electron-withdrawing groups para and ortho positions, are crucial. Thus, I designed a series of experiments that examined those qualities, both the ability of the compounds to elicit an immune response as well as the ability to react with nucleophilic amino acids.

2.4.1 Exploration of Quality of Leaving Group

Working from the previous report by Landsteiner in 1935,[27] the effect of the quality of leaving group of the aromatic compounds was tested (**Figure 2.2**). Skin sensitization of the derivatives of DNCB was evaluated by measuring the release of IL-8 from stimulated THP-1 cells, as it is a commonly used platform for a cell-based sensitization assay. THP-1 cells were incubated with the compounds at the concentration of 50 μM, which was the optimal condition for IL-8 production (**Figure A2**). Released IL-8 level was examined through either ELISA or intracellular cytokine staining. Broadly, the percentage of IL-8 expression decreased as the electronegative of the leaving group halides decreased (**Figure 2.2A**). Interestingly, the difference in IL-8 expression between dinitrofluorobenzene (–F) and DNCB was not significant. This could be due to the high reactivity of DNFB, which could result in loss of activity through hydrolysis. The percentage of IL-8 expressing cells for dinitrophenol (–OH) was 3.78 %, which was in level with that of resting (**Figure 2.2B**), and it suggested a total loss of immune activity. Alcohol is not a good leaving group, poorly reacting via nucleophilic addition mechanism. To explore further, the chemical structure of DNP was modified with tosyl (–OTs) and mesyl (–OMs) groups, which are both good leaving groups, to create DNP-based derivatives capable of reacting. Both derivatives activated THP-1 cells, resulting in IL-8 level comparable to or higher than that of DNCB. Interestingly, the mesyl (–OMs) group resulted in higher activity than the tosyl (–OTs) group and the parent

compound. It implies an additive positive effect of having a small and unhindered leaving group. Altogether, this result confirmed that the leaving group is necessary for the immune response.

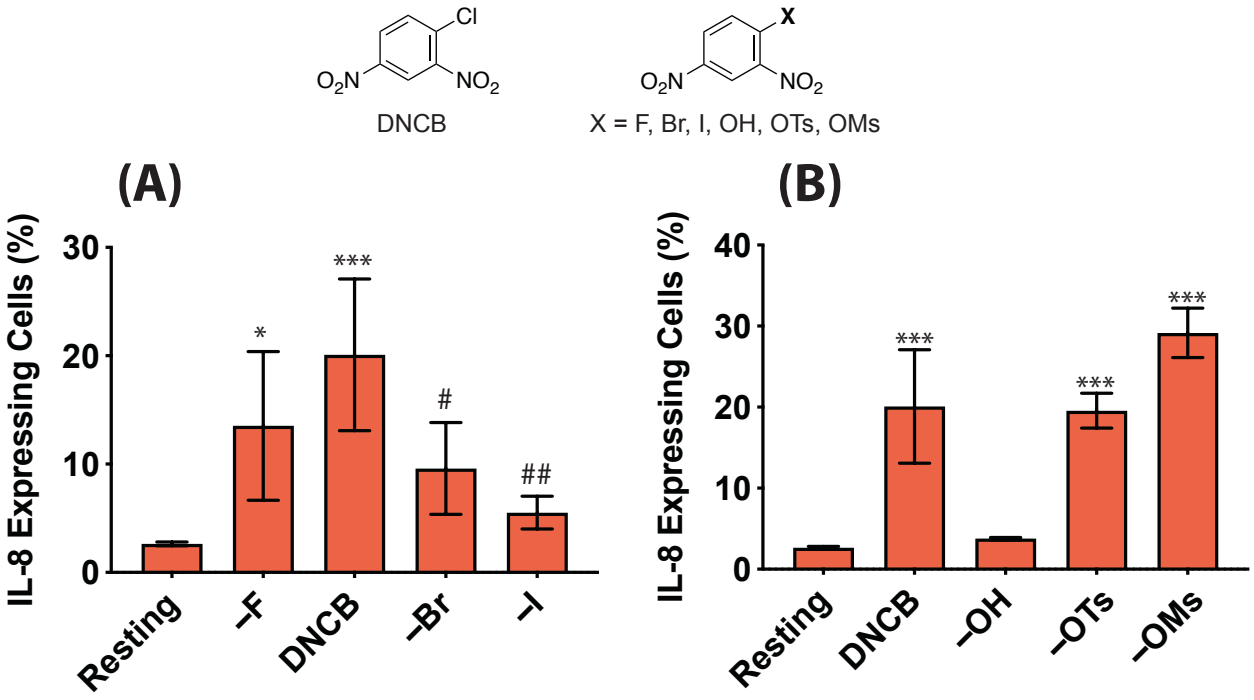

Figure 2.2 IL-8 response from different leaving groups. After THP-1 cells were incubated with 50 μM of the test compounds for 10 h with Brefeldin A treatment, they were intracellularly stained for IL-8 proteins. The percentage of IL-8 expressing cells was measured with a flow cytometer. **(A)** The effect of leaving group halides. IL-8 level reduced for decreasing electronegativity. **(B)** The effect of non-halide leaving groups. The tosyl and mesyl restored the IL-8 response, suggesting that non-sensitizers can be made to elicit sensitization potential. *$p \leq 0.05$ ***$p \leq 0.0005$ significance to resting, #$p \leq 0.05$ ##$p \leq 0.005$ significance to DNCB.

2.4.2 Exploration of Quality of Electron-Withdrawing Groups

Next, the quality of electron-withdrawing substituents was tested as the leaving group experiments indicated the S_NAr mechanism. One important element of the S_NAr reaction is the

ability to correlate reactivity with the electron density at the point of reaction in a molecule.[36,37] To test this hypothesis, I chose substituents with varying electron-withdrawing capabilities,[37] including cyano (–CN), carboxylic acid (–COOH), and a methyl ester (–COOMe) at the *para* and *ortho* positions relative to the leaving group (**Figure 2.3**). Using the same experimental procedure as above, the percent IL-8 expressing cells was examined. As expected, there was a decreasing trend of IL-8 production as the compounds assayed were more electron-rich than DNCB (**Figure 2.3A**). Although the electron-withdrawing capability of a carboxylic acid and a methyl ester were similar, the IL-8 response of carboxylic acids and methyl esters were different. Whereas the percent IL-8 expressing cells of carboxylic acids were 1.82 % and 1.52 % which were in level with that of resting, the responses of methyl esters were 2.30 % and 2.24 % which were slightly higher and elicited statistically significant compared to that of resting. One possible reason for this could be that carboxylic acids have pKa of ~5, thus they were deprotonated at the physiological pH. The negative charge on carboxylic acid might be interfering with the compound's interaction with proteins. Other than that, the percent IL-8 expressing cells of cyano derivatives was 5.00 % and 5.63 %, which were above-resting but still not comparable to that of DNCB. The results here suggest that DNCB-based scaffolds require substituents with electron-withdrawing capabilities comparable to the nitro group at the *para* and *ortho* positions. With that in mind, I sought to elucidate the effect of increasing the number of electron-withdrawing groups – balancing it with the activity of steric interactions with potential target proteins. To do so, derivatives with additional electron-withdrawing groups were synthesized. These derivatives included two nitro groups and extra carboxylic acid or ester groups (**Figure 2.3B**). Using the same experimental procedure, the IL-8 levels of the derivatives were determined. The IL-8 response of 4-chloro-3,5-dinitrobenzoic acid (4–COOH) was 15.4 %, which was comparable to that of DNCB. On the other hand, other

derivatives did not show IL-8 level comparable to DNCB, implying that steric and potentially charge density were also critical factors to skin sensitization potential. The results altogether demonstrate the cumulative effect of the electron-withdrawing groups in DNCB-based compounds.

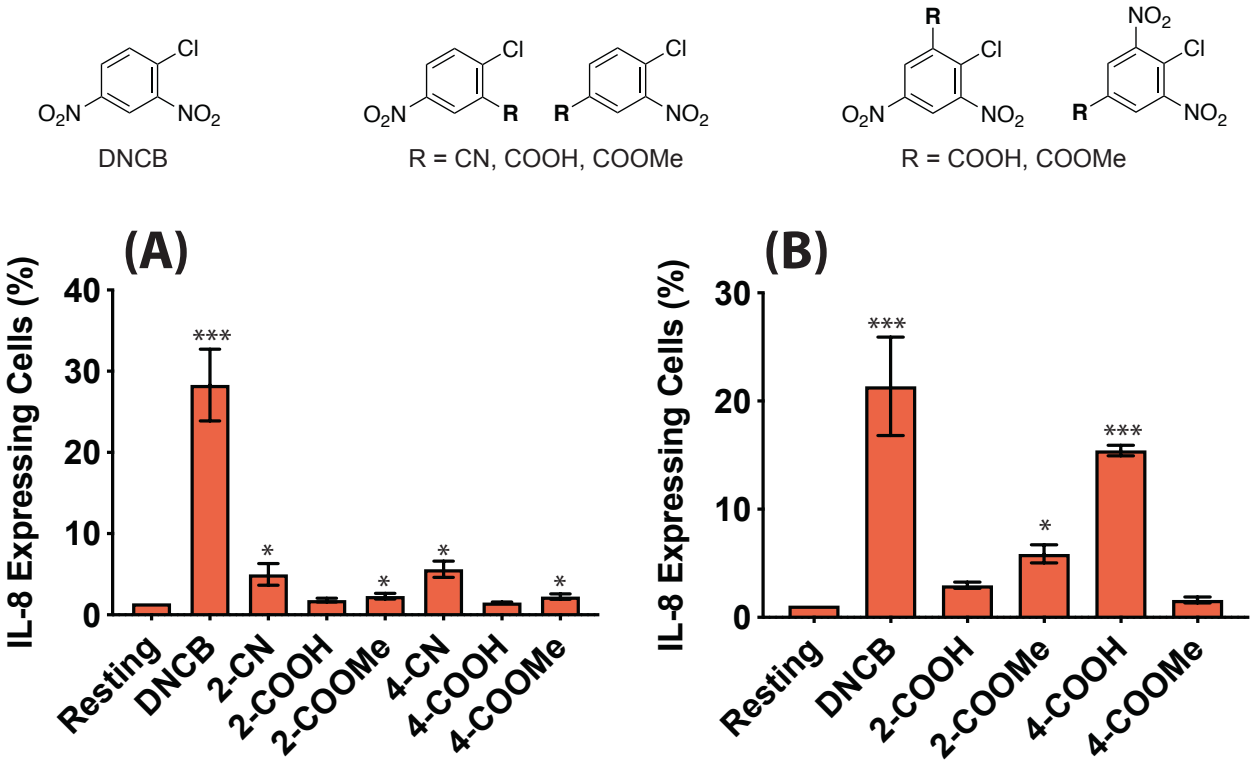

Figure 2.3 The quality of electron-withdrawing groups was explored. After THP-1 cells were incubated with 50 μM of the test compounds for 10 h with Brefeldin A treatment, they were intracellularly stained for IL-8 proteins. The percentage of IL-8 expressing cells was measured with a flow cytometer. **(A)** IL-8 level elicited by THP-1 cells treated with electron-withdrawing group derivatives. A series of electron-withdrawing groups were substituted in place of the nitro group. None of the derivatives elicited IL-8 response comparable to that of DNCB. **(B)** IL-8 level elicited by THP-1 cells treated with additive electron-withdrawing group derivatives. Ester and carboxylic acid groups were added to dinitrochlorobenzene compound. IL-8 level of 4–COOH was comparable to that of DNCB. *$p \leq 0.05$, ***$p \leq 0.0005$, significance to resting.

To investigate the effects of steric and charge density, more ester derivatives were synthesized and assayed (**Figure 2.4**). The hexyl and *tert*-butyl introduce bulkier ester groups to DNCB scaffolds. Derivatives with *tert*-butyl groups elicited higher IL-8 response compared to that of hexyl derivatives. However, none of the derivatives demonstrated IL-8 response comparable to that of DNCB. The IL-8 response for *ortho* substituents were above resting in contrast to that of *para* substituents. This suggests the nitro groups at both the ortho and para positions are important to elicit IL-8 response.

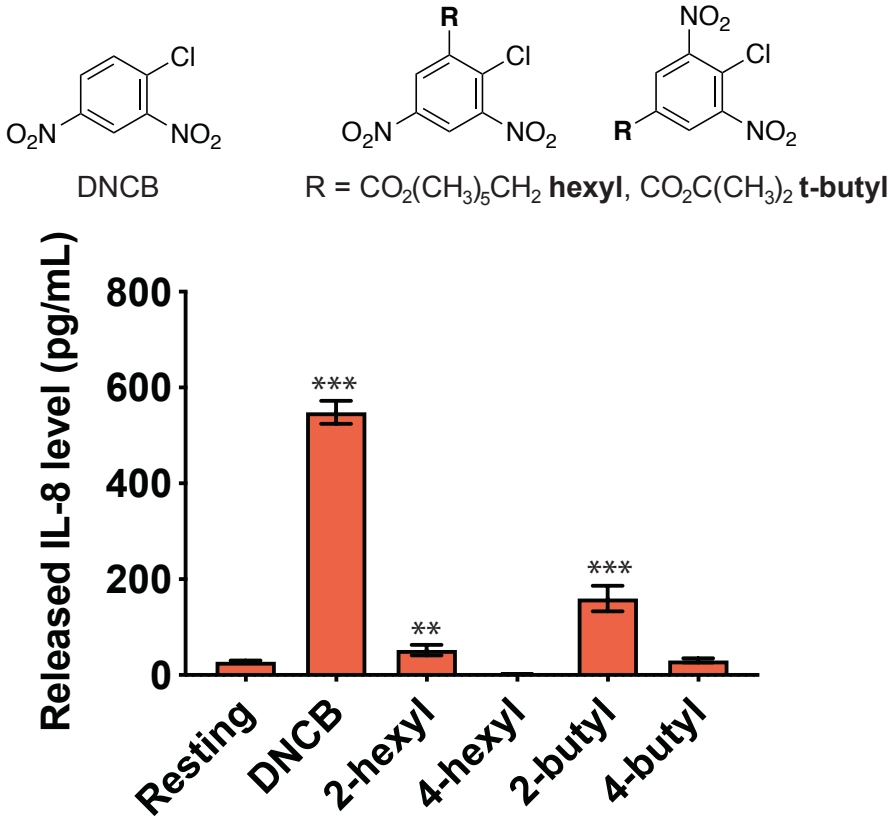

Figure 2.4 Exploration of steric effect with substituent ester derivatives. After THP-1 cells were incubated with 50 μM of the test compounds for 20 h, the supernatant was collected for quantification with human IL-8 ELISA. None of the derivatives showed IL-8 response in level with DNCB. **p ≤ 0.005, ***p ≤ 0.0005, significance to resting.

2.4.3 Contact Hypersensitivity of DNCB Derivatives

Observing such a clear IL-8 response from DNCB-based derivatives, I sought to investigate if the results would translate into a mouse model using a well-established murine contact hypersensitivity.[23,38,39] In this experiment, male Balb/c mice between 6-8 weeks of age are sensitized with test compounds for 2 consecutive days. After a rest period, the mice are challenged on the ear dorsum for five consecutive days, followed by ear thickness measurement 24 h after the last exposure (**Figure 2.5A**). The rest period between the sensitization and challenge phase adequately represents the delayed-type contact hypersensitivity, thus this experiment predicts the chemical sensitizer's ability to elicit clinically apparent symptoms. To minimize the use of animals and to obtain the best result, the compounds that showed comparable IL-8 response to DNCB's, which were the tosyl (–OTs) and 4-chloro-3,5-dinitrobenzoic acid (4-DNCBA or 4–COOH from Figure 2.3B), were chosen. Before the challenge, the average ear thickness was approximately 0.32 mm, which was about the same throughout the entire groups. After the challenge, DNCB- and 4-DNCBA-treated groups showed redness and swelling in the ear, which were notable signs of ear inflammation. The ear thickness of 4-DNCBA-treated mice was 0.391 mm on average, which was at a comparable level with that of DNCB-treated mice, 0.378 mm. Despite inflammation was expected from the tosyl-treated group as it showed comparable IL-8 response, the ear thickness turned out to be 0.311 mm, showing no change at all (**Figure 2.5B**). One possible reason for this is that tosyl was unable to cause sensitization and elicitation due to its inability to penetrate the skin barrier. To test this hypothesis, tosyl was dissolved in DMSO, the solvent that could enhance skin penetration. In this case, the tosyl-treated group showed inflammation that was statistically significant and in level with that of the DNCB-treated group, confirming our hypothesis (**Figure 2.5C**).

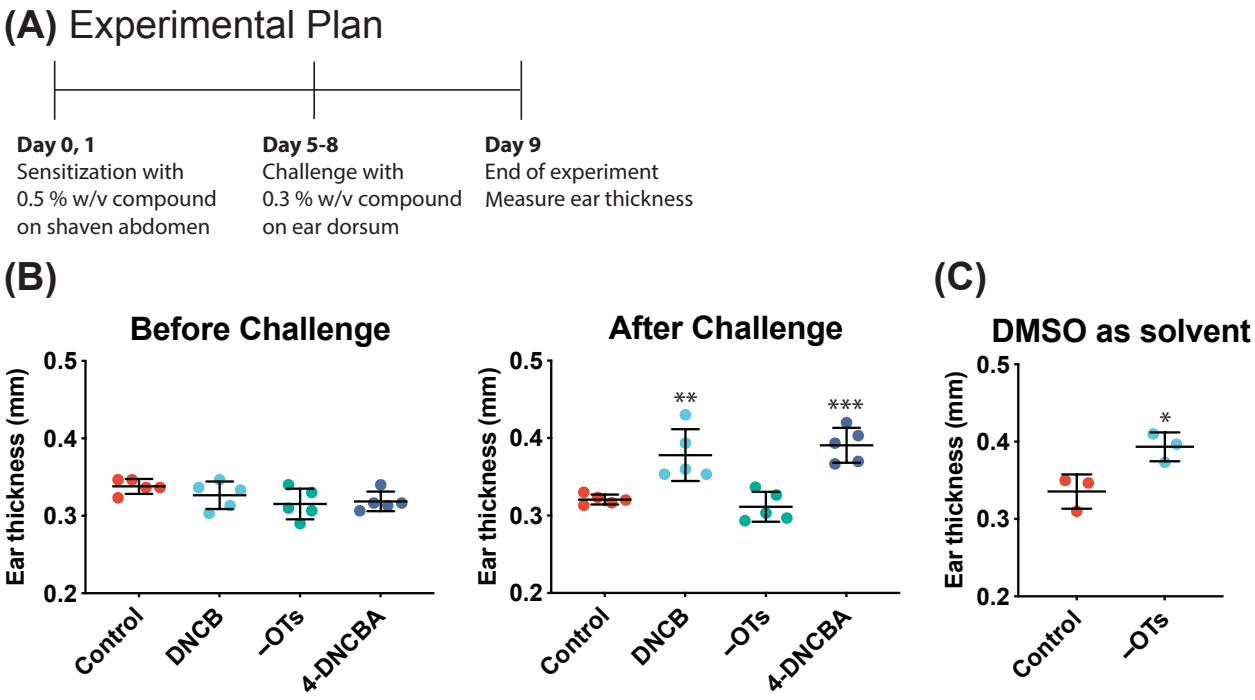

Figure 2.5 *In vivo* contact hypersensitivity model. **(A)** The experimental timeline for animal study. Test compounds were dissolved in 1:4 v/v olive oil and acetone to make 0.5 % w/v solution and applied on the shaven abdomen of Balb/c mice for 3 consecutive days. After 2 days of rest, the mice were challenged in the dorsum of both ears with tested compounds at the same concentration for 4 days. **(B)** The ear thickness was measured before challenge (left) and 24 h post-challenge (right). Change in ear thickness shows the manifestation of contact hypersensitivity. **(C)** The experiment was repeated with 5 % w/v tosyl solution in DMSO. It shows that DMSO enhances skin penetration, and chemical compounds can be fabricated to elicit contact hypersensitivity. *p $\leq$ 0.05, **p $\leq$ 0.005, *** p $\leq$ 0.0005, significance to control.

2.4.4 Correlation of Sensitization Potential to Rate of Reactivity

Observing such clear relationships between the molecular structure and overall immune response, I sought to examine the process of chemical binding by comparing the chemical reactivity of these compounds to the biological activity. To examine the rate of reactivity of

compound-protein binding, I first needed a simpler reaction setup that can reflect such process. One of the methods of contact allergen identification is the direct peptide reactivity assay, which involves reacting test compounds with cysteine at the physiological pH. The formation of cysteine adduct is usually accepted as an indication of sensitization. Thus, the test compounds were incubated with cysteine at physiological pH because it is a common proxy for a contact allergen's ability to form haptens.[40] Eight compounds, out of 20 tested for IL-8 response, were chosen for this experiment. The tosyl (–OTs) and 4-chloro-3,5-dinitrobenzoic acid (4-DNCBA or 4–COOH from Figure 2.3B) were chosen for showing comparable IL-8 response to that of DNCB, or as strong sensitizers. 2-cyano-4-nitrochlorobenzene (2–CN), 4-cyano-2-nitrochlorobenzene (4–CN), and methyl 2-chloro-3,5-dinitrobenzoate (2-DNCBE or 2–COOMe from Figure 2.3B) were chosen for moderate sensitizers. The others, methyl 4-chloro-3,5-dinitrobenzoate (4–DNCBE or 4–COOMe from Figure 2.3B) and 2-chloro-3,5-dinitrobenzoic acid (2-DNCBA or 2–COOH from Figure 2.3B), were chosen for weak sensitizers. From this, some type of reactivity vs biological activity trend was expected. However, plotting the log k_{obs} vs. IL-8 response normalized to DNCB, no simple correlation was observed (**Figure 2.6**). Although a linear correlation was not seen, there was a rate of reactivity window where a balance between compound stability and reactivity led to IL-8 expression. High cellular response did not immediately translate to high reactivity. The ester derivatives (4-DNCBE and 2-DNCBE) showed the highest rate of reactivity. These compounds, however, resulted in low IL-8 expression when they were treated with THP-1 cells compared to DNCB. A potential steric hindrance was also observed. The substituted esters (hexyl and *tert*-butyl derivatives) showed a similar rate of reactivity although they were not as potent as DNCB in eliciting IL-8 response. These results, altogether, demonstrate that a balance between the rate of

reactivity and steric hindrance is required for a chemically reactive compound to act as a skin sensitizer.

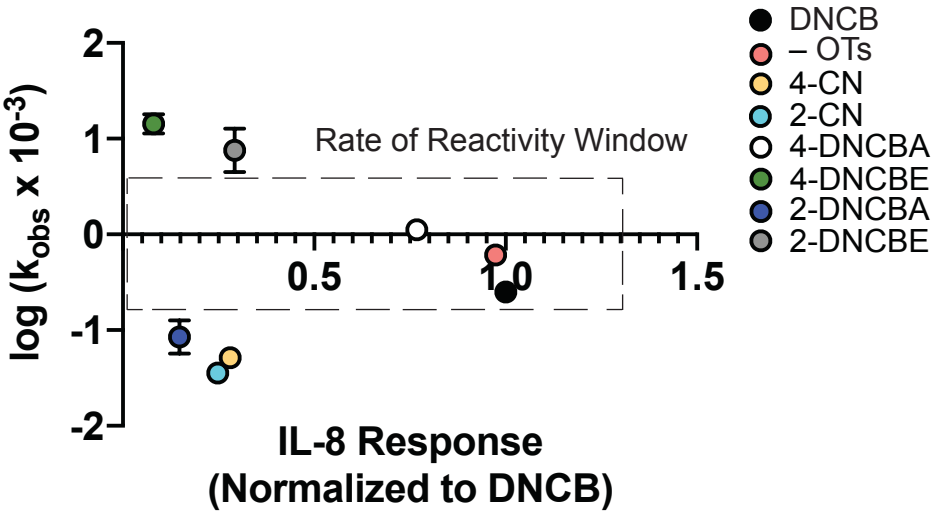

Figure 2.6 Correlation of IL-8 response to the rate of reactivity to cysteine. IL-8 response was normalized to DNCB. The rate of reactivity was measured by reacting test compounds to the solution of cysteine in physiological pH. This reveals that there is no linear correlation between the rate of reactivity to the skin sensitization potential of a compound.

Next, I sought to compare the nucleophilic reactivity of the derivatives at the site of nucleophilic substitution reaction using computer simulation that calculates electrophilicity map. Using a molecular modeling software (Spartan), an electrophilicity map was generated by calculating the molecular orbitals of electrophiles using B3LYP/6-31 + G (d,p) basis set (**Table A1**). This was done by mapping the absolute value of the lowest-unoccupied molecular orbital (LUMO) on the electron density. From the log k_{obs} vs. |LUMO| value plot (**Figure A7**), there was a loose but direct correlation between the experimental and computational reactivity. Also, the |LUMO| value vs. IL-8 activity indicated a similar trend with the experimental plot (**Figure 2.6**)

where there appeared a required balance of reactivity and stability for optimal cellular IL-8 response.

2.4.5 Reactivity of DNCB Derivatives to Cellular Protein

Based on this result, I sought to compare a trend of protein modification by DNCB and its derivatives with western blotting. Hapten formation is considered as the initial step towards the development of contact hypersensitivity.[3] Therefore, DNCB-based derivatives that elicited similar immune response and the rate of reactivity to DNCB, that is the halide derivatives and 4-DNCBA, would bind the same or similar proteins to DNCB. For instance, DNCB undergoes S_NAr mechanism to covalently bind proteins, yielding DNP-modified proteins. THP-1 cells were lysed to yield protein samples after they were incubated with the compounds. After quantification of protein samples with bicinchoninic acid (BCA) assay, the proteins were analyzed by western blotting with anti-DNP antibody, an antibody that binds dinitrophenol (DNP) moieties to provide a signal. DNP moieties do not exist naturally in mammalian cells, thus anti-DNP antibody provides a useful tool for the detection of small molecule's protein targets. The anti-DNP antibody also showed that it can detect DNP-modified proteins by binding DNP-moieties on the proteins (**Figure A6**). For this experiment, the halide derivatives such as dinitroiodobenzene (–I), tosyl (–OTs) and mesyl (–OMs), and the cyano derivatives, 2-CN and 4-CN, were used. Although 4-DNCBA showed promising results in cell, animal, and rate experiments, it could not be used because the anti-DNP antibody could not bind proteins modified by 4-DNCBA. From the western blot, treatment with halide derivatives resulted in a series of gel-staining pattern that was similar to that of DNCB (**Figure 2.7B**), suggesting that similar proteins were modified. The cyano derivatives,

however, showed no modified proteins, indicating that derivatives with low immune response and slow rate of reactivity are slow to modify proteins in cells as well.

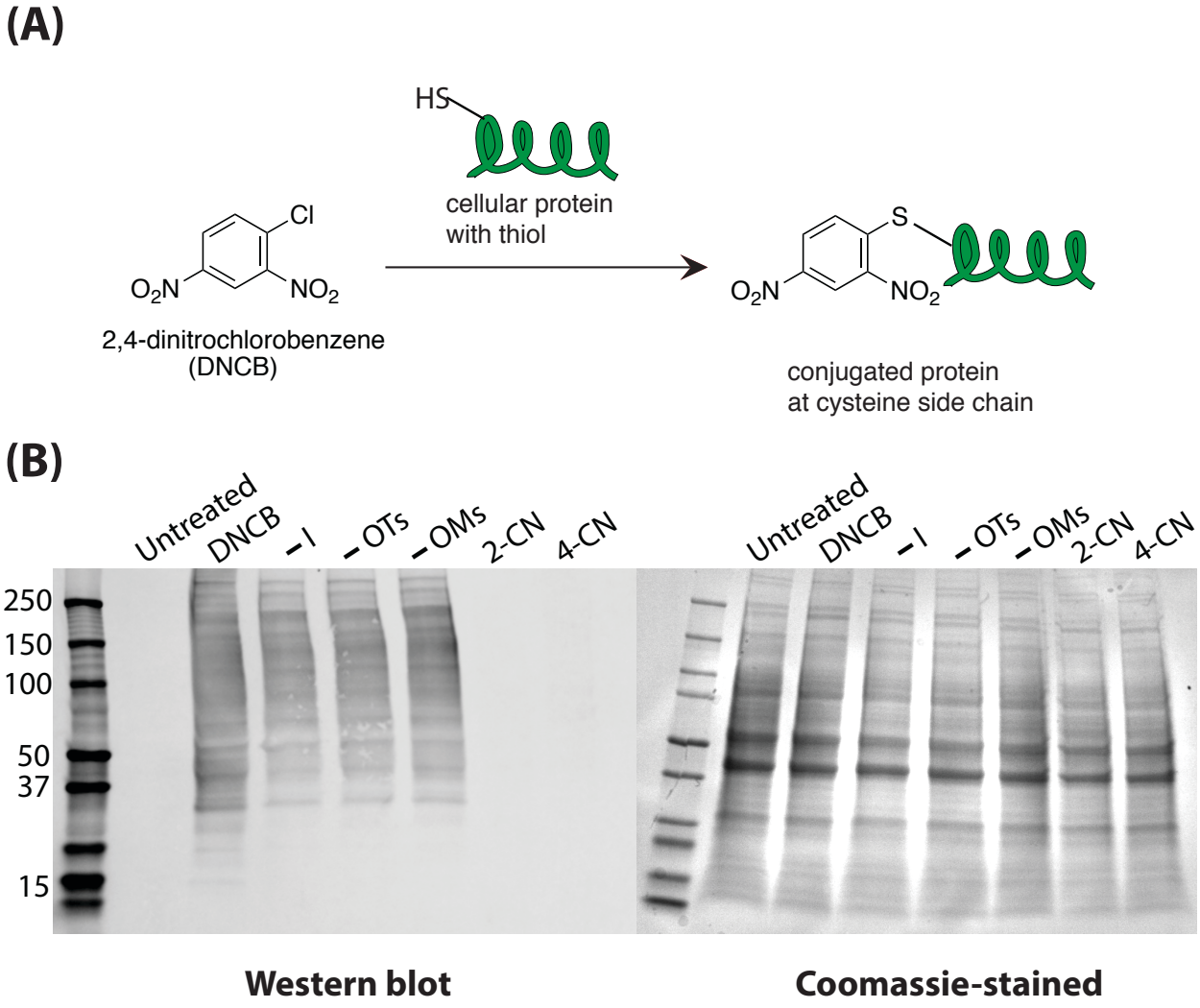

Figure 2.7 Cellular protein modification by DNCB and its derivatives. **(A)** Demonstration of DNCB binding cysteine amino acid residue of a protein. **(B)** THP-1 cells were treated with the labeled compounds and lysed. Modified proteins were analyzed by western blotting (left). To show that an equal amount of proteins were loaded in each lane, proteins were separated with the same material and methods and Coomassie-stained (right). While the halide derivatives (–I, –OTs, –OMs) show similar band pattern, the cyano derivatives (2-CN and 4-CN) show no protein bands.

2.5 Discussion

This study aims to find a correlation between the overall sensitization potential and the chemical structure of a contact allergen, DNCB. Here, this study shows a structure-activity relationship of DNCB. Unlike many other previous reports, this study used a systemic approach in designing derivatives of DNCB as well as in screening sensitization potential and reactivity of the compounds. The substitution reaction mechanism that DNCB undergoes occurs through a Meisenheimer complex, which is stabilized by electronegative leaving groups.[41] Thus, halogen derivatives of DNCB were chosen as an initial examination. Halogens express the highest electronegativity of any elements, fluorine being the highest. Including DNCB, total of 4 halogen leaving groups, fluorine to iodine, were tested. My result showed a decreasing IL-8 expression which corresponded to a decrease in electronegativity. In this study, non-halogen leaving groups, tosyl and mesyl derivatives, were also explored based on the hypothesis that any leaving groups capable of forming a Meisenheimer complex would cause contact hypersensitivity. The tosyl and mesyl derivatives not only showed high IL-8 response but also demonstrated a protein binding trend that was similar to DNCB (**Figure 2.7**). The tosyl derivative was tested for murine contact hypersensitivity model, and showed ear inflammation that was similar to DNCB's. These results show that non-allergenic compounds can be made to cause sensitization by controlling their rate of substitution reaction.

In addition to the ability of the leaving group, this study showed that the capabilities of the electron-withdrawing substituents, the nitro groups of DNCB, are important in an S_NAr mechanism as well. The effect of the electron-withdrawing substituents of the benzene ring is presented by Hammett sigma constant or substituent constant (σ), which is a value calculated based on the ionization constant of a substituted benzoic acid in water at 25 ^{O}C.[36,37,42] A large positive

σ-value implies high electron-withdrawing power by resonance effect whereas a large negative σ-value implies high electron-releasing power. In this study, the nitro groups, with σ value of 1.27, were replaced with cyano (σ value of 0.66), carboxylic acid, and methyl ester (σ value of 0.45 each) at the *para* and *ortho* position relative to the leaving group. The IL-8 response elicited by these compounds was in level with the resting cells, suggesting that electron-withdrawing capabilities were the determining factors for the skin sensitization potential of DNCB. The lack of IL-8 response by these substituents also aligns with observations from western blotting. The cyano groups showed no protein modification from western blotting, ultimately confirming the loss of sensitization potential. One limitation of this study is that none of the DNCB derivatives showed IL-8 level comparable to DNCB. Unfortunately, the nitro group is the strongest electron-withdrawing substituent, thus substitution that shows the opposite effect is not quite available. To do the best with the given ability, I explored the overall effects of electron-withdrawing groups by substituting another electron-withdrawing group in addition to two nitro groups (**Figure 2.3B and 2.4**). One of the derivatives in this group, 4-DNCBA, showed IL-8 response that was in level with DNCB, confirming that electron-withdrawing capabilities were the determining factors for skin sensitization potential of DNCB.

Protein binding by contact allergens is a critical step in the sensitization phase; however, the identity of this protein still has not been elucidated. The design of the derivatives with additional electron-withdrawing groups was balanced with the activity of steric interactions with potential target proteins. Hexyl and *tert*-butyl groups introduce more electron-rich alkyl chain and bulky group to the compound, affecting the kinetic stabilization. The results showed that all of the *para* substituents failed to elicit a strong IL-8 response that was comparable to that of DNCB or 4-DNCBA whereas *ortho*-substituted esters showed above-resting response. These observations

altogether could be implying that the potential protein target of DNCB has a binding pocket with an H-bonding acceptor. Taking a further step with this result, the rate of reactivity of the compounds was measured. Direct peptide reactivity assay (DPRA) is an assay that applies contact allergen's ability to covalently bind proteins. It evaluates the skin sensitization potential of a compound by directly reacting with an acetyl-capped model peptide (ex. Ac-RFAACAA-COOH). Instead of using a more common procedure of DPRA, this study used reactivity against one amino acid, cysteine to meet the goal of examining the effect of manipulating the reaction mechanism and the chemical structures. Unlike the hypothesis that a faster rate of reactivity would correspond to a high level of biological response, this study showed that there is a rate of reactivity window where a balance between compound stability and reactivity led to IL-8 expression.

2.6 Conclusion

In conclusion, this study shows that there are various aspects to the degree of sensitization potential of DNCB and its derivatives. The sensitization potential of DNCB-based derivatives were evaluated using three different screening methods: release of IL-8 by immune cells, the rate of reactivity to cysteine, and murine contact hypersensitivity model. The results showed that understanding the reactivity of the compounds can be used to manipulate and predict the sensitization more broadly than screening each compound individually. However, the rate of covalently bond formation of a contact allergen is not linearly correlated with its sensitization potential. This result strongly implies that there are specific protein targets that rely on spatial information along with reactivity to determine the activation of the sensitization phase. This work may also guide the use of DNCB analogs which elicit a stronger response than DNCB, improving the outcomes of immunological mechanisms probed via DNCB.

2.7 References

1. Ashby, J., Basketter, D. A., Paton, D. & Kimber, I. Structure activity relationships in skin sensitization using the murine local lymph node assay. *Toxicology* **103**, 177–194 (1995).

2. Kimber, I. *et al.* Alternative approaches to the identification and characterization of chemical allergens. *Toxicol In Vitro* **15**, 307–312 (2001).

3. Divkovic, M., Pease, C. K., Gerberick, G. F. & Basketter, D. A. Hapten-protein binding: from theory to practical application in the in vitro prediction of skin sensitization. *Contact Derm.* **53**, 189–200 (2005).

4. McKinney, J. D., Richard, A., Waller, C., Newman, M. C. & Gerberick, F. The Practice of Structure Activity Relationships (SAR) in Toxicology. *Toxicol Sci* **56**, 8–17 (2000).

5. Chipinda, I. *et al.* Rapid and simple kinetics screening assay for electrophilic dermal sensitizers using nitrobenzenethiol. *Chem. Res. Toxicol.* **23**, 918–925 (2010).

6. Mbiya, W., Chipinda, I., Siegel, P. D., Mhike, M. & Simoyi, R. H. Substituent Effects on the Reactivity of Benzoquinone Derivatives with Thiols. *Chem. Res. Toxicol.* **26**, 112–123 (2013).

7. Chipinda, I. *et al.* Pyridoxylamine reactivity kinetics as an amine based nucleophile for screening electrophilic dermal sensitizers. *Toxicology* **315**, 102–109 (2014).

8. Mbiya, W., Chipinda, I., Simoyi, R. H. & Siegel, P. D. Reactivity measurement in estimation of benzoquinone and benzoquinone derivatives' allergenicity. *Toxicology* **339**, 34–39 (2016).

9. Niwa, Y., Niwa, H., Kohmura, J., Ou, D. W. & Yokoyama, M. M. Studies on the dinitrochlorobenzene (DNCB) sensitization test. *Ann Allergy* **48**, 108–112 (1982).

10. Popov, A. *et al.* Contact allergic response to dinitrochlorobenzene (DNCB) in rats: insight from sensitization phase. *Immunobiology* **216**, 763–770 (2011).

11. Zhang, E. Y., Chen, A. Y. & Zhu, B. T. Mechanism of Dinitrochlorobenzene-Induced Dermatitis in Mice: Role of Specific Antibodies in Pathogenesis. *PLoS One* **4**, (2009).

12. Magnusson, B. & Kligman, A. M. The identification of contact allergens by animal assay. The guinea pig maximization test. *J. Invest. Dermatol.* **52**, 268–276 (1969).

13. Buehler, E. V. Occlusive patch method for skin sensitization in guinea pigs: the Buehler method. *Food Chem. Toxicol.* **32**, 97–101 (1994).

14. Frankild, S., Vølund, A., Wahlberg, J. E. & Andersen, K. E. Comparison of the sensitivities of the Buehler test and the guinea pig maximization test for predictive testing of contact allergy. *Acta Derm. Venereol.* **80**, 256–262 (2000).

15. Landsteiner, K. & Jacobs, J. STUDIES ON THE SENSITIZATION OF ANIMALS WITH SIMPLE CHEMICAL COMPOUNDS. *J Exp Med* **64**, 717–721 (1936).

16. Basketter, D. A. *et al.* Use of the local lymph node assay for the estimation of relative contact allergenic potency. *Contact Derm.* **42**, 344–348 (2000).

17. Rovida, C. *et al.* The Local Lymph Node Assay (LLNA). *Current Protocols in Toxicology* **51**, 20.7.1-20.7.14 (2012).

18. Basketter, D. A., Gerberick, G. F., Kimber, I. & Loveless, S. E. The local lymph node assay: a viable alternative to currently accepted skin sensitization tests. *Food Chem. Toxicol.* **34**, 985–997 (1996).

19. Sharma, N. S. *et al.* Perspectives on Non-Animal Alternatives for Assessing Sensitization Potential in Allergic Contact Dermatitis. *Cell Mol Bioeng* **5**, 52–72 (2012).

20. Sakaguchi, H. *et al.* Development of an in vitro skin sensitization test using human cell lines; human Cell Line Activation Test (h-CLAT) II. An inter-laboratory study of the h-CLAT. *Toxicology in Vitro* **20**, 774–784 (2006).

21. Python, F., Goebel, C. & Aeby, P. Assessment of the U937 cell line for the detection of contact allergens. *Toxicol. Appl. Pharmacol.* **220**, 113–124 (2007).

22. Gerlier, D. & Thomasset, N. Use of MTT colorimetric assay to measure cell activation. *Journal of Immunological Methods* **94**, 57–63 (1986).

23. Röse, L., Schneider, C., Stock, C., Zollner, T. M. & Döcke, W.-D. Extended DNFB-induced contact hypersensitivity models display characteristics of chronic inflammatory dermatoses. *Exp. Dermatol.* **21**, 25–31 (2012).

24. Aleksic, M. *et al.* Investigating protein haptenation mechanisms of skin sensitisers using human serum albumin as a model protein. *Toxicol In Vitro* **21**, 723–733 (2007).

25. Hirota, M. *et al.* Modification of cell-surface thiols elicits activation of human monocytic cell line THP-1: possible involvement in effect of haptens 2,4-dinitrochlorobenzene and nickel sulfate. *J Toxicol Sci* **34**, 139–150 (2009).

26. Aleksic, M. *et al.* Mass spectrometric identification of covalent adducts of the skin allergen 2,4-dinitro-1-chlorobenzene and model skin proteins. *Toxicology in Vitro* **22**, 1169–1176 (2008).

27. Landsteiner, K. & Jacobs, J. STUDIES ON THE SENSITIZATION OF ANIMALS WITH SIMPLE CHEMICAL COMPOUNDS. *J Exp Med* **61**, 643–656 (1935).

28. Landsteiner, K. & Chase, M. W. STUDIES ON THE SENSITIZATION OF ANIMALS WITH SIMPLE CHEMICAL COMPOUNDS : IX. SKIN SENSITIZATION INDUCED BY INJECTION OF CONJUGATES. *J. Exp. Med.* **73**, 431–438 (1941).

29. Landsteiner, K. & Di Somma, A. A. STUDIES ON THE SENSITIZATION OF ANIMALS WITH SIMPLE CHEMICAL COMPOUNDS : V. SENSITIZATION TO DIAZOMETHANE AND MUSTARD OIL. *J. Exp. Med.* **68**, 505–512 (1938).

30. Delaine, T., Hagvall, L., Rudbäck, J., Luthman, K. & Karlberg, A.-T. Skin Sensitization of Epoxyaldehydes: Importance of Conjugation. *Chem. Res. Toxicol.* **26**, 674–684 (2013).

31. Manabe, Y. *et al.* 1-Fluoro-2,4-dinitrobenzene and its derivatives act as secretagogues on rodent mast cells. *Eur. J. Immunol.* **47**, 60–67 (2017).

32. Roberts, D. W. & Aptula, A. O. Electrophilic Reactivity and Skin Sensitization Potency of SNAr Electrophiles. *Chem. Res. Toxicol.* **27**, 240–246 (2014).

33. Rosenkranz, H. S., Klopman, G., Zhang, Y. P., Graham, C. & Karol, M. H. Relationship between allergic contact dermatitis and electrophilicity. *Environ. Health Perspect.* **107**, 129–132 (1999).

34. Eisen, H. N. & Belman, S. Studies of Hypersensitivity to Low Molecular Weight Substances: Ii. Reactions of Some Allergenic Substituted Dinitrobenzenes with Cysteine or Cystine of Skin Proteins. *Journal of Experimental Medicine* **98**, 533–549 (1953).

35. Eisen, H. N., Kern, M., Newton, W. T. & Helmreich, E. A Study of the Distribution of 2,4-Dinitrobenzene Sensitizers Between Isolated Lymph Node Cells and Extracellular Medium in Relation to Induction of Contact Skin Sensitivity. *Journal of Experimental Medicine* **110**, 187–206 (1959).

36. Hammett, L. P. The Effect of Structure upon the Reactions of Organic Compounds. Benzene Derivatives. *J. Am. Chem. Soc.* **59**, 96–103 (1937).

37. McDANIEL, D. H. & BROWN, H. C. An Extended Table of Hammett Substitutent Constants Based on the Ionization of Substituted Benzoic Acids. *J. Org. Chem.* **23**, 420–427 (1958).

38. Noonan, F. P. & Halliday, W. J. Studies of Contact Hypersensitivity and Tolerance in vivo and in vitro. *IAA* **56**, 523–532 (1978).

39. Saint-Mezard, P., Berard, F., Dubois, B., Kaiserlian, D. & Nicolas, J.-F. The role of CD4+ and CD8+ T cells in contact hypersensitivity and allergic contact dermatitis. *Eur J Dermatol* **14**, 131–138 (2004).

40. Gerberick, G. F. *et al.* Development of a peptide reactivity assay for screening contact allergens. *Toxicol. Sci.* **81**, 332–343 (2004).

41. Meisenheimer, J. Ueber Reactionen aromatischer Nitrokörper. *Justus Liebigs Annalen der Chemie* **323**, 205–246 (1902).

42. Hammett, L. P. Some Relations between Reaction Rates and Equilibrium Constants. *Chem. Rev.* **17**, 125–136 (1935).

43. Crossland, R. K. & Servis, K. L. Facile synthesis of methanesulfonate esters. *J. Org. Chem.* **35**, 3195–3196 (1970).

44. Carballada, P. C. *et al.* Variation of the Viologen Electron Relay in Cyclodextrin-Based Self-Assembled Systems for Photoinduced Hydrogen Evolution from Water. *European Journal of Organic Chemistry* **2012**, 6729–6736 (2012).

45. Denehy, E., White, J. M. & Williams, S. J. Electronic Structure of the Sulfonyl and Phosphonyl Groups: A Computational and Crystallographic Study. *Inorg. Chem.* **46**, 8871–8886 (2007).

46. van der Aar, E. M. *et al.* Enzyme kinetics and substrate selectivities of rat glutathione S-transferase isoenzymes towards a series of new 2-substituted 1-chloro-4-nitrobenzenes. *Xenobiotica* **26**, 143–155 (1996).

47. Haydon, D. J. *et al.* Creating an Antibacterial with in Vivo Efficacy: Synthesis and Characterization of Potent Inhibitors of the Bacterial Cell Division Protein FtsZ with Improved Pharmaceutical Properties. *J. Med. Chem.* **53**, 3927–3936 (2010).

48. Al-Hiari, Y. M., Qaisi, A. M., El-Abadelah, M. M. & Voelter, W. Synthesis and Antibacterial Activity of Some Substituted 3-(Aryl)- and 3-(Heteroaryl)indoles. *Monatsh. Chem.* **137**, 243–248 (2006).

49. Shang, J. *et al.* Aromatic Triazole Foldamers Induced by C–H···X (X = F, Cl) Intramolecular Hydrogen Bonding. *J. Org. Chem.* **79**, 5134–5144 (2014).

CHAPTER III

IDENTIFICATION AND VALIDATION OF FUNCTIONALLY-RELEVANT PROTEIN TARGETS OF DNCB THROUGH PROTEOMICS AND INHIBITION STUDIES

3.1 Summary

Despite the known dangers of contact allergens, no clear molecular mechanism of action currently exists. In this chapter, we report how one of the most widely researched contact allergen, 1-chloro-2,4-dinitrobenzene (DNCB), induces skin sensitization via modification of select proteins within cells. We identify the protein and its mechanism of action via first mass spectrometry, gene suppressing assays, and protein inhibition with small molecules. Starting with an unbiased sampling, we identified 9 candidate proteins that showed DNCB-modified protein fragments. After the identification of these proteins, we found that HSP90, which was previously identified as a stress-response protein and damage-associated molecular pattern, showed the most unique sequences and sites of modification. We explored the functional relevance of the identified candidate proteins in skin sensitization by generating a THP-1 knockdown cell line and demonstrated that decreasing HSP90 levels in cells reduced DNCB-induced hypersensitivity below background level. Finally, we showed that DNCB activity was attenuated both in cells and *in vivo* by treatment with either geldanamycin (GA), an inhibitor of HSP90, or anti-CD91, an inhibitor of HSP90 receptor. Altogether, we identify HSP90 as a critical protein involved in skin sensitization induced by DNCB, or DNCB-induced hypersensitivity, and report that its effects can be reduced by inhibiting HSP90.

3.2 Introduction

As mentioned in Chapter 1 (Section 1.6-1.8), contact allergens react with self-proteins in the skin, which in turn activates the immune system to produce allergen-specific T cells. The consequence of this event is the manifestation of contact dermatitis that affects approximately 20 % of the general population. Despite the dangers that contact allergens pose, we are still without a proper cure, treatment, or even quantitative diagnostic test. One reason is that contact allergen's molecular mechanism of action is not clear to the level that we understand the elementals of this process. Here, this chapter sought to clarify this mechanism by identifying the protein targets of a contact allergen, DNCB, through mass spectrometry and gene-knockdown studies. This chapter not only aims to identify the protein but also elucidate the actions of the protein targets in contact hypersensitivity. Although DNCB is a well-established contact allergen, there has been no direct evidence of DNCB-protein modification by mass spectrometry or confirmation of the modified proteins in pathology of contact dermatitis.[1–5]

We show that heat shock protein 90 (HSP90) is critical in DNCB-induced contact hypersensitivity. Through western blot analysis and mass spectrometry, we showed that DNCB covalently binds HSP90 along with several other proteins. HSPs were first discovered as a family of stress-responsive proteins that maintain homeostasis of mammalian cells.[6–10] However, recent studies reported that HSPs are proteins that participate in the immune system by processing antigens and delivering antigens to neighboring cells.[11–14] By suppressing HSP90 expression in THP-1 cells, this work presents evidences that DNCB-modified HSP90 plays a role in skin sensitization. Also, we report that DNCB's sensitization potential can be attenuated by inhibiting HSP90 with either geldanamycin (GA), a known inhibitor of HSP90 protein, or anti-CD91, an inhibitor for a known receptor for HSP90. Altogether, this work provides new evidence that

contributes to the understanding of the fundamental pathology of contact dermatitis and offers insights into new potential therapeutic targets for individuals suffering from this disorder.

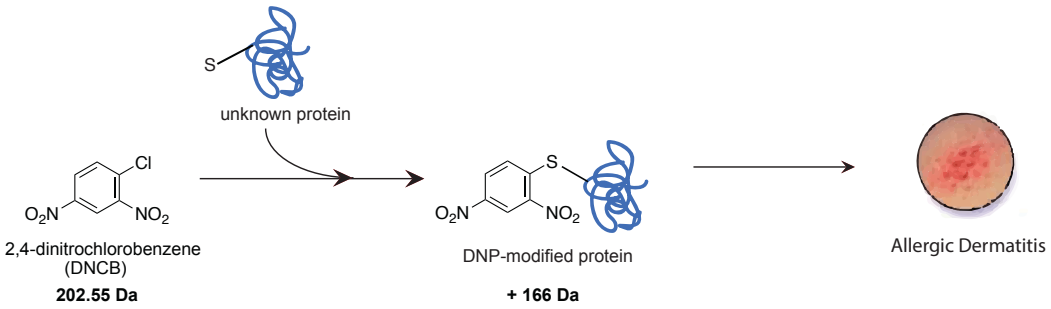

Figure 3.1 Graphic depiction of DNCB-protein modification. DNCB, with mass of 202.55 Da, covalently modifies unknown protein/s within cells, typically at cysteine or lysine functional groups. This modification yields a mass shift of 166 Da. DNCB modification of a protein will lead to activation of the immune response that elicits clinical symptoms of allergic contact dermatitis.

3.3 Materials and Methods

3.3.1 Cell Culture

Human monocyte cell line THP-1 was obtained from American Type Culture Collection (ATCC, Manassas, VA) and grown in Roswell Park Memorial Institute (RPMI) 1640 medium (Life Technologies, Carlsbad, CA) supplemented with 10 % fetal bovine serum (FBS, Thermo Fisher Scientific, Waltham, MA) and 1 % antibiotic-antimycotic (Thermo Fisher Scientific) at 37 ^{O}C in 5 % CO_2 incubator. Cells were passed every 3-4 days and plated at a density of 5 x 10^5 cells/mL.

3.3.2 Cell Lysate Preparation

DNCB (≥ 99 %) was purchased from Millipore Sigma and was dissolved in DMSO (Molecular Biology Grade, Millipore Sigma) to prepare 1 M DNCB stock solution. The stock was sterile filtered and stored in -80 ^{O}C freezer.

For the preparation of cell lysates, THP-1 cells were incubated with 50 μM DNCB which was diluted in cell culture medium from 1 M DNCB stock solution. About 18 x 10^6 THP-1 cells were resuspended in 18 mL medium with either buffer or 50 μM DNCB and seeded in a 6-well plate (3 mL per well). After incubation, the cells were harvested, washed with ice-cold 1X PBS (300 g, 5 min, 2x), lysed in 1X cell lysis buffer (50 mM Tris-HCl (pH 8.0), 150 mM NaCl, 1 % Triton X-100) containing 1 tablet of protease inhibitor (cOmplete™ ULTRA Tablets, Mini, EASYpack Protease Inhibitor, Millipore Sigma) for 30 min on ice, sonicated (15 s, 3x), and centrifuged at 16,000 g for 20 min to collect protein in supernatant. Protein samples were stored in -80 ^{O}C freezer if not used immediately.

Bicinchoninic acid (BCA) assay was performed to quantify protein samples. We used Pierce™ BCA Protein Assay Kit (Invitrogen) and the assay was performed following the manufacturer's protocol with few changes. Protein samples were diluted 1:9 in 1X PBS and bovine serum albumin (BSA) was run along with the protein samples to generate a standard curve.

3.3.3 Protein Separation by Gel Electrophoresis and Western Blotting

Protein samples were analyzed by gel electrophoresis and western blotting. To recite briefly, we used 4-15 % Mini-PROTEAN® TGX™ Precast Protein Gels (Bio-Rad, Hercules, CA) by running at 100 V for 60 min. Separated proteins were transferred to Immuno-Blot® PVDF Membrane (Bio-Rad) in a tank-blotting system for 16 h at 30 V. The membrane was blocked in blocking buffer (5 % w/v nonfat milk (Cell Signaling Technology, Danvers, MA) in 1X Tris Buffered Saline (TBS, Bio-Rad) with 0.1 % Tween-20 (Fisher Scientific)) for 1 h rt, rinsed in 1X TBS with Tween-20 (5 min, rt, shaking, 3x), stained with primary antibody overnight at 4 ^{O}C with shaking, rinsed in 1X TBS with Tween-20 (5 min, rt shaking, 3x), stained with a secondary antibody for 1 h rt with

shaking in dark, rinsed in 1X TBS with Tween-20 (5 min, rt shaking, 3x), and dried on a clean paper towel in dark. The primary and secondary antibodies were diluted in the blocking buffer. For primary antibodies, we used mouse anti-DNP antibody clone 9H8.1 (Millipore Sigma, 1:10,000 dilution), HSP90 alpha monoclonal antibody clone 5G5 (Invitrogen, 1:1,000 dilution). Purified anti-LRP1 (CD91) antibody (BioLegend, 1:500 dilution), and phosphotyrosine monoclonal (pY20) antibody (Invitrogen, 1:500 dilution). For secondary antibodies, we used goat anti-mouse IgG (H+L) Secondary Antibody, DyLight 650 (Invitrogen, 1:10,000 dilution). Dried membranes were imaged using Azure Biosystems c600 (Thermo Fisher).

3.3.4 Immunoprecipitation

For immunoprecipitation, we purchased μMACS^{TM} Separator from Miltenyi Biotec (Germany) and performed following the manufacturer's protocol with few changes. About 1 mg of protein was mixed with 1 μg monoclonal antibody and 50 μl μMACS Protein G MicroBeads (Miltenyi Biotec). After vigorous vortexing, the mixture was placed in ice for 30 min. To purify antibody-bound proteins, the mixture was applied to μ Columns (Miltenyi Biotec). The columns were primed with 200 μl 1X cell lysis buffer before applying the mixtures. Then, the column was washed with 200 μl high salt wash buffer (50 mM Tris-HCl (pH 8.0), 500 mM NaCl, 1 % NP-40 alternative, 4x), and 100 μl low salt wash buffer (20 mM Tris-HCl (pH 7.5)). For elution, we used 2X Laemmli Buffer (Bio-Rad) heated to 95 ^{O}C. Eluent was directly loaded on 4-15 % MiniPROTEAN® TGX^{TM} Precast Protein Gels for separation and western blotting analysis.

3.3.5 Sample Preparation for Mass Spectrometry

About 3 mg of protein samples were shipped to Kendrick Labs, Inc. (Madison, WI, US) for 2D gel electrophoresis and western blotting. Proteins separated from a gel were excised and sent to Northwestern Proteomics for mass spectrometry.

3.3.6 Generation of THP-1 Knockdown Cell Lines Using shRNA

To generate knockout cells, we purchased MISSION® shRNA Custom Lentiviral Particles from Millipore Sigma, three shRNA template oligonucleotides targeting each of mRNA sequences. The shRNA templates were designed with puromycin selection marker for positively selecting for cells with shRNA. Briefly summarizing transduction procedure, 2 x 10^4 THP-1 cells were seeded in a 96 well plate with 105 µl cell culture medium containing 8 µg/ml hexadimethrine bromide and 15 µl lentiviral particles. The supernatant was replaced with fresh cell culture medium on the next day. Successfully transduced cells were selected with 5 µg/ml puromycin beginning day 5 post-transduction. Empty vectors, MISSION® PLKO.1-puro Empty Vector Control Transduction Particles, were used as a control for transduction procedure.

3.3.7 Real-Time PCR (qPCR)

Stably transduced cells were seeded in a 6-well plate (3 x 10^6 cells per well, 10^6 cells per ml) and incubated in 37 ^{O}C incubator under two conditions: 1) cell culture medium only and 2) cell culture medium containing 50 µM DNCB. Then, total RNA was isolated using Direct-zol RNA Miniprep Kit with TRI Reagent Treatment (Zymo Research, Irvine, CA) following the manufacturer's protocol with one change: RNA was eluted with 10 µl of DNase/RNase-Free Water included in the kit. Elution was repeated once to produce 20 µl of total RNA eluent.

Recovered RNA samples were reverse-transcribed using SuperScript™ IV First-Strand Synthesis System (Invitrogen). To produced unbiased cDNA templates, we used Oligo(dT)$_{20}$ primer provided with the First-Strand Kit. Synthesized cDNA templates were quantified with Qubit 4 Fluorometer (Invitrogen) using 1X dsDNA HS Assay Kit (Invitrogen) and stored in -20 ^{O}C freezer if not used immediately.

For qPCR, we used RT^2 SYBR Green ROX qPCR Mastermix (Qiagen, Hilden, Germany) following the manufacturer's protocol with several changes. Per run, approximately 50 ng of cDNA was mixed with 200 nM primers and qPCR Mastermix. Primers were purchased from Integrative DNA Technologies (Coralville, IA). Beta-actin was used as an endogenous control and sequences for IL-8 and beta-actin were selected based on previous publications.[15–17] A complete list of primers used can be found in the Appendix. qPCR was repeated 3x and statistical significance was calculated based on ddCt values.

3.3.8 Co-Dosing of Chemical Inhibitors and Contact Allergens

Geldanamycin (GA) ≥ 98 % purity, 1 mg was purchased from Stemcell Technologies (Vancouver, Canada). It was dissolved in 180 µl DMSO to make a 10 mM stock solution, aliquoted, and stored in -20 ^{O}C freezer. Prior to usage, GA was further diluted in DMSO to reach 1,000X more concentrated than the desired final concentration. For example, GA stock solution was diluted to 1 mM in DMSO prior to addition to cell culture, and 1 µl of this was added to the cell culture to reach 1 µM GA treatment. DNCB was diluted to 500 µM in the cell culture medium. For the assay, 10^6 THP-1 cells were seeded in a 24 well plate with 900 µl of cell culture medium and 1 µl of 1,000X GA solution. After 5 min in the incubator, 100 µl of 500 µM DNCB was added to make a

final concentration of 50 μM. After incubating for 16-20 h, the release of IL-8 chemokine in the supernatant was measured using human IL-8 ELISA (BioLegend, San Diego, CA).

3.3.9 CD91 Blocking Assay

For the wells with anti-CD91, THP-1 cells were pre-incubated with 0.06 μg of anti-CD91 antibody for 24 h. The cells were washed in 300 μl 1X PBS (3x), resuspended in cell culture medium containing 50 μM DNCB, and incubated for 16-20 h. The release of IL-8 was measured using human IL-8 ELISA kit (BioLegend).

3.3.10 Murine Model of Contact Hypersensitivity

This experiment was performed following previously published protocols with several minor changes.[18,19] For GA inhibition study, BALB/c mice aged 6-8 weeks were obtained from Jackson Laboratory. For the HSP90 knockout experiment, mice deficient in HSP90-alpha proteins (colony strain C57BL/6N-Hsp90aa1tm1(KOMP)Wtsi/Mmucd) were obtained from Mutant Mouse Resource and Research Center (MMRRC) at University of California, Davis and bred on site. All the animal studies and mice maintenance were approved by the Institute of Animal Care and Use (IACUC #72517). For all experiments, mice were sensitized with 25 μl of 0.5 % w/v DNCB dissolved in 1:4 v/v olive oil and acetone solution, applied on the shaven abdomen for 2 consecutive days (Day 0 and 1). From day 5 to 8, mice were challenged with 10 μl of 0.5 % w/v DNCB on the ear. On day 9 or 24 h post-challenge, ear thickness was measured using electric caliber and the ears were cut with a scalpel. For the GA inhibition study, 0.5 mM GA solution prepared in 1:4 olive oil and acetone solution was applied on the same spots of sensitization and

challenge 30 min before they were treated with 0.5 % w/v DNCB. As a negative control, a group of mice were sensitized and challenged with 1:4 olive oil and acetone solution only.

3.4 Results

3.4.1 Identification of DNCB-Modified Proteins

In Chapter 2, I showed that DNCB undergoes nucleophilic aromatic substitution (S_NAr) reaction to bind proteins, which is consistent with previously reported literature.[1,2,4,20–24] Cysteine or lysine side chains of a protein serve as nucleophilic functional groups, producing DNCB-modified proteins that can be detected in mass spectrometry by a shift of 166 Da in a mass spectrum (**Figure 3.1**). To directly identify DNCB-modified proteins and isolate them from cellular debris, we used anti-DNP antibodies for western blotting and affinity purification. A part of Chapter 2 reports the observation of DNCB-modified protein bands using this antibody (**Figure 2.7**). THP-1 cells were treated with 50 μM DNCB for 30 min. The cellular lysate was separated via gel electrophoresis and immunoblotted with the anti-DNP antibody to identify any proteins that had been modified by DNCB. From the western blot, we observed protein band patterns that were similar to those in a Coomassie-stained gel, indicating that DNCB reacted with many different proteins (**Figure 3.2B**).

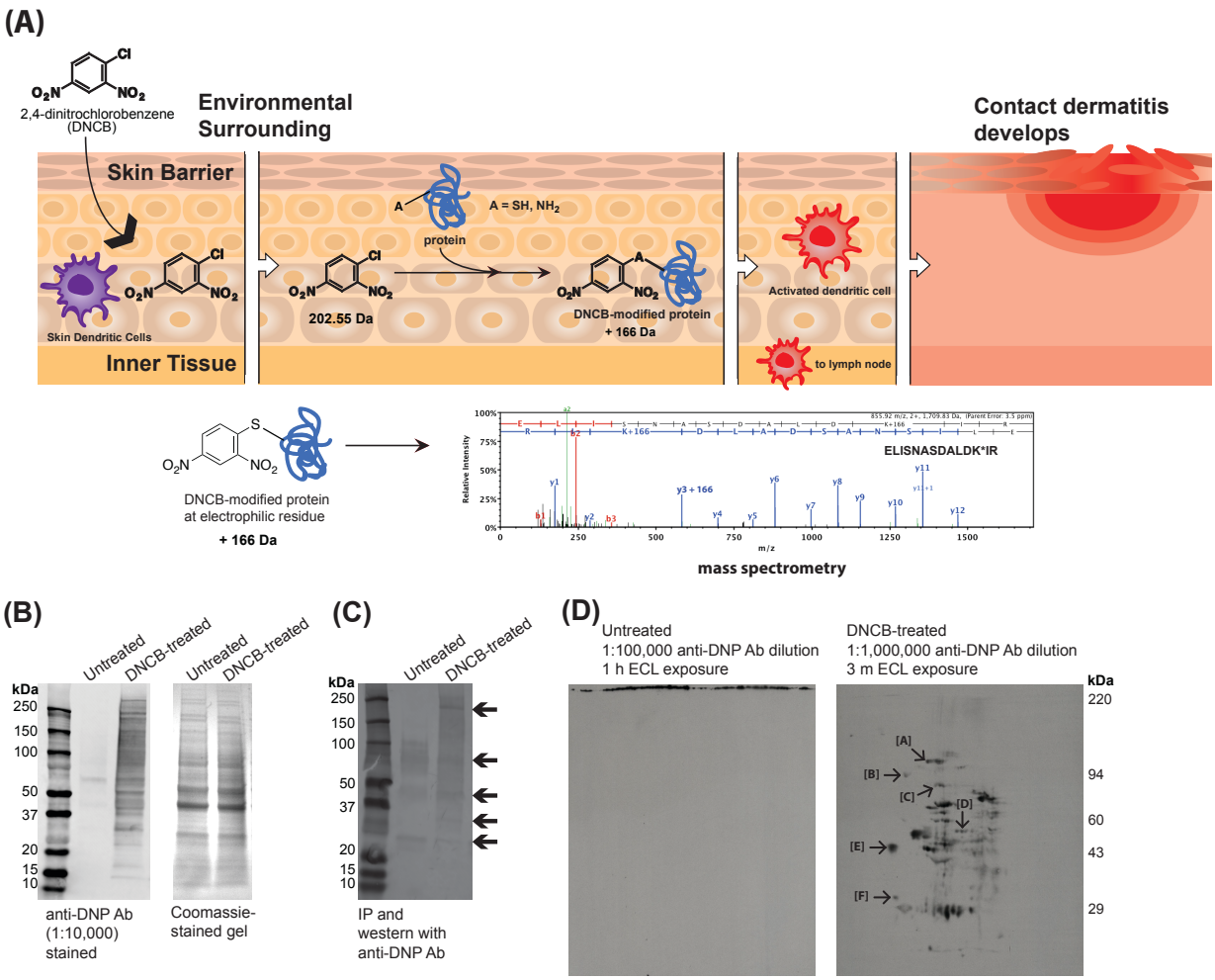

Figure 3.2 DNCB modifies many proteins quickly in a nonselective manner. **(A)** A simplified overview of allergic contact dermatitis in the skin. DNCB modifies lysine and cysteine residues of the protein to result in a shift of 166 Da detectable by mass spectrometry. Modification of proteins activates the skin dendritic cells. **(B)** Western blot showing untreated and DNCB-modified proteins probed with anti-DNP antibody (1:10,000 dilution, left), and a Coomassie-stained gel showing all proteins (right). **(C)** Western blot showing immunoprecipitated untreated and DNCB-modified proteins. Proteins were purified using the anti-DNP antibody (1 µg) and western blot was stained with the same antibody. The arrows indicate the positions of protein bands. **(D)** Western blot showing protein samples separated in 2D gel electrophoresis and stained with anti-DNP antibody (1:100,000 dilution for untreated (left) and 1:1,000,000 dilution for DNCB-treated (right)). Spots labeled from [A] to [F] were excised for mass spectrometry.

To enrich for DNCB-modified proteins, we used affinity-based purification with the anti-DNP antibody. Anti-DNP antibody was first mixed with magnetic beads to form an antibody-bead complex, which was mixed with cellular lysates for the selection of proteins with the highest level of modification. The number of protein bands was reduced to 5 (**Figure 3.2C**), but the total concentration of DNCB-modified proteins provided an insufficient quantity of proteins for analysis (data not shown). To address this issue, we separated cellular lysates by 2-dimensional gel electrophoresis and again immunoblotted using anti-DNP antibody. Similar to the 1D gel results (**Figure 3.2 B**), many protein spots were visible (**Figure 3.2D**). To increase our likelihood of identifying DNCB-modified proteins, we excised spots that were clearly distinct from neighboring proteins, became darker over time under chemiluminescence exposure (**Figure A8**), and corresponded to the molecular weight observed from our previous immunoprecipitation (**Figure 3.2C**). A total of 6 spots containing multiple proteins were excised and analyzed through mass spectrometry.

For identification of proteins, excised samples were disgested with trypsin, and the resulting peptides were analyzed by tandem mass spectrometer. Mass spectrometric data containing peptide masses and peptide fragments were searched against Mascot database search software. To summarize, we identified a total of 270 proteins from 6 spots (**Table A1)**. All of the proteins identified as putative DNCB-modified were cytosolic proteins that are predominantly found in the nucleus or endoplasmic reticulum. Each of our putative DNCB-modified proteins showed at least one unique DNCB modification on a peptide fragment. These unique peptide fragments appeared at least twice in the mass spectrum (**Table A2**). Among the identified DNCB-modified proteins, peptide fragments from HSP90 showed a high Mascot ion score (**Table 1**) and thus a higher probability of DNCB modification. Of all peptides identified, 13 of 21 belonged to

proteins in the HSP90 family, with each variant of HSP90 having multiple sites of potential modification and some modifications occurring at similar sites within the structure. To determine the potential for each of these proteins to contribute to a sensitization response in skin, we examined the relative abundance of identified proteins in human monocytes and human skin tissue.[25] Interestingly, all of the DNCB-modified proteins were in the top 25 % of proteins expressed in the skin. Our results suggest that the self-proteins which elicit an immune response may be common skin proteins which then elicit an inflammatory response separately from an antigen-specific response.

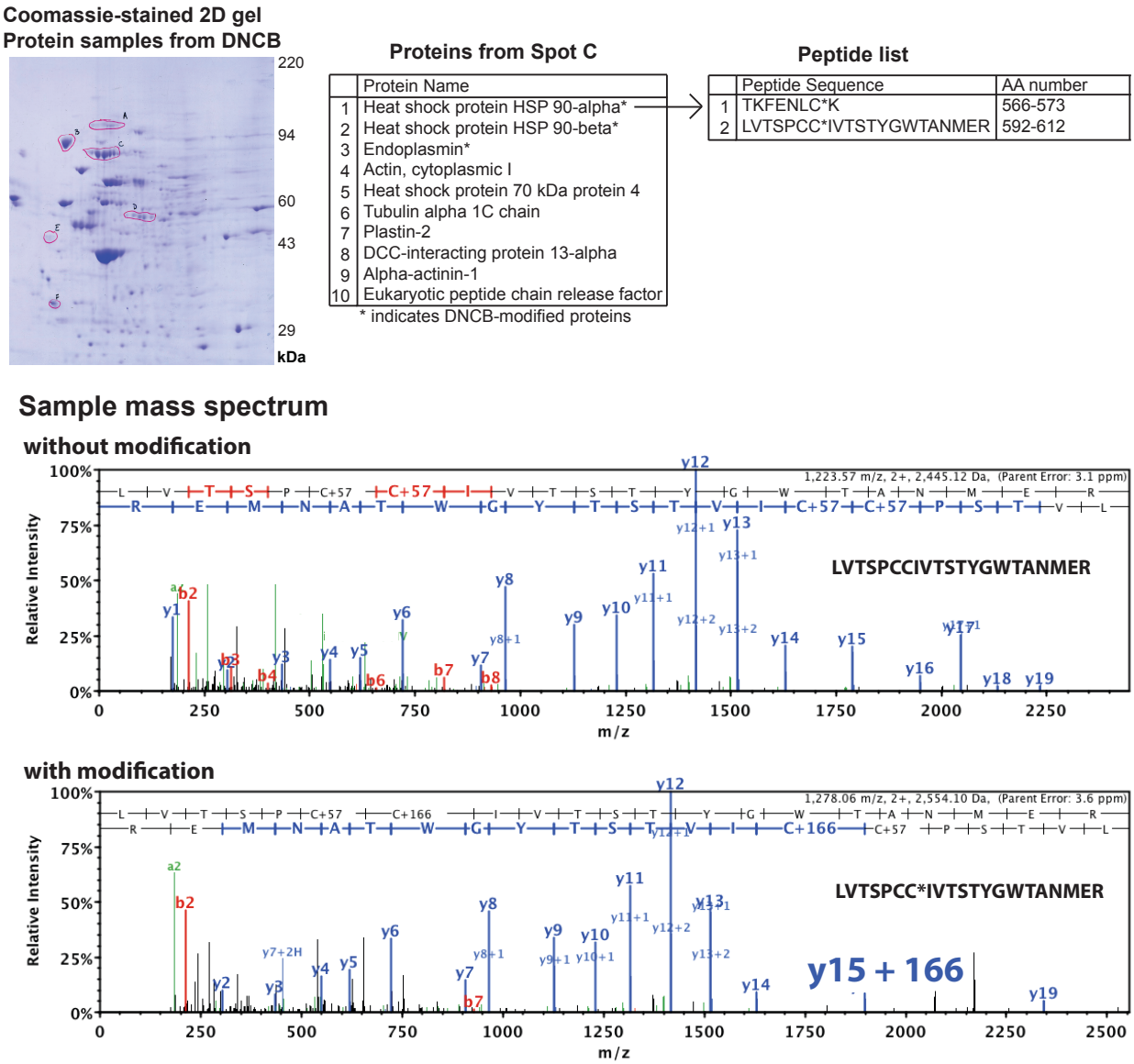

Figure 3.3 Overview of mass spectrometry flow and example data. A full list of the identified proteins and DNCB-modified peptide sequences with a mass spectrum can be found in the Appendix (Table A1 and Table A2). **(Top left)** An image of Coomassie-stained gel is shown with spot markings. **(Top Middle)** The list of proteins identified from Spot C is shown as an example that represents the full data. A total of 10 proteins were identified from Spot C. Three of them were DNCB-modified and they were marked with asterisks. **(Top Right)** HSP90-alpha has two unique DNCB-modified peptide fragments. **(bottom)** Mass spectrum of one of HSP90-alpha's peptide fragments, LVTSPCCIVTSTYGWTANMER. DNCB modification occurred on cysteine (marked with asterisks). This y15 ion of this fragment has a mass of 1,788 Da without modifications. With DNCB modification, this fragment has a mass of 1,897 Da, which is what is shown in this figure.

Table 3.1 List of DNCB-Modified Proteins

	Name of protein	Gene ID	Location of protein	Relative abundance (ppm)[25]		Peptide sequence found	Mascot score	MW (kDa)
				Monocyte	Skin			
1	60 S ribosomal protein L13	RPL13	Cytosol	232	42.2	RNKSTESLQANVQRLK*	19.2	24
2	DnaJ heat shock protein family (HSP40) member B11	DNAJB11	Cytosol, ER	318	194	QLLK*QGSVQK	29.7	41
3	Endoplasmin	HSP90B1	Cytosol, ER	766	1399	ELISNASDALK*IR NLGTIAK*SGTSEFLNK EFEPLLNWMK*DK LTESPC*ALVASQYGWSGNMER IMK*AQAYQTGK	100.5 77.1 33.0 98.6 40.5	92
4	Heat shock protein HSP90-alpha	HSP90AA1	Cytosol, ER	663	864	TKFENLC*K LVTSPCC*IVTSTYGWTANMER	15.2 61.0	85
5	Heat shock protein HSP90-beta	HSP90AB1	Cytosol, ER	1057	832	ADLINNLGTIAK*SGTK VILHLK*EDQTEYLEER VFIMDSC*DELIPEYLNFIR LVSSPC*CIVTSTYGWTANMER QK*AEADKNDK	75.8 25.9 83.0 98.6 35.3	83
6	Protein disulfide-isomerase A3	PDIA3	ER	1025	1174	VDC*TANTNTCNK FIQENIFGIC*PHMTEDNK	30.2 45.4	57
7	Ribonuclease inhibitor	RNH1	Cytosol	2332	264	DSPC*QLEALK LGDVGMAELC*PGLLHPSSR	42.2 33.5	50
8	Spectrin beta chain, non-erythrocytic 1	SPTBN1	Cytosol	200	236	K*QQMLENQMEVR	15.6	275
9	Tubulin alpha-1C	TUBA1C	Nucleus, cytoskeleton	1042	401	TIQFVDWC*PTGFK	28.8	50

3.4.2 Validation of DNCB-Modified Proteins

To validate mass spectrometry data and to understand the roles that the candidate proteins play in skin sensitization, we conducted a gene suppression experiment. If the candidate proteins were functionally relevant to skin sensitization, the knockdown cells would show reduced sensitization potential to DNCB. We successfully generated gene-knockdown cell lines for the following 6 proteins: DNAJB11, HSP90AA1, HSP90AB1, PDIA3, RNH1, and SPTBN1 (**Figure A9**). RPL13 and TUBA1C were excluded because they are ribosomal and cytoskeletal proteins which are essential for housekeeping functions. The knockdown of these proteins results in non-viable cell lines. Endoplasmin, despite its promising mass spectrum result, was also excluded from the study because previous reports showed that it is necessary for cell survival.[8] Data for knockdown experiments can be misinterpreted if it is done without proper control, such as an empty vector. Empty vectors are essentially the same shRNA design without any known gene target and serve to prove that transduction procedure or the virus itself has a negligible effect on the expression of the gene of interest. For each knockdown experiment, there were three experimental groups: (i) no transduction, which were the wild type THP-1 cells, (ii) empty vector, and (iii) target gene knockdowns. Each of these experimental groups were incubated under one of the two conditions – either left untreated (resting) or treated with 50 μM DNCB for 3 h (DNCB-treated) – before their total RNA was isolated for reverse-transcription. Similar to the analyses in Chapter 2, I used IL-8 for the marker of sensitization potential; IL-8 was amplified from the cDNA templates. While the wild-type THP-1 cells showed a 3-fold increase in IL-8 level under DNCB-stimulation, the cells without HSP90AB1, PDIA3, and SPTBN1 expressions showed only about 1.5 fold increase under the same condition. This was about 55 % less DNCB-induced IL-8 production. When cells without DNAJB11 and HSP90AA1 expression were stimulated with

DNCB, they showed IL-8 level indistinguishable from the resting cells, implying DNCB did not induce sensitization in these cells (**Figure 3.4**). This result implies that the modification of these two proteins, of the many proteins that DNCB modifies, results in IL-8 production, providing one molecular mechanism for elicitation of inflammatory responses in the skin.

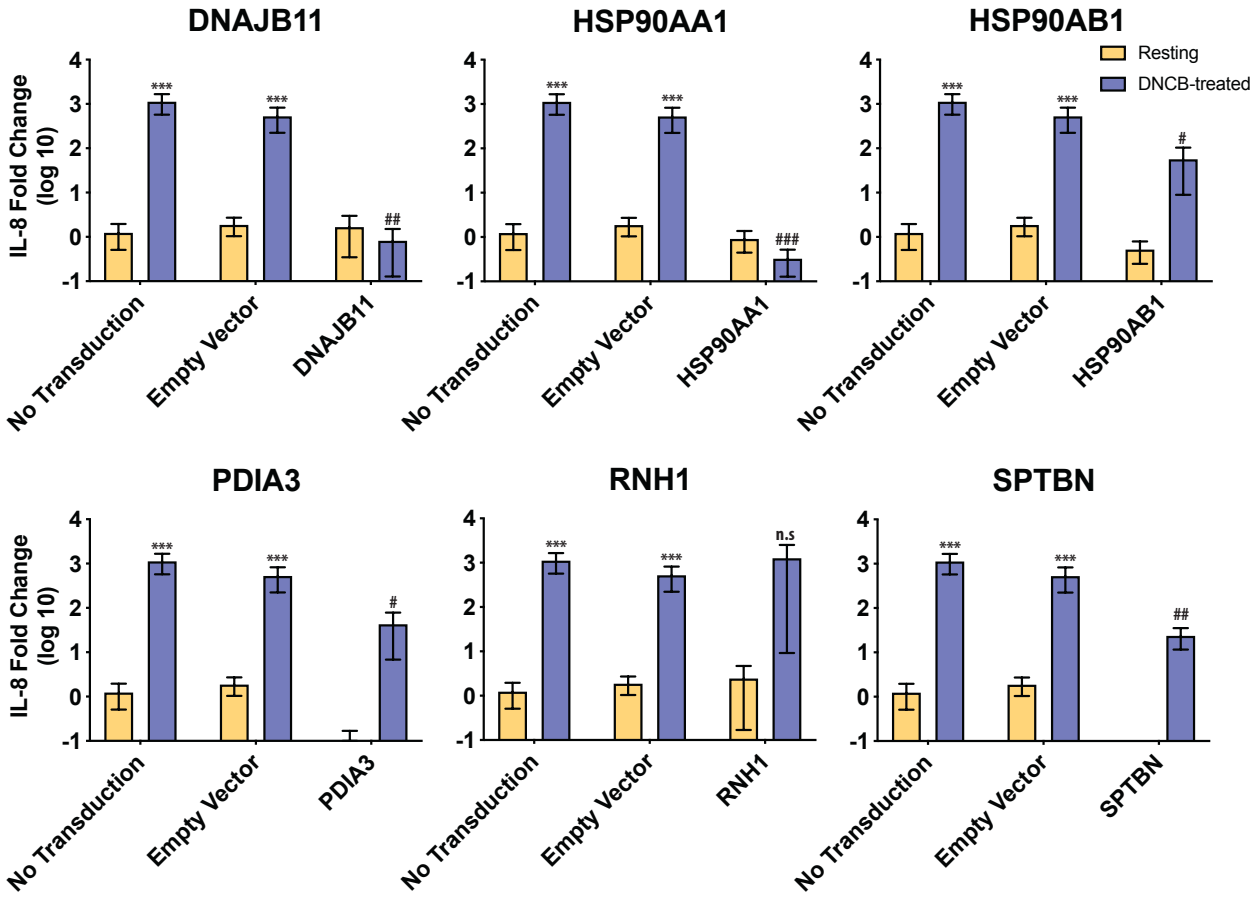

Figure 3.4 Protein knockdown with shRNA shows that DNAJB11 and HSP90AA1 can be critical proteins involved in DNCB-induced hypersensitivity. THP-1 cells were transduced with lentivirus packaged shRNA that suppresses the expression of gene targets before they are translated into proteins. There were three experimental groups: the wild type THP-1 cells (no transduction), the empty vector, and the knockdown cells. Each experimental group was either left untreated (resting, yellow bars) or treated with 50 μM DNCB for 3 h (DNCB-treated, purple bars). Each graph title describes the target genes. mRNA expression was normalized to that in the no transduction-resting condition. All experiments were repeated in triplicates, and the ddCt value was used for p-value calculation. * indicates statistical significance compared to the no transduction resting condition. *$p < 0.05$, **$p < 0.005$, ***$p < 0.0005$. # indicates statistical significance compared to no transduction DNCB-treated condition. #$p < 0.05$, ##$p < 0.005$, ###$p < 0.0005$.

3.4.3 Investigation of Molecular Mechanism of DNCB-HSP90

Next, we sought to explore the attenuation in DNCB-induced skin sensitization by using chemical inhibitors of the protein. Geldanamycin (GA) is a drug compound that selectively binds the ATP-binding site to ultimately block the activity of HSP90.[9,26–31] We hypothesized that DNCB-modification of HSP90 would be hindered by this inhibitor and that the subsequent IL-8 secretion would be reduced. To test this hypothesis, THP-1 cells were first incubated with 0.1 μM GA to allow inhibition of HSP90, and then they were stimulated with 50 μM DNCB. The release of IL-8 by cotreatment with GA was decreased by 76 % compared to the level dosed without GA (**Figure 3.5A**). Observing the reduction in DNCB-induced IL-8 response using GA, we sought to test the hypothesis directly in murine models of contact hypersensitivity. The experimental procedure was similar to described previously (**Figure 2.5**) with a few changes. GA was dissolved in 1:4 olive oil and acetone with 10 % DMSO to increase its solubility. For the group treated with GA (DNCB+GA/DNCB+GA), 0.5 mM GA was applied and dried before the mice were treated with 0.5 % DNCB solution. This group of mice showed less inflamed ears, with the average ear thickness of 0.534 mm, which was 19.3 % less than the group treated with DNCB only (**Figure 3.5B**). In addition to the control groups (solvent only, GA/GA, and DNCB/DNCB), one group of mice were treated with 0.5 mM GA during the sensitization period and treated with 0.5 % DNCB during the challenge period. This experimental group was to account for the inherent DNCB-induced inflammation that was not part of DNCB-induced hypersensitivity. The average ear thickness of this group was within the range of error of the DNCB+GA group, suggesting that the observed inflammation from the GA+DNCB group was due to the toxic effects of DNCB and that GA reduced DNCB-induced hypersensitivity. The results here indicate that the sensitization

potential of DNCB can be reduced by blocking the activity of HSP90 and it also reduces DNCB-induced hypersensitivity.

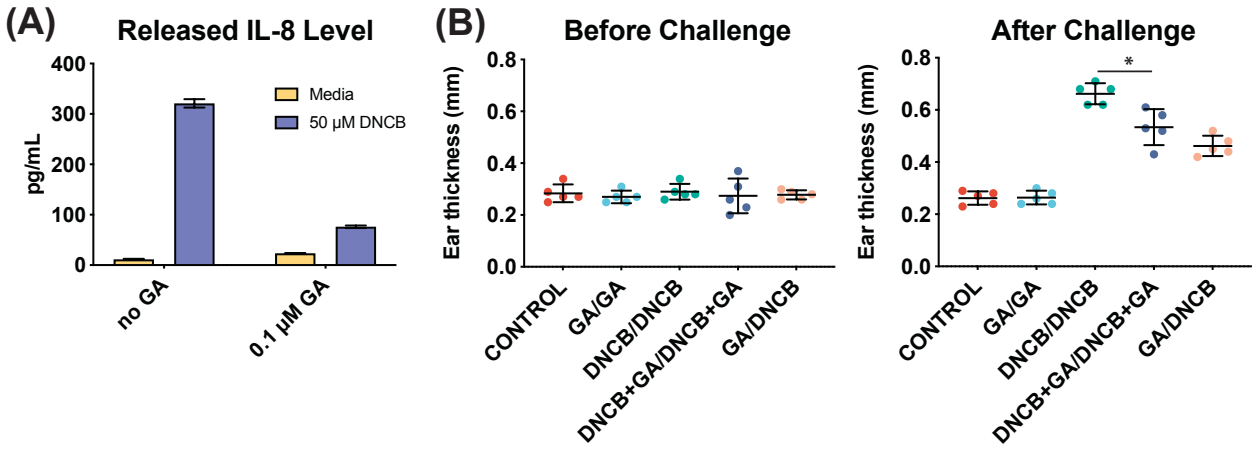

Figure 3.5 Treatment with GA and DNCB reduces skin sensitization potential. **(A)** Measurement of released IL-8 in the supernatant after cotreating THP-1 cells with 0.1 µM GA and 50 µM DNCB. Cells were cultured for 20 h. n = 3. The released IL-8 was reduced by 76 %. **(B)** Murine model of contact hypersensitivity to test the efficacy of GA *in vivo*. The ear thickness was measured before (left) and after (right) the challenge. n = 5. Control: treatment with solvent only, GA/GA: sensitize and challenge with 0.5 mM GA to show that GA is not a sensitizer. DNCB/DNCB: sensitize and challenge with 0.5 % w/v DNCB. DNCB+GA/DNCB+GA: sensitize and challenge with 0.5 mM GA and 0.5 % DNCB. DNCB was applied after GA was completely dried on the mouse skin. GA/DNCB: applied GA only during the sensitization period and DNCB only during the challenge period to show inherent DNCB-induced inflammation. * indicates significance compared to DNCB/DNCB. * $p < 0.05$.

Heat shock proteins (HSPs) carry out many functions that are necessary for the maintenance of cells. HSPs are highly conserved protein across many species, and they function as molecular chaperones involved in protein folding, assembly of protein complexes, molecular

trafficking into and out of the cell, cell cycle regulation and control.[6–8,10,12,32–34] Recently, several studies revealed that some families of HSPs, such as HSP90s, participate in antigen processing and presentation of antigen by major histocompatibility complexes (MHC) class I molecules. Extracellular HSP90s can bind antigenic peptides to form complexes to deliver peptides to the antigen-presenting cells.[11,13,14,35] These extracellular HSPs carrying antigenic peptides are endocytosed by CD91, a common surface receptor for the heat shock proteins gp96, HSP90, and HSP70.[36–38] As the final experiment, I sought to investigate if DNCB-induced hypersensitivity was also mediated by CD91 signaling pathway. To inhibit CD91, THP-1 cells were pre-incubated with antibodies to CD91 for 24 h. The cells preincubated with antibodies demonstrated less DNCB-induced IL-8 level (**Figure 3.6**) than the cells without preincubation. Lipopolysaccharide (LPS) elicits an IL-8 response in THP-1 cells via receptors other than CD91. When cells with and without preincubation were stimulated with LPS, they did not show a significant difference in IL-8 level. These results altogether indicate that CD91 signaling could be a pathway of DNCB-induced hypersensitivity.

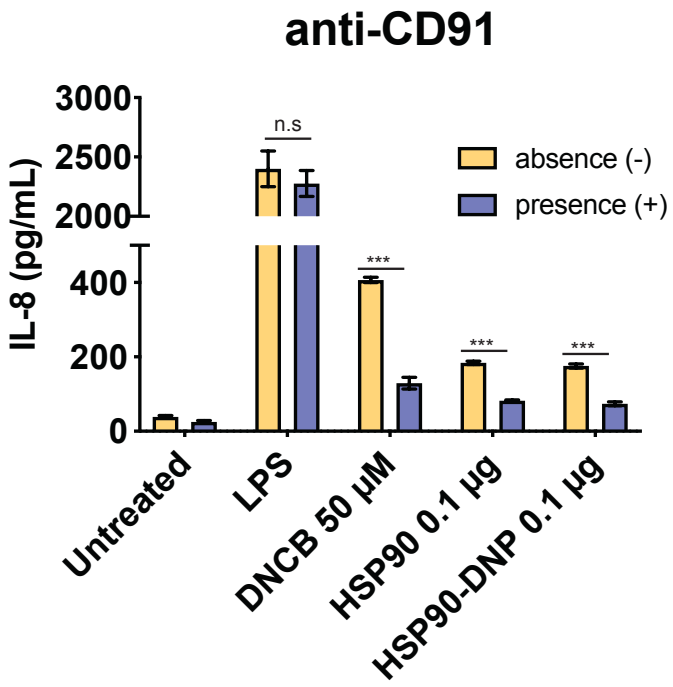

Figure 3.6 Blocking the cell surface receptor CD91 attenuates DNCB-induced IL-8 response. THP-1 cells were incubated with the anti-CD91 antibody for 24 h, washed in PBS, and replenished in the cell culture medium containing 50 µM DNCB. After 20 h incubation with DNCB, the supernatant was collected for human IL-8 ELISA. The above graph shows IL-8 response comparing absence (yellow bar) and presence (purple bar) of anti-CD91 antibody. DNCB-induced IL-8 production decreased by more than 80 %, suggesting the inhibition of contact hypersensitivity. HSP90 proteins and HSP90 pre-modified with DNCB (HSP90-DNP) were the positive controls for the reagents that bind CD91. LPS was the negative control as an immune activator that does not undergo CD91 pathway. * indicates statistical significance between absence (-) and presence (+). n.s = not significant, ***$p < 0.0005$.

3.5 Discussion

This study aims to identify functionally-relevant protein targets of DNCB to clarify one of the many molecular mechanisms of allergic contact dermatitis. The pathology of contact dermatitis is

hypothesized to begin when contact allergens covalently bind proteins, the event that leads to activation of Langerhans cells. Because protein modification by DNCB, or any contact allergens, happens in a manner similar to a post-translational modification, a common protein modification process for cellular functions, identification of the protein targets has been an active area of research in the past few decades. To best of our knowledge, this work is the first to confirm modification by mass shift and demonstrate the functional relevance of protein targets by protein knockdown and inhibition.

This study used the anti-DNP antibody as a tool for affinity-based purification of cell lysates. The usage of anti-DNP antibody for DNCB-modified protein staining was first reported in 2009 by Hirota *et al*.[39] These researchers fractionated DNCB-treated cell lysates into cell membrane proteins and cytosolic proteins in the attempt to clarify the location of DNCB modification. Their experiments revealed, however, that band staining patterns of cell membrane proteins were not different from those of cytosolic proteins, suggesting that DNCB could be membrane-permeable and did not necessarily affect only cell membrane proteins. This chapter also revealed similar protein-staining patterns of DNCB-treated cell lysates in the first set of experiments. The protein staining patterns observed in western blot were very similar to those of a Coomassie-stained gel, indicating that DNCB reacted with many different proteins within cells. This observation is consistent with the previous report of Hirota *et al*. However, I was surprised to find that many protein modification resulted from just 30 min of incubation time because previous experiments had been for at least 2 h. This result suggests that protein modification by DNCB occurs in a relatively short timeframe in a non-selective manner. These findings were confirmed by monitoring the progress of DNCB-modification over time (**Figure A10**). DNCB modification started to appear as early as 10 min of compound exposure in cells, peaked at 30 min, and then

started to diminish beginning 8 h time-point. While I could not determine the reason for the disappearance of DNCB-modified proteins from 8 h timepoint, I speculate that at this point, the cells could become activated to eliminate proteins that were misfolded and damaged by DNCB modification. Furthermore, all of the proteins identified as putative DNCB-modified were cytosolic proteins that are predominantly found in the nucleus or endoplasmic reticulum. This result implies that DNCB not only modifies proteins quickly but is also internalized within 30 min.

This study used RNAi to validate the functional relevance of the identified DNCB-modified proteins. Assessed by IL-8 mRNA expression, DNCB demonstrated a reduced sensitization potency in all of the knockdown cells except for RNH1 knockdown cells. RNH1-knockdown cells did not show a decrease in DNCB-induced IL-8 level compared to that of non-transduced or empty vector control cells. RNH1 interacts with intracellular and extracellular ribonucleases to regulate its activity.[40] I assume that the deletion of RNH1 could cause uncontrollable RNase activity within the cell, which might also explain the high error bars in data from RNH1–knockdown cells. The results from the knockdown experiment showed that DNCB's interaction with the shown five proteins – DNAJB11, HSP90AA1, HSP90AB1, PDIA3, and SPTBN1 – somehow induced hypersensitivity. One limitation of this experiment is that although RNAi is a powerful tool that enables the discovery of new pathways, it can often have off-target effects that lead to false discovery.[41] The off-target effect is currently the main challenge of the RNAi technique as a whole. Therefore, chemical and pathway inhibitors such as GA or anti-CD91 provide an additional method of confirmation for functional relevance. DNCB displayed a reduced sensitization potential when it was treated with GA or anti-CD91, providing additional evidence of HSP90's involvement in the sensitization phase.

Identification of the modified proteins and confirmation of these proteins in a cellular model indicated that HSP90 was a protein of interest for its interaction with DNCB. However, the complex interplay of factors that results in the ultimate manifestation of symptoms can be difficult to entangle. As such, animal models could be useful to test HSP90's involvement in contact hypersensitivity. Future experiments could be testing DNCB's sensitization potency in HSP90 knockout mice or local injection of anti-CD91. HSP90 knockout mice would validate DNCB-HSP90 interaction in contact hypersensitivity, proposing a mechanism of DNCB-induced sensitization phase. On the other hand, anti-CD91 injection could provide information regarding HSP90's involvement in the elicitation phase as well. If blocking CD91 in sensitized mice reduces the elicitation of ear inflammation, it would be a sign of new potential therapeutic targets of allergic contact dermatitis.

3.6 Conclusion

In this chapter, I identify several proteins of a contact allergen, DNCB. Elucidating the molecular mechanism of delayed-type hypersensitivity remains a challenge; thus I aimed to propose at least one potential mechanism, of many, for the sensitization phase. Contact hypersensitivity is an allergen-specific T cell response, indicating that it relies heavily on adaptive immunity that has been primed by the activation of the innate immunity. For this reason, I sought to identify an example pathway for this innate immunity. Knowing that contact allergens bind proteins to initiate the sensitization phase, I identified 9 DNCB-modified proteins through mass spectrometry. One of the identified proteins was HSP90, a molecular chaperone protein involved in many cellular functions including stress response, protein folding, cellular trafficking, and antigen-presentation by MHC class I molecule. Through shRNA knockdown and chemical and pathway inhibition

experiments, I revealed that HSP90 plays a crucial role in skin sensitization induced by DNCB. The results, however, only indicate the pathway of one protein and one contact allergen. Thus, generalizing the results of this should be undertaken with caution. DNCB is only one of the many contact allergens, and the protein targets of other contact allergens could be different. Overall, we hope these results provide others with a better understanding of the sensitization pathway as well as new insights for potential therapeutic targets of allergic contact dermatitis.

3.7 References

1. Aleksic, M. *et al.* Investigating protein haptenation mechanisms of skin sensitisers using human serum albumin as a model protein. *Toxicology in Vitro* **21**, 723–733 (2007).

2. Aleksic, M. *et al.* Mass spectrometric identification of covalent adducts of the skin allergen 2,4-dinitro-1-chlorobenzene and model skin proteins. *Toxicology in Vitro* **22**, 1169–1176 (2008).

3. Parkinson, E. *et al.* Stable Isotope Labeling Method for the Investigation of Protein Haptenation by Electrophilic Skin Sensitizers. *Toxicol Sci* **142**, 239–249 (2014).

4. Parkinson, E. *et al.* Determination of Protein Haptenation by Chemical Sensitizers Within the Complexity of the Human Skin Proteome. *Toxicol Sci* **162**, 429–438 (2018).

5. Guedes, S. *et al.* Contact dermatitis: in pursuit of sensitizer's molecular targets through proteomics. *Arch. Toxicol.* **91**, 811–825 (2017).

6. Schlesinger, M. J. Heat shock proteins. *J. Biol. Chem.* **265**, 12111–12114 (1990).

7. Kregel, K. C. Invited Review: Heat shock proteins: modifying factors in physiological stress responses and acquired thermotolerance. *Journal of Applied Physiology* **92**, 2177–2186 (2002).

8. Sanchez, E. R. Chaperoning steroidal physiology: Lessons from mouse genetic models of Hsp90 and its cochaperones. *Biochimica et Biophysica Acta (BBA) - Molecular Cell Research* **1823**, 722–729 (2012).

9. Whitesell, L., Mimnaugh, E. G., Costa, B. D., Myers, C. E. & Neckers, L. M. Inhibition of heat shock protein HSP90-pp60v-src heteroprotein complex formation by benzoquinone ansamycins: essential role for stress proteins in oncogenic transformation. *PNAS* **91**, 8324–8328 (1994).

10. Buchner, J. & Li, J. Structure, Function and Regulation of the Hsp90 Machinery. *Biomedical Journal* **36**, 106 (2013).

11. Srivastava, P. Roles of heat-shock proteins in innate and adaptive immunity. *Nat Rev Immunol* **2**, 185–194 (2002).

12. Haase, M. & Fitze, G. HSP90AB1: helping the good and the bad. *Gene* **575**, 171–186 (2016).

13. Imai, T. *et al.* Heat shock protein 90 (HSP90) contributes to cytosolic translocation of extracellular antigen for cross-presentation by dendritic cells. *PNAS* **108**, 16363–16368 (2011).

14. Asea, A. *et al.* Novel Signal Transduction Pathway Utilized by Extracellular HSP70. Role of Toll-Like Receptor (TLR) 2 and TLR4. *Journal of Biological Chemistry* **277**, 15028–15034 (2002).

15. Cao, X. *et al.* Critical selection of internal control genes for quantitative real-time RT-PCR studies in lipopolysaccharide-stimulated human THP-1 and K562 cells. *Biochemical and Biophysical Research Communications* **427**, 366–372 (2012).

16. Jung, D. *et al.* Discrimination of skin sensitizers from non-sensitizers by interleukin-1α and interleukin-6 production on cultured human keratinocytes. *Journal of Applied Toxicology* **36**, 1129–1136 (2016).

17. Yun, J. J. *et al.* Genomic DNA functions as a universal external standard in quantitative real-time PCR. *Nucleic Acids Res* **34**, e85 (2006).

18. Röse, L., Schneider, C., Stock, C., Zollner, T. M. & Döcke, W.-D. Extended DNFB-induced contact hypersensitivity models display characteristics of chronic inflammatory dermatoses. *Exp. Dermatol.* **21**, 25–31 (2012).

19. Freudenberg, M. A., Esser, P. R., Jakob, T., Galanos, C. & Martin, S. F. Innate and adaptive immune responses in contact dermatitis: analogy with infections. *G Ital Dermatol Venereol* **144**, 173–185 (2009).

20. Martin, S. F. *et al.* Mechanisms of chemical-induced innate immunity in allergic contact dermatitis. *Allergy* **66**, 1152–1163 (2011).

21. Karjalainen, K. & Mäkelä, O. Concentrations of three hapten-binding immunoglobulins in pooled normal human serum. *Eur. J. Immunol.* **6**, 88–93 (1976).

22. Mussotter, F. *et al.* Proteomics analysis of dendritic cell activation by contact allergens reveals possible biomarkers regulated by Nrf2. *Toxicology and Applied Pharmacology* **313**, 170–179 (2016).

23. Bauch, C. *et al.* Putting the parts together: Combining in vitro methods to test for skin sensitizing potentials. *Regulatory Toxicology and Pharmacology* **63**, 489–504 (2012).

24. Kimani, F., Kim, S.-M., Steinhardt, R. & Esser-Kahn, A. P. Correlating the structure and reactivity of a contact allergen, DNCB, and its analogs to sensitization potential. *Bioorganic & Medicinal Chemistry* **27**, 2985–2990 (2019).

25. Wang, M., Herrmann, C. J., Simonovic, M., Szklarczyk, D. & von Mering, C. Version 4.0 of PaxDb: Protein abundance data, integrated across model organisms, tissues, and cell-lines. *Proteomics* **15**, 3163–3168 (2015).

26. Schulte, T. W., Blagosklonny, M. V., Ingui, C. & Neckers, L. Disruption of the Raf-1-Hsp90 Molecular Complex Results in Destabilization of Raf-1 and Loss of Raf-1-Ras Association. *J. Biol. Chem.* **270**, 24585–24588 (1995).

27. Prodromou, C. *et al.* Identification and structural characterization of the ATP/ADP-binding site in the Hsp90 molecular chaperone. *Cell* **90**, 65–75 (1997).

28. Neckers, L. *et al.* Methods to validate Hsp90 inhibitor specificity, to identify off-target effects, and to rethink approaches for further clinical development. *Cell Stress Chaperones* **23**, 467–482 (2018).

29. Li, Y.-H., Lu, Q.-N., Wang, H.-Q., Tao, P.-Z. & Jiang, J.-D. Geldanamycin, a ligand of heat shock protein 90, inhibits herpes simplex virus type 2 replication both *in vitro* and *in vivo*. *The Journal of Antibiotics* **65**, 509–512 (2012).

30. Ochel, H.-J., Eichhorn, K. & Gademann, G. Geldanamycin: the prototype of a class of antitumor drugs targeting the heat shock protein 90 family of molecular chaperones. *Cell Stress Chaperones* **6**, 105–112 (2001).

31. Park, J.-W. *et al.* The heat shock protein 90-binding geldanamycin inhibits cancer cell proliferation, down-regulates oncoproteins, and inhibits epidermal growth factor-induced invasion in thyroid cancer cell lines. *J. Clin. Endocrinol. Metab.* **88**, 3346–3353 (2003).

32. Chen, K.-C. *et al.* The endoplasmic reticulum HSP40 co-chaperone ERdj3/DNAJB11 assembles and functions as a tetramer. *The EMBO Journal* **36**, 2296–2309 (2017).

33. Grunwald, M. S. *et al.* The oxidation of HSP70 is associated with functional impairment and lack of stimulatory capacity. *Cell Stress Chaperones* **19**, 913–925 (2014).

34. Li, T., Jiang, H.-L., Tong, Y.-G. & Lu, J.-J. Targeting the Hsp90-Cdc37-client protein interaction to disrupt Hsp90 chaperone machinery. *J Hematol Oncol* **11**, (2018).

35. Triantafilou, M. & Triantafilou, K. Heat-shock protein 70 and heat-shock protein 90 associate with Toll-like receptor 4 in response to bacterial lipopolysaccharide. *Biochemical Society Transactions* **32**, 636–639 (2004).

36. Basu, S., Binder, R. J., Ramalingam, T. & Srivastava, P. K. CD91 is a common receptor for heat shock proteins gp96, hsp90, hsp70, and calreticulin. *Immunity* **14**, 303–313 (2001).
37. Binder, R. J., Han, D. K. & Srivastava, P. K. CD91: a receptor for heat shock protein gp96. *Nat. Immunol.* **1**, 151–155 (2000).

38. Pawaria, S. & Binder, R. J. CD91-dependent programming of T helper cell responses following Heat Shock Protein immunization. *Nat Commun* **2**, 521 (2011).

39. Hirota, M. *et al.* Modification of cell-surface thiols elicits activation of human monocytic cell line THP-1: possible involvement in effect of haptens 2,4-dinitrochlorobenzene and nickel sulfate. *J Toxicol Sci* **34**, 139–150 (2009).

40. Thomas, S. P., Kim, E., Kim, J.-S. & Raines, R. T. Knockout of the Ribonuclease Inhibitor Gene Leaves Human Cells Vulnerable to Secretory Ribonucleases. *Biochemistry* **55**, 6359–6362 (2016).

41. Sharma, S. & Rao, A. RNAi screening: tips and techniques. *Nat Immunol* **10**, 799–804 (2009).

CHAPTER IV

CONCLUSION

4.1 Conclusions

Contact hypersensitivity is a type IV hypersensitivity reaction mediated by allergen-specific T cells. This dissertation investigates the early stages of the pathology of contact hypersensitivity, preliminary focused on understanding the interaction between the contact allergen and its protein targets. DNCB was chosen as a model contact allergen for this study because it was a well-studied model in the field of contact hypersensitivity.

Chapter 2 reports on the structure-activity relationship of DNCB. Based on DNCB's reaction mechanism, this study chose structural derivatives of DNCB to screen for the sensitization potential. IL-8 response of stimulated cells corresponded to the electronegative strength of leaving groups and substituents. Tosyl and mesyl derivatives, which are not contact allergens, induced IL-8 level that was comparable to DNCB's both in cells and in vivo. This result indicates that non-allergenic compounds can be made to elicit contact hypersensitivity. The capabilities of electron-withdrawing substituents were also important factors in the sensitization potential as DNCB derivatives with cyano and carboxylic acid substituents failed to elicit IL-8 responses. While DNCB derivatives with bulkier substituents, hexyl and *tert*-butyl groups, did not appear to be as potent as DNCB, the *ortho* substituents showed higher IL-8 response than *para* substituents. These evidences could be implying the protein-allergen binding mechanism. Based on the results from cell-based assays, a linear correlation between cellular response and the rate of reactivity was

expected. Surprisingly, both fast and slow rates of reactivity to cysteine resulted in the background level of cellular response, demonstrating that there needs a balance among the electronegativity, reactivity, and spatial information to elicit hypersensitivity.

Chapter 3 attempts to elucidate a molecular mechanism of contact allergen by identifying the protein target and analyze its pathway. Mass spectrometry analysis revealed a total of nine DNCB-modified proteins, all of which were cytosolic and highly abundant in human skin. This result shows that DNCB both modifies proteins and gets internalized in a rather short timeframe. To validate the functional relevance, the gene expressions of the identified DNCB-modified proteins were suppressed with shRNA. Real-time PCR indicated in the reduction of DNCB-induced IL-8 response by more than half with gene suppression. HSP90, one of the identified protein targets that showed the most promising mass spectrometry result, showed IL-8 reduction to the background level. This result led to the hypothesis that HSP90 is involved in the sensitization pathway. HSP90's involvement in contact hypersensitivity will be discussed in the next section. HSP90 is an ATPase, requiring energy from ATP to activate. The inhibitor of HSP90, or GA, selectively binds the ATP-binding site of HSP90 to reduce its activity in cells. Using GA, the result from knockdown cells was validated. When THP-1 cells were stimulated with DNCB in the presence of GA, they showed a reduction in IL-8 level compared to DNCB-stimulated cells without GA. Similar phenomena were observed *in vivo*. Mice that were sensitized and challenged with DNCB in the presence of GA showed a reduction in ear thickness, and this reduction was at the comparable level with the ear thickness that was not sensitized with DNCB. These results suggest that DNCB-induced contact hypersensitivity can be attenuated by reducing the activity of HSP90. To investigate a mechanism at which DNCB-induced contact hypersensitivity activates, cells were stimulated with DNCB in the presence of the anti-CD91 antibody. Supposedly, the anti-

CD91 antibody should bind the cell surface receptor, CD91, a known receptor for HSP90. IL-8 level of the cells stimulated in the presence of anti-CD91 was significantly lower than that of DNCB-induced cells without anti-CD91. These results indicate that DNCB-modified HSP90s are acquired via CD91.

This dissertation aimed to elucidate a molecular mechanism at which DNCB undergoes to elicit contact hypersensitivity. Based on the SAR, the rate of reactivity did not linearly correlate with the sensitization potential, implying that there might be a specific protein targets of DNCB despite it modifies many different proteins. This dissertation demonstrated that DNCB modifies HSP90, which then, mediates the sensitization phase by activating antigen-presenting cells bearing CD91.

4.2 HSP90 in Contact Hypersensitivity

Heat shock proteins (HSPs) are highly conserved among many organisms, and they participate in many different functions, including the elicitation of the adaptive immune response.[1,2] This dissertation revealed a new role of HSP90 as a mediator of contact hypersensitivity. This dissertation showed that a contact allergen, DNCB, covalently binds HSP90, the event that leads to activation of the dendritic cells by CD91 signaling. There are two possibilities as to how HSP90 leads to the development of allergen-specific lymphocytes via antigen presentation. The first possibility is that DNCB-modification could disrupt the conformation of HSP90, which is then recognized as non-self by free HSP90s. In support of this idea, the previous studies of Gerberick and Hirota have shown DNCB's ability and sensitivity to modify thiols. For strong contact allergens such as DNCB, modification of thiols can occur in disulfide bonds, disrupting the conformation of HSP90.[3,4] Previous studies have also shown upregulation of the heat shock

proteins shortly upon the induction of stress response.[5] This could also mean that the protein modification of DNCB induces a stress response in cells, upregulating the expressions of HSPs, which ultimately lead to the processing of DNCB-modified HSP90s to antigenic peptides. In addition to respond to stress, HSP90 is a molecular chaperone that forms complexes with many different proteins. DNCB-modification could somehow lead to the disruption of protein-protein interaction that can signal the cell's malfunctions.[6–8] This dissertation also showed a preliminary result of CD91 signaling in the DNCB-induced sensitization phase. Of many families of HSPs, HSP90 plays a critical role in the interface of innate and adaptive immunity by contributing to the cross-presentation of antigens.[9,10] According to the report of Imai et al., both HSP90a-dull dendritic cells and mice showed diminished translocation of extracellular antigens into the cytosol, and thus decreasing cross-presentation and cross-priming. Based on this finding, HSP90s could have been contributing to the translocation of DNCB-HSP90 antigens from the extracellular compartments.

This dissertation, however, could not reveal whether DNCB-HSP90 binding occurs during the elicitation phase. A recently published study showed that the concentration of anti-HSP90a antibodies was higher in patients with psoriasis compared to those of healthy individuals,[11] which strongly suggests (i) DNCB-HSP90 antigens could be cross-presented in contact hypersensitivity, (ii) HSP90 peptides could be presented by APCs in addition to the allergens themselves, and (iii) DNCB-modified HSP90 could be the ones initiating the elicitation by allergen-specific T cells. To test the last suggestion, mice that were sensitized with DNCB could be challenged with HSP90.

4.3 Future Work

This dissertation showed that reducing HSP90 activity by geldanamycin (GA) attenuated DNCB-induced sensitization both in cellular and *in vivo* assays (**Figure 3.5**). One addition to this work could be to investigate if DNCB-induced sensitization could be reversed by inhibiting HSP90. This work could be done in both cells and *in vivo*. To do so in the cellular model, DNCB-stimulated THP-1 cells could be re-incubated with GA before they are collected for IL-8 measurement. If released IL-8 level is less than that of cells induced only with DNCB, it could suggest that sensitization can be halted by inhibiting HSP90 activity. However, this experiment might not be feasible because the DNCB-modification of proteins can cause distortion in protein conformation that could hinder GA from binding its HSP90-binding site.

To run this experiment in the animal model, mice will be first sensitized with 0.5 % DNCB and then challenged in the presence of GA (DNCB/DNCB+GA). In addition to measuring the ear thickness, valuable information could be gathered from ear tissue histology or local cytokine measurement in the ear. Furthermore, treating mice with GA after they are sensitized and challenged with 0.5 % DNCB could be a good experiment as well. If ear inflammation decreases by GA treatment, it will be an evidence of HSP90 as a therapeutic target and support the claim that reducing HSP activity attenuates contact hypersensitivity.

In addition, this dissertation showed HSP90's involvement in DNCB-induced sensitization by demonstrating that (i) HSP90-knockdown cells were less likely to induce sensitization response by DNCB and (ii) DNCB-induced contact hypersensitivity could be mediated by CD91, the receptor for HSP90. There are several experiments that would be a good addition to the findings shown in this dissertation. So far, HSP90's involvement in contact hypersensitivity was demonstrated mostly in cell-based models. To investigate the complex interplay of immune cells

in contact hypersensitivity, DNCB's sensitization potential can be tested in mice deficient in HSP90 genes. HSPs are highly conserved protein across many species and they are abundant in mouse skin tissue as well. Although deletion of HSP90 genes in mice should not be detrimental, because their cellular functions are not necessary cell's survival, pre-mature lethality has been previously reported in mice deficient in HSP90β gene and failure of spermatogenesis in HSP90α-deficient mice.[12–14] For this experiment, HSP90α-deficient mice will be sensitized and challenged with DNCB, following the protocol used in this dissertation and many other publications. If the average ear thickness of HSP90α-deficient mice after the challenge period is less than that of wild type, it would support our findings that HSP90 is a critical protein involved in the pathology of contact dermatitis.

This dissertation has shown some evidence that DNCB-induced contact hypersensitivity could be mediated by CD91. However, this concept still needs to be supported by more evidences. The first, and the most important, the experiment would be on the investigation of CD91 activation. CD91 has been shown to act as an NF-κB signaling receptor for immunogenic HSPs, which is initiated by phosphorylation of the cytosolic domain of CD91.[15] To investigate CD91-dependence of DNCB-induced hypersensitivity, DNCB-treated cell lysate will be purified with CD91 β-chain antibody and be probed with phosphotyrosine antibody. Based on previous reports that showed phosphorylation in samples treated with HSPs, we are also expecting to see similar results with DNCB. If this experiment shows CD91-dependence, an *in vivo* CD91 inhibition study could be conducted. This study will have two main goals: (i) to test CD91 dependence in animal model, and (ii) to test the hypothesis that CD91 pathway could be a therapeutic target of contact hypersensitivity. The inhibition of CD91 in animal can be done by intravenous (iv) tail injecting the monoclonal antibody as reported previously.[16–18] To make the study consistent with the IL-8

observation (**Figure 3.6**), the anti-CD91 antibody would be injected before the sensitization period. However, to look at the therapeutic effects of CD91, another experiment will be conducted by injecting anti-CD91 antibody in between sensitization and challenge period. If DNCB-sensitized mice show less inflammation with anti-CD91 injection in comparison with mice without the injection, it will be a solid proof that inhibition of CD91 is a therapeutic target.

4.4 References

1. Schlesinger, M. J. Heat shock proteins. *J. Biol. Chem.* **265**, 12111–12114 (1990).

2. Srivastava, P. Roles of heat-shock proteins in innate and adaptive immunity. *Nat Rev Immunol* **2**, 185–194 (2002).

3. Gerberick, G. F. *et al.* Development of a peptide reactivity assay for screening contact allergens. *Toxicol. Sci.* **81**, 332–343 (2004).

4. Hirota, M. *et al.* Modification of cell-surface thiols elicits activation of human monocytic cell line THP-1: possible involvement in effect of haptens 2,4-dinitrochlorobenzene and nickel sulfate. *J Toxicol Sci* **34**, 139–150 (2009).

5. Parsell, D. A. & Sauer, R. T. Induction of a heat shock-like response by unfolded protein in Escherichia coli: dependence on protein level not protein degradation. *Genes Dev.* **3**, 1226–1232 (1989).

6. Buchner, J. & Li, J. Structure, Function and Regulation of the Hsp90 Machinery. *Biomedical Journal* **36**, 106 (2013).

7. Seo, Y. H. Small Molecule Inhibitors to Disrupt Protein-protein Interactions of Heat Shock Protein 90 Chaperone Machinery. in *Journal of cancer prevention* (2015). doi:10.15430/JCP.2015.20.1.5.

8. Riggs, D. L. *et al.* Functional specificity of co-chaperone interactions with Hsp90 client proteins. *Crit. Rev. Biochem. Mol. Biol.* **39**, 279–295 (2004).

9. Imai, T. *et al.* Heat shock protein 90 (HSP90) contributes to cytosolic translocation of extracellular antigen for cross-presentation by dendritic cells. *PNAS* **108**, 16363–16368 (2011).

10. Rock, K. L. & Goldberg, A. L. Degradation of cell proteins and the generation of MHC class I-presented peptides. *Annu. Rev. Immunol.* **17**, 739–779 (1999).

11. Damasiewicz-Bodzek, A., Szumska, M. & Tyrpień-Golder, K. Antibodies to Heat Shock Proteins 90α and 90β in Psoriasis. *Archivum Immunologiae et Therapiae Experimentalis* **68**, (2020).

12. Sanchez, E. R. Chaperoning steroidal physiology: Lessons from mouse genetic models of Hsp90 and its cochaperones. *Biochimica et Biophysica Acta (BBA) - Molecular Cell Research* **1823**, 722–729 (2012).

13. Voss, A. K., Thomas, T. & Gruss, P. Mice lacking HSP90beta fail to develop a placental labyrinth. *Development* **127**, 1–11 (2000).

14. Grad, I. *et al.* The molecular chaperone Hsp90α is required for meiotic progression of spermatocytes beyond pachytene in the mouse. *PLoS ONE* **5**, e15770 (2010).

15. Pawaria, S. & Binder, R. J. CD91-dependent programming of T helper cell responses following Heat Shock Protein immunization. *Nat Commun* **2**, 521 (2011).

16. Chisholm, P. L., Williams, C. A. & Lobb, R. R. Monoclonal antibodies to the integrin α−4 subunit inhibit the murine contact hypersensitivity response. *European Journal of Immunology* **23**, 682–688 (1993).

17. Brok, H. P. M. *et al.* Prevention of Experimental Autoimmune Encephalomyelitis in Common Marmosets Using an Anti-IL-12p40 Monoclonal Antibody. *The Journal of Immunology* **169**, 6554–6563 (2002).

18. Cingoz, O. Ustekinumab. *MAbs* **1**, 216–221 (2009).

APPENDIX

1. Synthesis of DNCB Derivatives

Characterization of synthesized compounds

Unless otherwise noted, spectroscopic characterization was done on Bruker Avance III HD 500 11.7 Tesla NMR (500 MHz) for ^{1}H NMR and ^{13}C NMR. NMR spectra were analyzed using MestreNova software. Coupling on the spectra is expressed in hertz and abbreviations for multiplicities given as s = singlet, d = doublet, t = triplet, dd = doublet of doublets and m = multiplet where applicable. Mass spectral analysis was performed on Agilent 6224 TOF-MS.

2,4-dinitrophenyl 4-methylbenzenesulfonate (tosyl derivative, –OTs)

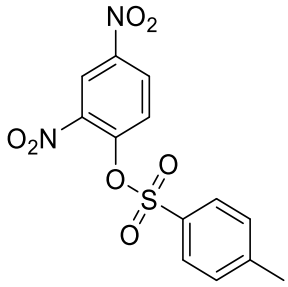

Tosyl derivative was synthesized according to literature procedure.[1] A solution of 2,4-dinitrophenol (–OH) (10 mmol, 1.84 g, 1 equiv.) in 10 ml dichloromethane (DCM) was first cooled in an ice-bath. Triethylamine (10 mmol, 1.02 g, 1.4 ml total) was added under argon and constant stirring. Subsequently, a solution of tosyl chloride (10 mmol, 1.9 g) dissolved in 5.0 ml DCM was added slowly over 5 min. The mixture was allowed to warm up to room temperature and stirred for 18 h. The reaction mixture was extracted with dilute HCl (3 x 25 ml) and the solvent layer was dried over sodium sulfate and evaporated in vacuo. The crude product was purified using column chromatography with mobile phase hexane/ethyl acetate to yield an off-white product (2.00 g, 60 % yield). ^{1}H NMR ($CDCl_3$) δ = 8.76 (d, *J* = 2.8 1H), 8.48 (dd, *J* = 9.0, 2.8, 1H), 7.80 (d, *J* = 8.4, 2H), 7.73 (d, *J* = 9.0, 1H), 7.39 (d, *J* =7.8, 2H), 2.49 (s, 3H).

^{13}C NMR ($CDCl_3$) δ = 147.2, 145.9, 145.3, 142.5, 130.9, 130.3, 128.6, 128.6, 126.3, 121.6, 21.8. NMR matched the literature procedure.[2]

2,4-dinitrophenyl methanesulfonate (mesyl derivative, –OMs)

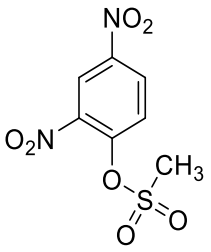

Mesyl derivative was synthesized according to literature procedure.[3] A solution of 2,4-dinitrophenol (0.50 g, 2.72 mmol, 1 equiv.) was prepared by dissolving in 10 ml of DCM in an ice-bath. Triethylamine (0.50 mL, 0.36 g, 3.5 mmol, 1.3 equiv.) was added to the solution under argon with constant stirring. Methane sulfonyl chloride (0.23 mL, 0.34 g, 2.90 mmol, 1.1 equiv.) was subsequently added over 5 min and the reaction mixture was stirred for 10 min. Then, the reaction was extracted into 10 mL ice water followed by 10 % HCl, 10 mL of saturated sodium bicarbonate, and brine. The organic layer was dried over sodium sulfate and the solvent was removed in vacuo to yield the crude product (252 mg, 38 % yield). ^{1}H NMR ($CDCl_3$) δ = 8.91 (d, *J* = 2.6, 1H), 8.54 (dd, *J* = 9.0, 2.7, 1H), 7.79 (d, *J* =9.0, 1H), 3.44 (s, 3H). ^{13}C NMR ($CDCl_3$) δ = 145.5, 145.3, 141.9, 128.9, 126.3, 121.9, 39.6. NMR matched the literature procedure.[3]

Synthesis of methyl esters

Methyl esters, such as methyl 2-chloro-5-nitrobenzoate, methyl 4-chloro-3-nitrobenzoate, methyl 4-chloro-2,5-dinitrobenzoate, and methyl 2-chloro-3,5-dinitrobenzoate, were synthesized according to the following published protocol:[4]

A solution of benzoic acid (0.03 mM) was prepared in 12 mL of methanol and was cooled in an ice bath. Concentrated sulfuric acid (1.2 mL total) was added to the solution dropwise. The resulting mixture was stirred while refluxing for 18 h. After the reaction was cooled to rt, organic layer was removed by extraction with 7.5 ml of water and removed with methanol in vacuo. After

cooling, reaction mixture was poured into 5.0 g of ice to precipitate the product. After filtering the product, it was washed with cold water and dried. Recrystallization from methanol gave the desired product.

methyl 2-chloro-5-nitrobenzoate

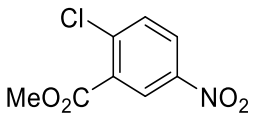

This compound was synthesized using 2-chloro-4-nitrobenzoic acid (0.50 g, 2.5 mmol) as the starting material. The crude product was recrystallized from methanol (260 mg, 48 % yield). ^{1}H NMR ($CDCl_3$) δ = 8.71 (d, *J* = 2.5, 1H), 8.27 (dd, *J* = 8.8, 2.8, 1 H), 7.65 (d, *J* = 8.8, 1H), 3.99 (s, 3H). ^{13}C NMR ($CDCl_3$) δ = 163.9, 146.1, 140.8, 132.3, 131.0, 126.8, 126.6, 53.1. NMR spectrum matched the published literature.[4]

Methyl 4-chloro-3-nitrobenzoate

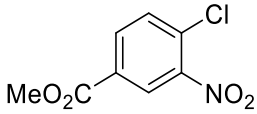

This compound was synthesized using 4-chloro-3-nitrobenzoic acid (0.50 g, 2.5 mmol) as the starting material. The crude product was recrystallized from methanol (420 mg, 78 % yield). ^{1}H NMR ($CDCl_3$) δ = 8.51 (d, *J* = 2.0, 1H), 8.16 (dd, *J* = 8.4, 2.0, 1H), 7.65 (dd, *J* = 8.5, 3.7, 1H), 3.97 (d, *J* =3.8, 3H). ^{13}C NMR ($CDCl_3$) δ = 164.2, 147.9, 133.6, 132.2, 131.7, 130.0, 126.6, 52.9. NMR spectrum matched the published literature.[5]

Methyl 4-chloro-3,5-dinitrobenzoate

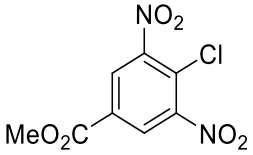

This compound was synthesized using 4-chloro-3,5-dinitrobenzoic acid (0.50 g, 2.0 mmol) as the starting material. The crude product was recrystallized from methanol (285 mg, 51 % yield). ^{1}H NMR ($CDCl_3$) δ = 8.60 (d, *J* = 1.9, 2H), 4.03 (s, 3H). ^{13}C NMR ($CDCl_3$) δ = 162.4, 149.7, 130.9, 128.2, 124.7, 53.6. NMR spectrum matched the published literature.[6]

Methyl 2-chloro-3,5-dinitrobenzoate

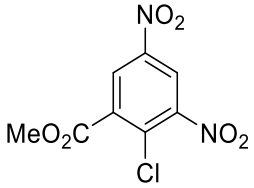

This compound was synthesized using 2-chloro-3,5-dinitrobenzoic acid (0.50 g, 2.0 mmol) as the starting material. The crude product was recrystallized from methanol (260 mg, 51 % yield). ^{1}H NMR ($CDCl_3$) δ = 8.81 (d, *J* = 2.6, 1H), 8.68 (d, *J* = 2.6, 1H), 4.05 (s, 3H). ^{13}C NMR ($CDCl_3$) δ = 162.7, 149.9, 145.6, 134.5, 132.5, 127.9, 121.9, 53.7. HRMS (ESI/TOF) Calculated for $C_{13}H_{15}ClN_2O_6$ $[M+H]^+$ 259.9925; found 260.9925

Synthesis of hexyl esters

Hexyl esters, such as hexyl 2-chloro-3,5-dinitrobenzoate and hexyl 4-chloro-2,6-dinitrobenzoate, were synthesized according to the following protocol:[7]

Oxalyl chloride (3.0 equiv.) and dimethylformamide (0.1 ml) were added to a solution of dinitrobenzoic acid (0.08 M, 1 equiv.) in dry DCM (30 ml) with stirring under argon. The reaction was stirred at rt for 2 h, and then DCM and excess oxalyl chloride was removed in vacuo to yield the crude product of acid chloride. A solution of Hexanol (1.2 equiv.) and N,N-diisopropylethylamine (1.5 equiv.) dissolved in DCM (10 ml) was cooled in ice-bath and added to the solution of crude product dissolved in 10 mL DCM. After stirring the mixture overnight under argon, the reaction was pumped down in rotary evaporator and purified by flash chromatography (hexanes / ethyl acetate 80/20) to yield the desired final product.

Hexyl 2-chloro-3,5-dinitrobenzoate

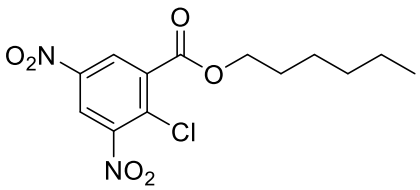

This compound was synthesized using 2-chloro-3,5-dinitrobenzoic acid (0.50 g, 2.5 mmol) as the starting benzoic acid. The final product was 430 mg, resulting in 40 % yield. ^{1}H

NMR ($CDCl_3$) δ = 8.82 (m, 1H), 8.79 (m, 1H), 8.70 (d, *J* = 2.7, 1H), 4.46 (t, *J* = 6.7, 3H), 1.87 (m, 3H), 1.79 (m, 3H), 1.52 (m, 3H), 1.42 (m, 3H), 1.41 (m, 6H), 1.31 (m, 6H), 0.98 (m, 4H), 0.89 (m, 4H). ^{13}C NMR (125 MHz, $CDCl_3$) δ = 162.5, 149.9, 145.6, 135.1, 132.3, 127.8, 121.8, 67.6, 31.3, 28.4, 25.6, 13.9. HRMS (ESI/TOF) Calculated for $C_{13}H_{15}ClN_2O_6$ $[M+H]^+$ 330.0619; found 330.0678

Hexyl 4-chloro-2,6-dinitrobenzoate

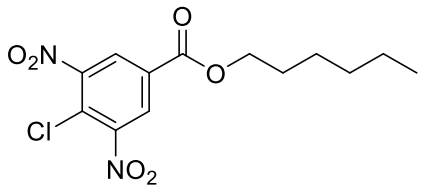

This compound was synthesized using 4-chloro-3,5-dinitrobenzoic acid (0.8 g, 3.24 mmol, 1 equiv.) as the starting material. The final product was 590 mg, resulting in 54 % yield. ^1H NMR ($CDCl_3$) δ = 8.70 (m, 3H), 8.55 (m, 3H), 4.44 (dd, *J* = 13.0, 6.3, 4H), 1.93 (m, 4H), 1.75 (m, 4H), 1.56 (m, 12H), 1.27 (m, 12H), 1.06 (m, 6H), 0.83 (m, 6H). ^{13}C NMR (125 MHz, $CDCl_3$) δ = 161.9, 149.7, 131.3, 128.1, 124.5, 67.2, 31.4, 28.5, 25.5, 22.5, 13.9. HRMS (ESI/TOF) Calculated for $C_{13}H_{15}ClN_2O_6$ $[M+H]^+$ 330.0619; found 330.0674

Synthesis of *tert*-butyl esters

Tert-butyl ester, such as *tert*-butyl 4-chloro-3,5-dinitrobenzoate and *tert*-butyl 2-chloro-3,5-dinitrobenzoate, were synthesized according to the following protocol:[7]

Tert-butanol (2.1 equiv.) was added to the solution of dinitrobenzoic acid (0.2 M, 1.0 equiv.) dissolved in dry DCM (20 ml) and stirred under argon. To this solution, 1-ethyl-3-(3-dimethylaminopropyl) carbodiimide (1.6 equiv) and a catalytic amount of dimethylaminopyridine (DMAP) were added. The reaction was stirred for 18 h at rt, extracted into 20 ml DCM, and washed with brine (2 x 10 ml). After the organic layer was removed, the crude product was purified with column chromatography (hexanes / ethyl acetate 80/20) to yield the desired final product.

Tert-butyl 4-chloro-3,5-dinitrobenzoate

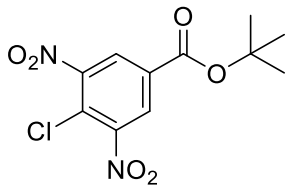

This compound was synthesized using 4-chloro-3,5-dinitrobenzoic acid (1.0 g, 4.05 mmol, 1.0 equiv.) as the starting material. The final product was 493 mg, resulting in 40 % yield. ^{1}H NMR ($CDCl_3$) δ = 8.53 (d, *J* = 2.7, 1H), 1.65 (s, 7H). ^{13} C NMR (126 MHz, $CDCl_3$) δ = 160.8, 149.6, 132.9, 127.9, 123.9, 84.6, 28.0. HRMS (ESI/TOF) Calculated for $C_{11}H_{11}ClN_2O_6$ $[M+H]^+$ 302.0306; Found 302.0279.

Tert-butyl 2-chloro-3,5-dinitrobenzoate

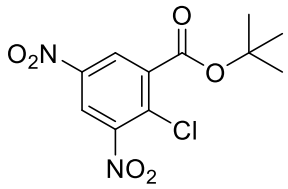

This compound was synthesized using 2-chloro-3,5-dinitrobenzoic acid as the starting material. The final product was 98 mg, resulting in 41 % yield. ^{1}H NMR ($CDCl_3$) δ = 8.68 (dd, *J* = 8.4, 2.7, 1H), 1.67 (s, 7H). ^{13}C NMR (125 MHz, $CDCl_3$) δ = 161.6, 149.7, 145.6, 136.9, 131.7, 127.3, 121.2, 85.6, 28.1. HRMS (ESI/TOF) Calculated for $C_{11}H_{11}ClN_2O_6$ $[M+H]^+$ 302.0306; Found 302.0294.

2. Detailed Protocol for Rate of Reactivity and Analysis of DNCB-Cysteine Adduct

DNCB was dissolved in 10 % CH_3CN in PBS (1 mM, 1 mL). The reaction was initiated by adding 100 µl of cysteine (10 mM, 10 equiv.) in PBS to the fully dissolved compound. At each time point, 10 µl aliquots of solution were quenched with 0.1 % trifluoroacetic acid (TFA) and the content was analyzed by HPLC. HPLC analysis was performed using Agilent Zorbax SB-C8 column (50 mm x 4.6 mm). The areas under the compound curve and the compound-cysteine curve were calculated and used to generate pseudo first-order rate.

Rate analysis was performed according to the protocol described in the main text. The following structure is an example demonstrating DNCB binding to cysteine. **Figure A1** was analyzed by HRMS comparison to a characterized compound. ^{1}H NMR (DMSO) δ = 8.88 (dd, *J*

= 5.5, 2.0, 1H), 8.50 (dd, *J* = 8.6, 1.8, 6H), 8.01 (m, 2H), 7.92 (m, 2H), 4.34 (m, 2H), 4.26 (m, 2H), 3.83 (dd, *J* =14.4, 4.8, 2H), 3.60 (dd, *J* =14.4, 7.5, 2H). ^{13}C NMR (125 MHz, DMSO) δ = 169.5, 162.2, 158.9, 146.2, 144.7, 143.3, 129.1, 128.1, 121.7, 50.8, 32.3. HRMS (ESI/TOF) Calculated for $C_9H_{10}N_3O_6S$ $[M+H]^+$ 288.029; Found 288.0283.

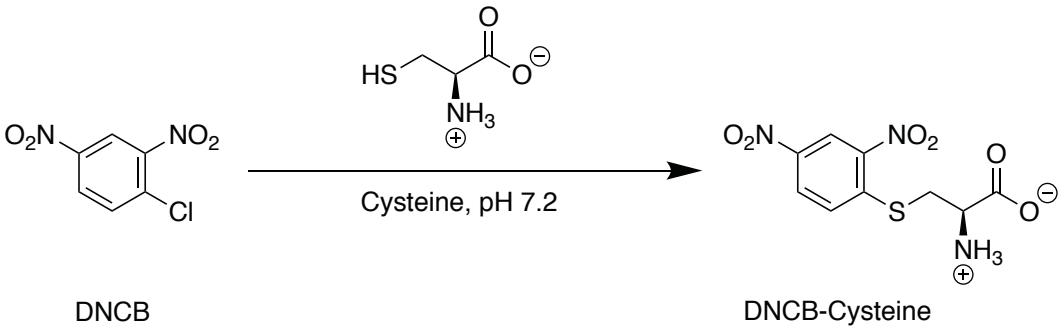

Figure A1. Reaction mechanism of DNCB binding cysteine.

This procedure was repeated for the derivatives with the aliquots quenching intervals determined by the rate of the respective reactions.

3. Optimization of IL-8 Assay

Because the production of IL-8 in THP-1 cells is transient, the assay condition had to be optimized. The goal of this experiment was to find the concentration and the incubation time that were ideal for the evaluation of the IL-8 response of DNCB. Finding the optimal assay condition for DNCB was crucial because it provided a baseline of comparison for DNCB-based derivatives. THP-1 cells were incubated at 11 different concentrations of DNCB – ranging from 400 μM to 6.25 μM – for 3 different incubation times – 14 h, 20 h, and 40 h. The supernatants were collected for IL-8 ELISA and the cells were collected for subsequent MTT assay. For all incubation time points, there was a reverse-parabolic trend of IL-8 release; concentrations higher than 80 μM appeared to

be too toxic to the cells, judging from the low cell viability assessed by MTT result and the IL-8 quantity lower than the background level (resting). While the cells that were treated with concentrations lower than 25 μM – 12.5 and 6.25 μM – showed 100 % cell viability, they failed to elicit an IL-8 response, suggesting that these concentrations failed to stimulate the cells at all. The duration of cell incubation seemed to matter in eliciting IL-8 response. Broadly, the overall IL-8 release seemed to be the greatest at 20 h incubation time. The longer incubation time, on the other hand, showed low cell viability as well as IL-8 response overall, indicating that incubating for a longer time only induces cytotoxicity. From this experiment, I concluded that the optimal assay condition for DNCB was 50 μM and 20 h.

Figure A2.

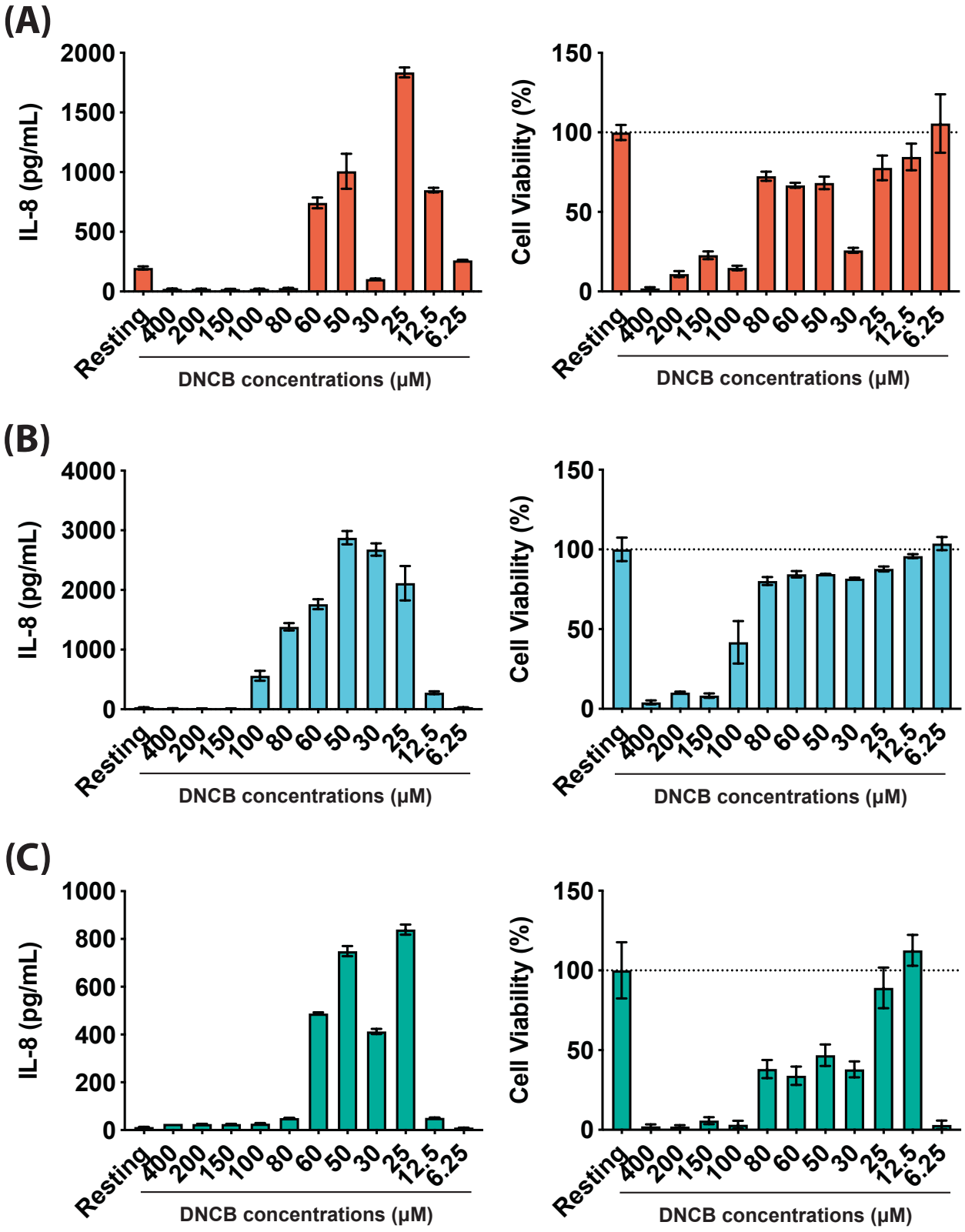
(A)
IL-8 (pg/mL)
2000
1500
1000
500
0
Cell Viability (%)
150
100
50
0
Resting
400
200
150
100
80
60
50
30
25
12.5
6.25
DNCB concentrations (μM)
(B)
IL-8 (pg/mL)
4000
3000
2000
1000
0
Cell Viability (%)
150
100
50
0
DNCB concentrations (μM)
(C)
IL-8 (pg/mL)
1000
800
600
400
200
0
Cell Viability (%)
150
100
50
0
DNCB concentrations (μM)

Figure A2, continued. DNCB dosage curve. To optimize DNCB incubation time and its dosage on THP-1 cells, they were incubated at a cell density of 10^6 cells/mL with 11 different concentration points for **(A)** 14 hrs, **(B)** 20 hrs, and **(C)** 40 hrs. IL-8 secretion to the supernatant was measured using ELISA and the viability of the cells was analyzed with MTT assay. The optimum assay condition was 50 μM DNCB for 20 h incubation.

4. Validation of Anti-DNP Antibody

The specificity of the anti-DNP antibody needs to be validated to ensure that it could bind the leaving group and cyano derivatives. To do so, bovine serum albumin (BSA) was used as a model protein. If BSA modified by DNCB and its derivatives appear in western blotting with anti-DNP antibody, it would confirm that its performance. BSA and the selected compounds (DNCB, –OTs, –OMs, 4–CN, and 2–CN) were dissolved in a solvent mixture composed of 17 parts 1X PBS and 3 parts 100 % CH_3CN (HPLC grade) and incubated in 37 ^{O}C for 7 days. To ensure conjugation, 10 μl of the sample was desalted and analyzed using MALDI (**Figure A3-A5**). Shift in mass was observed from the MALDI spectrum, confirming that DNCB and the derivatives were loaded on BSA. After confirming modification with MALDI, 5 μg of each sample was analyzed by western blotting (**Figure A6**). The samples were separated in SDS-PAGE, transferred to PVDF membrane, and stained using anti-DNP antibody and a secondary antibody with DyLight® 650 conjugate. The membrane was imaged using a gel imager. To ensure that equal amount of protein was used per sample, 5 μg of samples were separated again under the same condition, fixed in gel-fixing solution (50 % v/v ethanol in water with 10 % v/v acetic acid) for 1 h, washed in gel-washing solution (50 % v/v methanol in water with 10 % v/v acetic acid) overnight, stained in Coomassie solution (0.1 % w/v Coomassie blue R350, 20 % v/v methanol in water with 10 % v/v acetic acid) for 3 h, and then

destained with gel-washing solution until the desired intensity of the bands appeared. Band intensity was quantified using ImageJ software and normalized to the band intensity of DNCB sample. All of the tested compounds showed high intensity from western blotting.

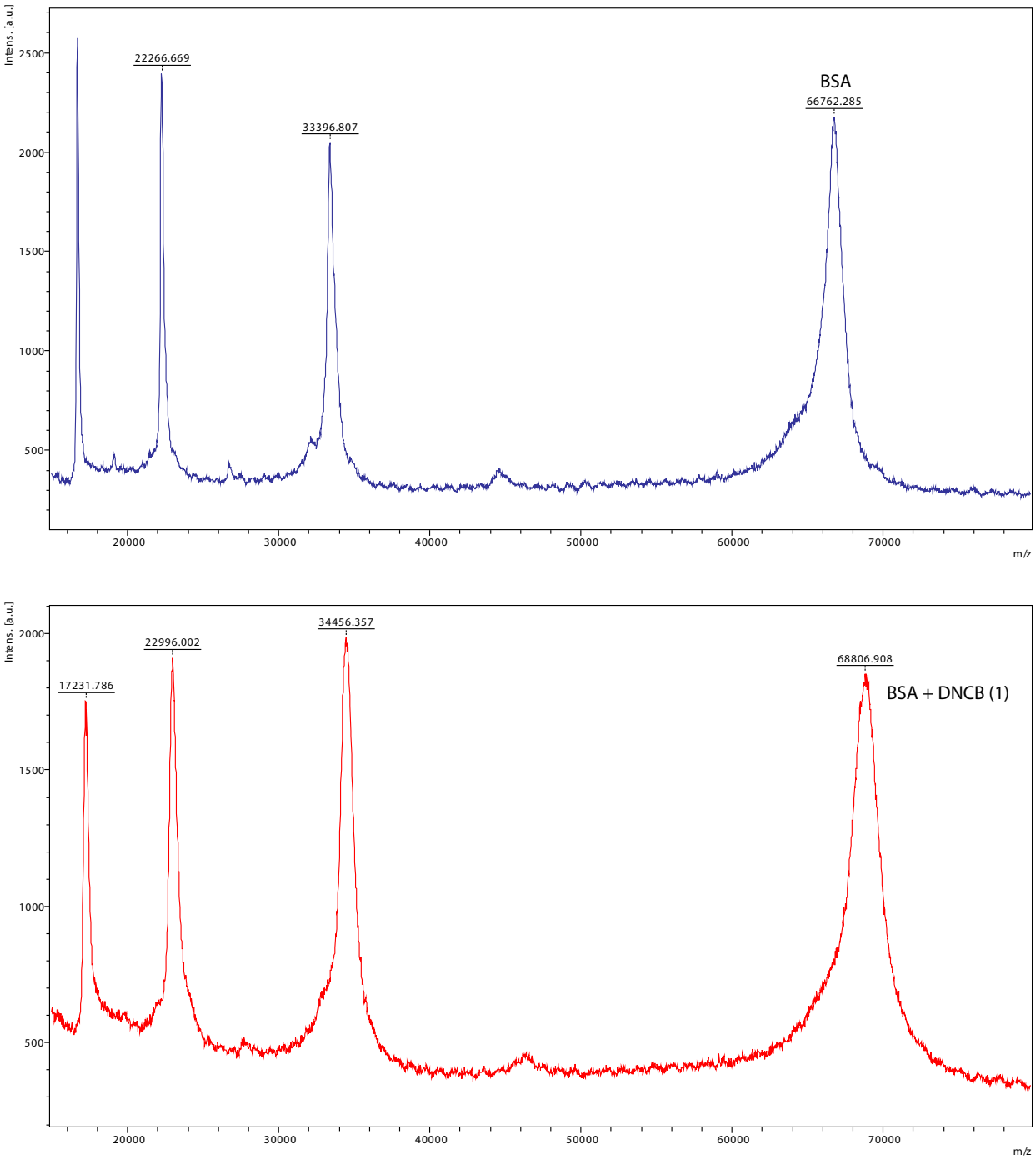

Figure A3. MALDI spectrum showing modification of BSA. **(Top)** Mass of BSA was observed at 66,762 Da. **(Bottom)** Mass of BSA incubated with DNCB was observed at 68,806 Da. The shift of the peak confirms DNCB modification.

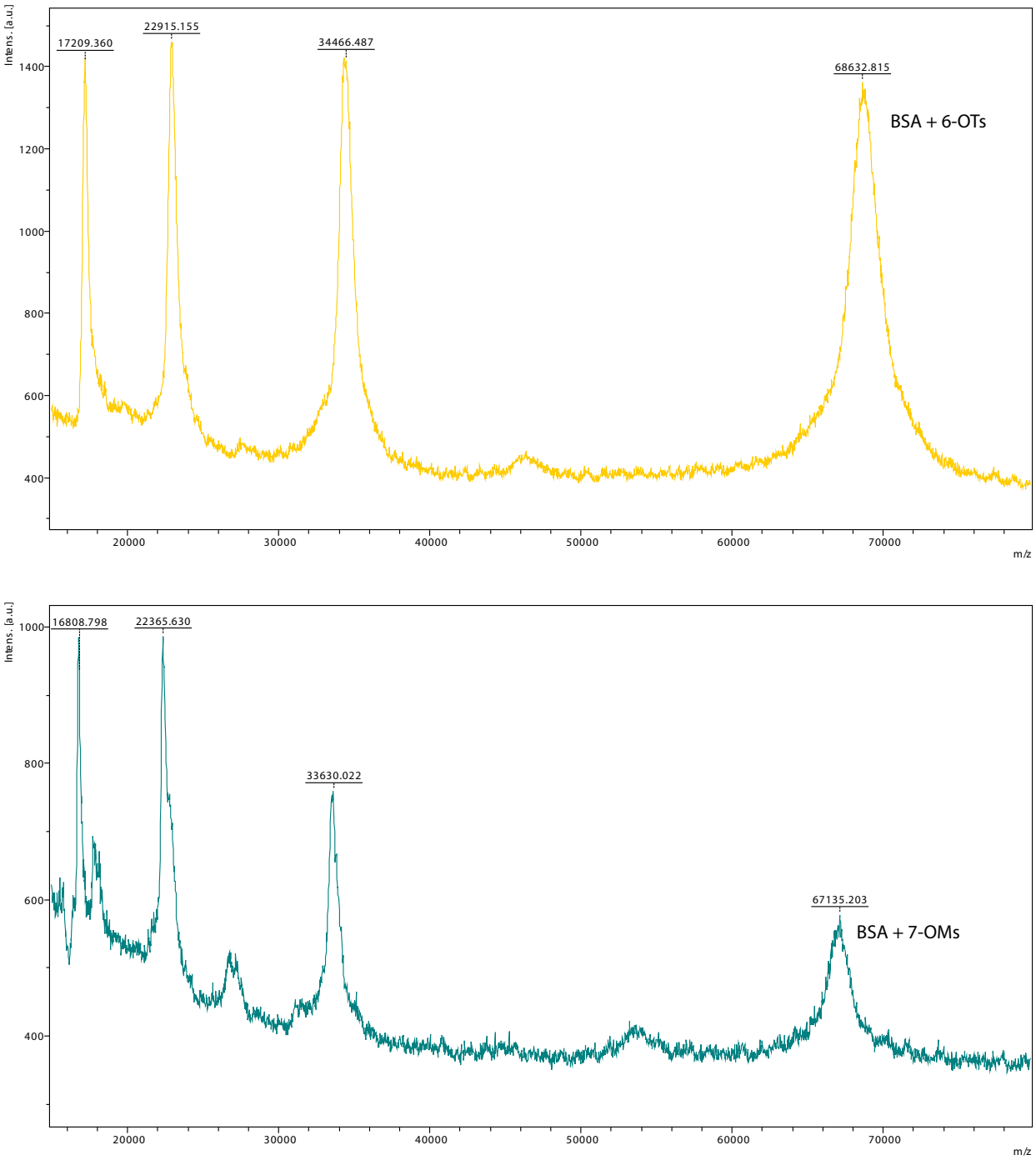

Figure A4. MALDI spectrum showing modification of BSA by **(top)** tosyl derivative (–OTs) at mass of 66,762 Da and **(bottom)** mesyl derivative (–OMs) at mass of 67,135 Da. Figure A3 showed that the mass of BSA was 66,762 Da. The shift of the peak confirms that compounds were successfully loaded on BSA.

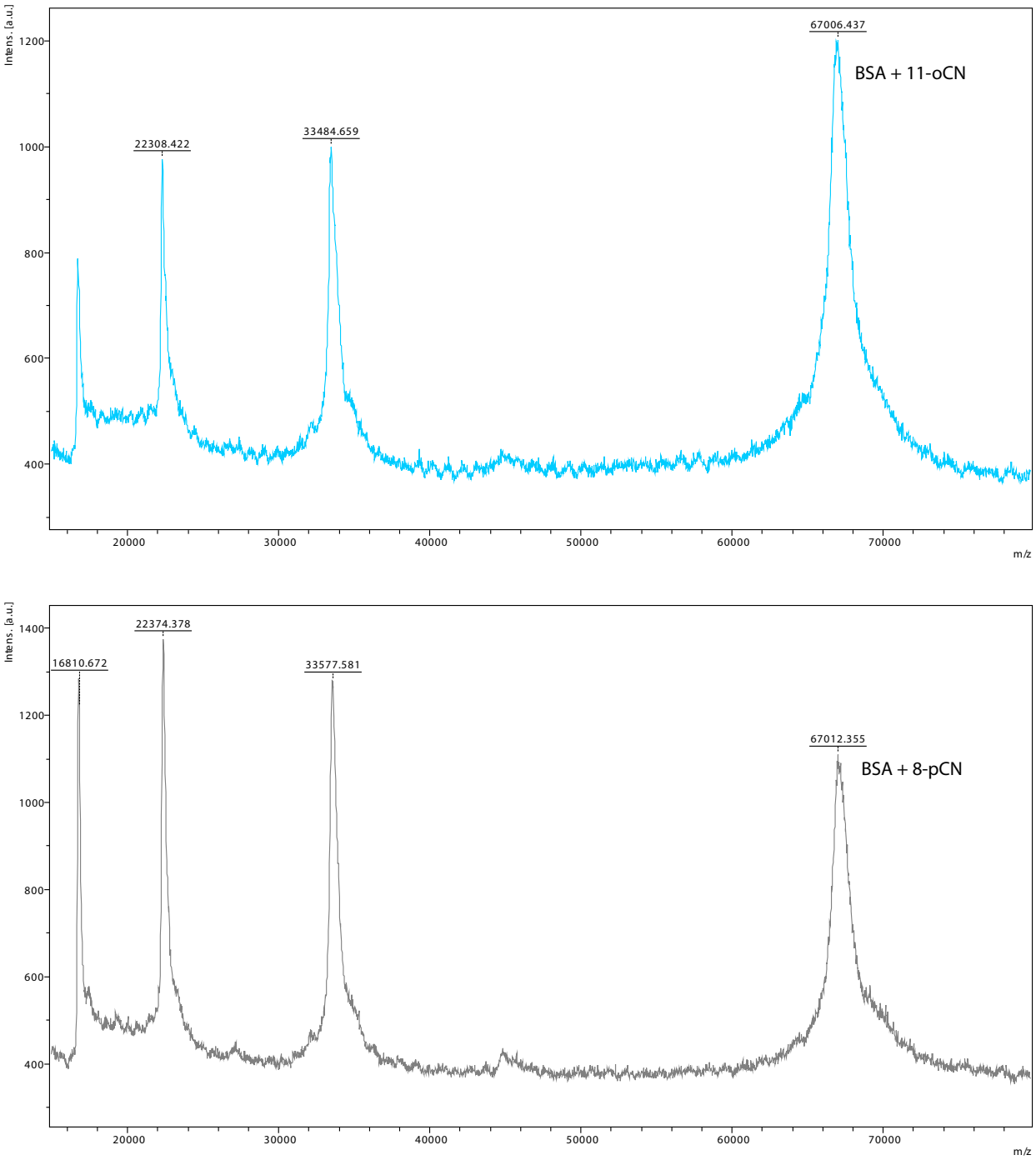

Figure A5. MALDI spectrum showing modification of BSA by cyano derivatives: **(top)** 2–CN at mass of 67,006 Da and **(bottom)** 4–CN at mass of 67,012 Da. Figure A3 showed that the mass of BSA was 66,762 Da. The shift of the peak confirms that compounds were loaded on BSA

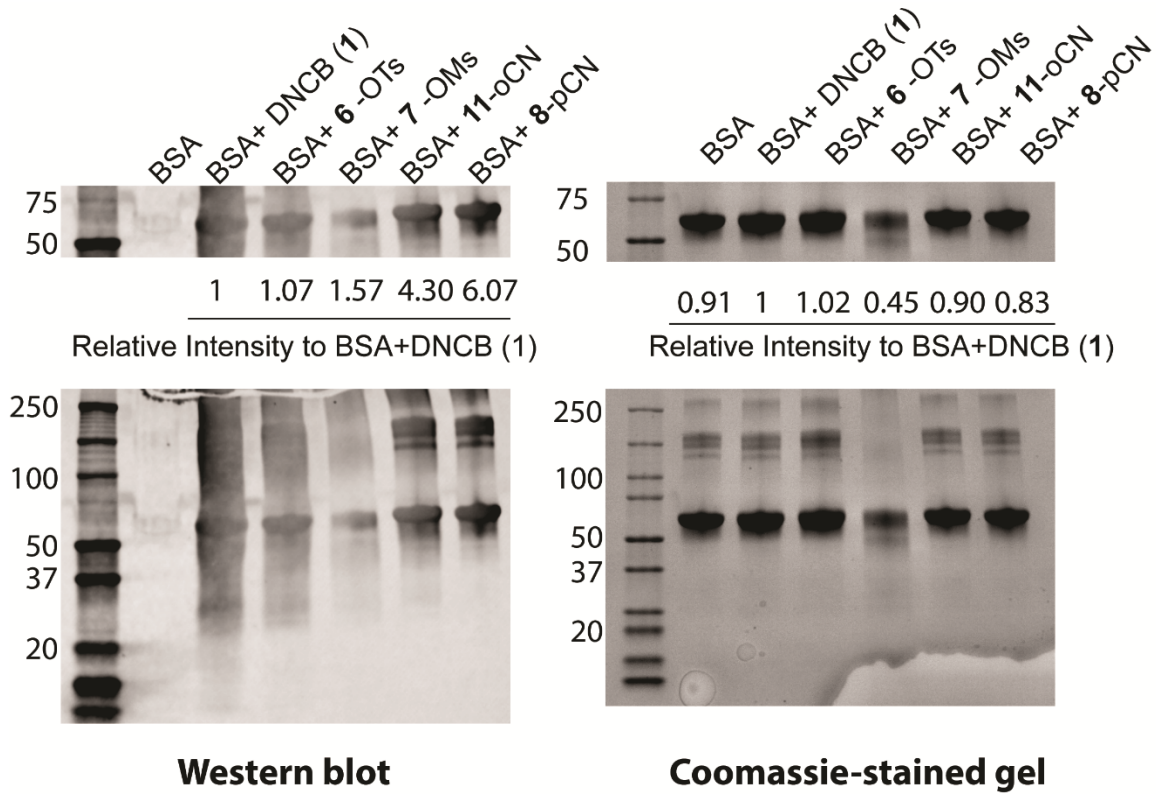

Figure A6. Analysis of BSA and BSA modified with selected DNCB derivatives. **(left)** An image of western blot stained with anti-DNP antibody. Whereas BSA lane is clean, the other lanes clearly show a protein band in between 50 and 75 kDa. Band intensity has been quantified using ImageJ. Relative to the band intensity from BSA + DNCB, they are similar or stronger, which validates the performance of the anti-DNP antibody. **(right)** Image of Coomassie-stained gel, indicating that the same or similar amount of proteins were loaded in each lane.

5. Computational Analysis of Compound Electron Density

All computations were performed using Spartan software (Wavefun. Inc.). Ground state geometrics and energies were optimized in gas phase using the B3LYP functional and 6-31 + G (d,p) basis set for all atoms. The electron density, and the composite surface of |LUMO| mapped onto the electron density were then calculated. Hexyl-2-chloro-3,5-dinitrobenzoate, hexyl-4-

chloro-2,5-dinitrobenzoate, *tert*-butyl-4-chloro-3,5-dinitrobenzoate, and *tert*-butyl-2-chloro-3,5-dinitrobenzoate were truncated to propyl-4-chloro-3,5-dinitrobenzoate, propyl-4-chloro-2,5-dinitrobenzoate, isopropyl-4-chloro-3,5-dinitrobenzoate, isopropyl-2-chloro-3,5-dinitrobenzoate respectively for feasible calculation (**Supplementary Table 1**).

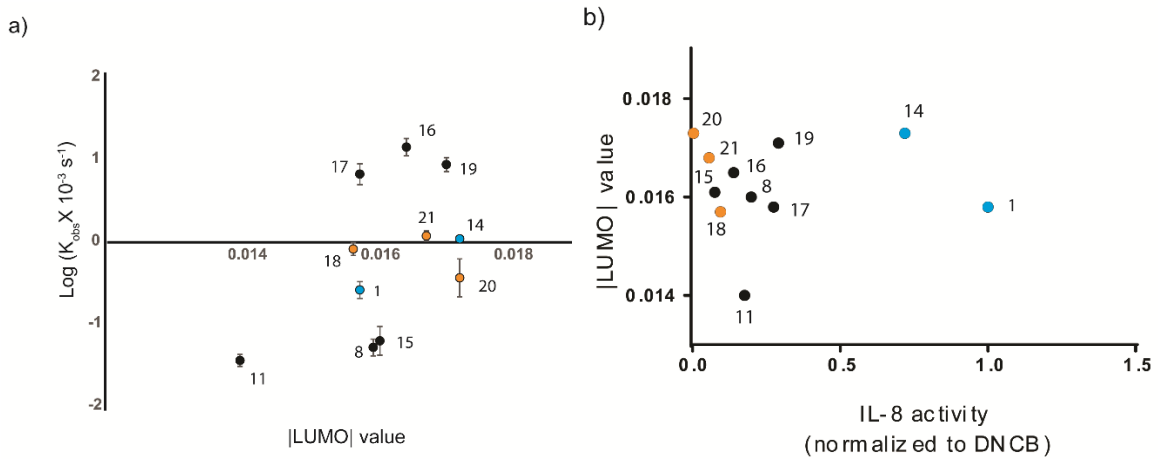

Figure A7. Plot of |LUMO| value at the site of reactivity of DNCB and its derivatives in respect to **(a)** experimental rate of reactivity and **(b)** IL-8 expression. Legends: DNCB (**1**), 4-chloro-3-nitrobenzonitrile (4-CN, **8**), 2-chloro-5-nitrobenzonitrile (2-CN, **11**), 2-chloro-3,5-dinitrobenzoic acid (2-DNCBA or 2-COOH from Figure 2.3B, **14**), 4-chloro-3,5-dinitrobenzoate (4-DNCBA or 4-COOH from Figure 2.3B, **15**), methyl 4-chloro-3,5-dinitrobenzoate (4-DNCBE, 4-COOMe from Figure 2.3B, **16**), methyl 2-chloro-3,5-dinitrobenzoate (2-DNCBE or 2-COOMe from Figure 2.3B, **17**), hexyl 2-chloro-3,5-dinitrobenzoate (2-hexyl, **18**), *tert*-butyl 4-chloro-3,5-dinitrobenzoate (4-butyl, **19**), hexyl 4-chloro-2,5-dinitrobenzoate (4-hexyl, **20**), tert-butyl 2-chloro-3,5-dinitrobenzoate (2-butyl, **21**).

Cartesian Coordinates (Output Report of DFT calculation)

2,4-dinitrochlorobenzene (DNCB, 1)

Cartesian Coordinates (Angstroms)

Atom X Y Z
--- --- --- ---

1 H H1 0.4492974 -0.0860932 -2.8910388
2 C C1 0.2973010 -0.0458389 -1.8188100
3 C C4 -0.1162017 0.0058314 0.9493564
4 C C2 -1.0072315 -0.0387787 -1.3147574
5 C C6 1.3895778 -0.0058344 -0.9604984
6 C C5 1.1640551 0.0193295 0.4146621
7 C C3 -1.2007562 -0.0083314 0.0780202
8 H H6 2.3996365 -0.0008503 -1.3507184
9 H H4 -0.2751247 0.0184154 2.0192049
10 Cl Cl1 -2.3112995 -0.1415958 -2.4597905
11 N N1 -2.5311618 0.0177209 0.7032887
12 O O1 -3.4283999 0.6357692 0.1376124
13 O O2 -2.6538162 -0.5647953 1.7804841
14 N N2 2.3084140 0.0556736 1.3316291
15 O O3 2.0788384 0.0733338 2.5409884
16 O O4 3.4368712 0.0660442 0.8403672

4-chloro-3-nitrobenzonitrile (4-CN, 8)

Cartesian Coordinates (Angstroms)
Atom X Y Z
--- --- --- ---

1 C C1 0.4391560 -0.0286664 -1.3671031
2 C C4 0.4125992 0.0405592 1.4350496
3 C C2 -0.7808862 -0.0139955 -0.6845644
4 C C6 1.6462805 0.0010100 -0.6487395
5 C C5 1.6250523 0.0459491 0.7395207
6 C C3 -0.7890276 0.0061994 0.7074767
7 H H2 -1.7215238 -0.0309135 -1.2211223
8 H H6 2.5946554 -0.0044051 -1.1748205
9 H H5 2.5536176 0.0889888 1.2972360
10 Cl Cl1 0.4813954 0.1500055 3.1710637
11 N N2 -2.1132203 -0.0161819 1.3458743
12 O O1 -3.0279995 0.5586893 0.7554772
13 O O2 -2.2413194 -0.6221461 2.4062803
14 C C7 0.4522863 -0.0707584 -2.7996747
15 N N1 0.4689340 -0.1043342 -3.9619539

2-chloro-5-nitrobenzonitrile (2-CN, 11)

Cartesian Coordinates (Angstroms)

Atom X Y Z
--- --- --- ---

1 C C1 -0.0372451 0.0000000 1.1034450
2 C C4 -0.5858833 0.0000000 -1.6027066
3 C C2 1.0273170 0.0000000 0.2112652
4 C C6 -1.3648898 0.0000000 0.6771844
5 C C5 -1.6371530 0.0000000 -0.6872637
6 C C3 0.7547085 0.0000000 -1.1625302
7 H H2 2.0486671 0.0000000 0.5701481
8 H H6 -2.1705881 0.0000000 1.4008158
9 H H5 -2.6618632 0.0000000 -1.0407518
10 C C7 1.8448437 0.0000000 -2.0908190
11 N N1 2.7437080 0.0000000 -2.8281164
12 Cl Cl1 -0.9418016 0.0000000 -3.3067652
13 N N2 0.2513879 0.0000000 2.5418520
14 O O1 1.4312942 0.0000000 2.8942032
15 O O2 -0.7025021 0.0000000 3.3200392

4-chloro-3,5-dinitrobenzoic acid (12)

Cartesian Coordinates (Angstroms)
Atom X Y Z
--- --- --- ---

1 C C1 0.1264008 -0.2132394 -1.4493297
2 C C4 -0.0686273 -0.2548410 1.3128548
3 C C2 0.2093503 -1.4554281 -0.7986465
4 C C6 -0.0509933 0.9785126 -0.7538415
5 C C5 -0.1350719 0.9631372 0.6379671
6 C C3 0.1074166 -1.4363061 0.6030249
7 H H6 -0.1161367 1.9065303 -1.3078466
8 H H4 -0.1484803 -0.2836308 2.3929053
9 Cl Cl1 0.2860072 -2.9390397 -1.6846832
10 N N1 0.2224601 -0.0940314 -2.9155380
11 O O3 -0.5383779 0.7062412 -3.4557593
12 O O4 1.0699815 -0.7628734 -3.4979240
13 N N2 0.1802349 -2.6693078 1.4079347
14 O O5 -0.5847464 -2.7483642 2.3670039
15 O O6 1.0124069 -3.5164537 1.0998026
16 C C7 -0.3102425 2.2098945 1.4436492
17 O O1 -0.3794297 2.2190876 2.6574538
18 O O2 -0.3836064 3.3079032 0.6774090
19 H H1 -0.4985462 4.0822089 1.2635634

2-chloro-3,5-dinitrobenzoic acid (14)

Cartesian Coordinates (Angstroms)
Atom X Y Z
--- --- --- ---

1 H H1 0.0138182 0.4887702 -2.3308442
2 C C1 0.0130871 0.3669816 -1.2553677
3 C C4 0.0326286 0.0728886 1.4987965
4 C C2 0.0847166 -0.9179259 -0.7100412
5 C C6 -0.0561796 1.4741655 -0.4225532
6 C C5 -0.0362351 1.3498855 0.9587288
7 C C3 0.1057001 -1.0774657 0.6908445
8 H H5 -0.0778132 2.2188498 1.6023378
9 N N1 -0.1375306 2.8157666 -1.0134356
10 O O1 -0.2026273 3.7755923 -0.2467692
11 O O2 -0.1352669 2.9023893 -2.2401522
12 N N2 0.0236770 0.0043181 2.9719563
13 O O3 -0.6669359 -0.8561717 3.5075051
14 O O4 0.6869195 0.8498892 3.5690233
15 Cl Cl1 0.3493564 -2.6367073 1.4094676
16 C C7 0.1624136 -2.0267330 -1.7283120
17 O O5 0.7166838 -1.8767021 -2.7988711
18 O O6 -0.4845907 -3.1384324 -1.3684314
19 H H2 -0.3918218 -3.7893585 -2.0938822

Methyl 4-chloro-3,5-dinitrobenzoate (15)

Cartesian Coordinates (Angstroms)
Atom X Y Z
--- --- --- ---

1 H H1 -0.0369360 -0.7211779 -1.8122120
2 C C1 -0.0277991 -0.7002817 -0.7298653
3 C C4 -0.0191005 -0.7141566 2.0428620
4 C C2 -0.0398607 -1.9024490 -0.0289548
5 C C6 0.0031731 0.5086108 -0.0356608
6 C C5 -0.0097392 0.4947629 1.3578149
7 C C3 -0.0347998 -1.9504219 1.3751307
8 H H5 -0.0037422 1.4260076 1.9115040
9 Cl Cl1 -0.1807649 -3.4445218 2.2356615
10 C C7 0.0371952 1.8355954 -0.7281075
11 O O1 0.0487955 2.8973751 -0.1330761
12 O O2 0.0543055 1.7087018 -2.0577144
13 N N1 -0.0592575 -3.1257915 -0.8512624
14 O O3 -0.7659207 -3.1037878 -1.8570751

15 O O4 0.6483054 -4.0680817 -0.5097067
16 N N2 -0.0089345 -0.6209891 3.5137025
17 O O5 0.7155288 -1.3887491 4.1387410
18 O O6 -0.7083013 0.2558954 4.0168129
19 C C8 0.0904240 2.9392525 -2.8171428
20 H H2 0.9887376 3.5074260 -2.5659349
21 H H3 -0.7991766 3.5360961 -2.6042621
22 H H4 0.1078681 2.6306847 -3.8612546

Hexyl 2-chloro-3,5-dinitrobenzoate (18)

Cartesian Coordinates (Angstroms)
Atom X Y Z
--------- ------------ ------------ ------------

1 C C1 -0.7053936 -2.1927823 -2.1602347
2 C C4 -0.1591117 -1.8831881 0.5385827
3 C C2 -0.3516414 -3.3082511 -1.4126380
4 C C6 -0.8057237 -0.9114513 -1.5864408
5 C C5 -0.5180056 -0.7631347 -0.2155223
6 C C3 -0.0704548 -3.1290474 -0.0663607
7 H H2 -0.2932253 -4.2849666 -1.8745114
8 H H4 0.0460796 -1.7726354 1.5956977
9 N N1 -0.9667282 -2.4423286 -3.5893662
10 O O1 -1.5818131 -3.4697351 -3.8683869
11 O O2 -0.5271047 -1.6411708 -4.4076059
12 N N2 0.3161154 -4.2936685 0.7392947
13 O O3 0.3659284 -5.3874062 0.1781178
14 O O4 0.5678829 -4.1090787 1.9290106
15 C C7 -0.5965805 0.5291666 0.5612916
16 O O5 -1.0332755 0.5622330 1.6962946
17 O O6 -0.0892360 1.5635793 -0.1037535
18 Cl Cl1 -1.4005793 0.4275244 -2.5161478
19 C C8 -0.1020486 2.8642056 0.5625414
20 H H3 -1.0158381 2.9407203 1.1558322
21 H H5 -0.1397069 3.5806098 -0.2605407
22 C C9 1.1453738 3.0558249 1.4154996
23 H H1 2.0316876 2.9102461 0.7861396
24 H H6 1.1690484 2.2856715 2.1951977
25 C C10 1.1717803 4.4498087 2.0532781
26 H H8 0.3019745 4.6055288 2.7024922
27 H H9 1.1679059 5.2367675 1.2897671
28 H H7 2.0726899 4.5769583 2.6624711

***Tert*-butyl 4-chloro-3,5 dinitrobenzoate (19)**

Cartesian Coordinates (Angstroms)
Atom X Y Z
--- --- --- ---

1 C C1 0.0747392 0.0197820 -3.4234814
2 C C4 -0.2729775 0.0079309 -0.6083184
3 C C2 -1.2017717 0.0196777 -2.8355857
4 C C6 1.1683062 0.0201775 -2.5417308
5 C C5 1.0074928 0.0236356 -1.1595720
6 C C3 -1.3783821 0.0201128 -1.4566490
7 C C7 -0.5164504 -0.0110537 0.8742057
8 O O1 -1.6397630 -0.0413793 1.3457176
9 O O2 0.6276007 0.0094435 1.5551746
10 N N1 -2.4347385 0.0170065 -3.6434198
11 O O3 -2.4746436 -0.6944679 -4.6422270
12 O O4 -3.3647472 0.7100419 -3.2352436
13 N N2 2.5600597 0.0135821 -3.0271095
14 O O5 3.3618833 0.7199025 -2.4189437
15 O O6 2.8417220 -0.7156562 -3.9727935
16 Cl Cl1 0.2896933 0.1564452 -5.1354263
17 C C8 0.6419593 -0.0121516 3.0335545
18 C C9 0.0735602 -1.3206554 3.5705546
19 C C11 0.0065678 1.2473351 3.6114292
20 H H5 1.8852552 0.0303880 -0.5261101
21 H H3 -2.3795720 0.0233308 -1.0430779
22 H H6 -1.0070456 -1.3837473 3.4234521
23 H H7 0.2837225 -1.3786199 4.6440993
24 H H2 0.5519970 -2.1766176 3.0833846
25 H H11 0.2141156 1.2812517 4.6865770
26 H H1 -1.0758558 1.2587984 3.4653006
27 H H10 0.4394910 2.1424654 3.1529679
28 H H12 1.7177813 0.0130413 3.2232710

Hexyl 4-chloro-2,5-dinitrobenzoate (20)

Cartesian Coordinates (Angstroms)
Atom X Y Z
--- --- --- ---

1 C C1 2.1863776 -0.1461477 -1.7864526
2 C C4 2.2735615 0.0950071 0.9706097
3 C C2 3.4458112 -0.1130870 -1.1650215

4 C C6 1.0000756 -0.0618112 -1.0644440
5 C C5 1.0391937 0.0461237 0.3251091
6 C C3 3.4496040 0.0077762 0.2350210
7 N N1 4.7016521 0.0482866 1.0118148
8 O O1 5.6086835 -0.7140389 0.6930499
9 O O2 4.7380073 0.8283546 1.9614009
10 N N2 2.0421132 -0.2732814 -3.2478748
11 O O3 2.7668772 -1.0694327 -3.8360306
12 O O4 1.1677650 0.4091021 -3.7783132
13 Cl Cl1 4.9108005 -0.0769464 -2.0852912
14 C C7 -0.2013449 0.1282524 1.1609551
15 O O5 -0.1776532 0.2488003 2.3726900
16 O O6 -1.3101527 0.0534858 0.4227435
17 H H1 2.3200744 0.1938896 2.0484293
18 H H3 0.0564673 -0.0863961 -1.5945607
19 C C8 -2.5796147 0.1280249 1.1345945
20 H H2 -2.6265049 1.0922884 1.6500286
21 H H4 -2.5977849 -0.6679869 1.8854360
22 C C9 -3.6925968 -0.0260284 0.1127590
23 H H5 -3.6039766 0.7691592 -0.6377004
24 H H7 -3.5665547 -0.9809467 -0.4121596
25 C C10 -5.0716947 0.0311458 0.7795979
26 H H6 -5.2246652 0.9865432 1.2954492
27 H H8 -5.1903076 -0.7723970 1.5160147
28 H H9 -5.8642130 -0.0777394 0.0321455

***Tert*-butyl 2-chloro-3, 5-dinitrobenzoate (21)**

Cartesian Coordinates (Angstroms)
Atom X Y Z
--- --- --- ---

1 H H1 0.5907576 1.8294588 -1.4638057
2 C C1 0.3604655 1.7981312 -0.4071967
3 C C4 -0.2519112 1.7465179 2.2861241
4 C C2 -0.0963723 0.6122208 0.1606849
5 C C6 0.5132118 2.9282237 0.3760474
6 C C5 0.2021255 2.9262596 1.7228867
7 C C3 -0.4211575 0.5779846 1.5271093
8 H H5 0.3112078 3.8169550 2.3265488
9 C C7 -0.2324085 -0.5403473 -0.7997203
10 O O1 -0.6115670 -0.3605897 -1.9392321
11 O O2 0.1636135 -1.6834767 -0.2702025
12 Cl Cl1 -1.1366657 -0.8279347 2.2267673
13 N N1 1.0011817 4.1618344 -0.2336519

14 O O3 1.1254680 5.1444076 0.4887570
15 O O4 1.2572156 4.1432865 -1.4320184
16 N N2 -0.5412847 1.8024227 3.7224444
17 O O5 -0.2250273 0.8449115 4.4130533
18 O O6 -1.0529155 2.8334270 4.1425462
19 C C8 0.0921186 -2.9396098 -1.0333161
20 C C9 -1.3422481 -3.2833198 -1.3890571
21 H H3 -1.7420494 -2.6086111 -2.1478646
22 H H6 -1.9790658 -3.2426836 -0.5015982
23 H H7 -1.3699864 -4.3041461 -1.7812517
24 C C11 1.0515694 -2.9227359 -2.2078697
25 H H2 2.0538144 -2.6291287 -1.8842997
26 H H10 0.7158751 -2.2415402 -2.9912106
27 H H11 1.1103985 -3.9328485 -2.6243249
28 H H12 0.4536366 -3.6490691 -0.2863493

6. Determination of Protein Spots to Analyze from 2-Dimensional Gel Electrophoresis

Two-dimensional gel electrophoresis and western blotting were performed by Kendricks Laboratory (Madison, WI). Briefly summarizing, proteins were first separated according to the carrier ampholyte method of isoelectric focusing in a glass tube using 2.0 % pH 3-10 Isodalt Servalytes.[8,9] Then, each tube gel was sealed to the top of a stacking gel that overlaid 10 % acrylamide slab gel (1.0 mm thick) for the secondary separation by molecular weight. The gel was transblotted on a PVDF membrane, blocked in a blocking buffer, stained with anti-DNP antibody, and then stained with anti-mouse IgG-HRP for two hours. After treating with ECL, the membrane was exposed to x-ray film.

To monitor protein spot development, the membrane was treated with different amounts of anti-DNP antibody and ECL. First, the membrane was treated with anti-DNP antibody diluted 1:100,000 in blocking buffer and exposed for 10 s, 30 s, and 1 min (**Figure A8** top row). Due to the strong signal ECL, spots are hard to distinguish from each other, and smears are also visible. Western blot was repeated using anti-DNP antibody diluted 1:1,000,000 in blocking buffer

(**Figure A8** bottom row), and I was able to remove smears and background signals. There were certain spots with weak signals that ultimately develop into strong signal over time (1 min to 10 min). Those spots were labeled from [A] to [F] and they were excised for downstream analysis.

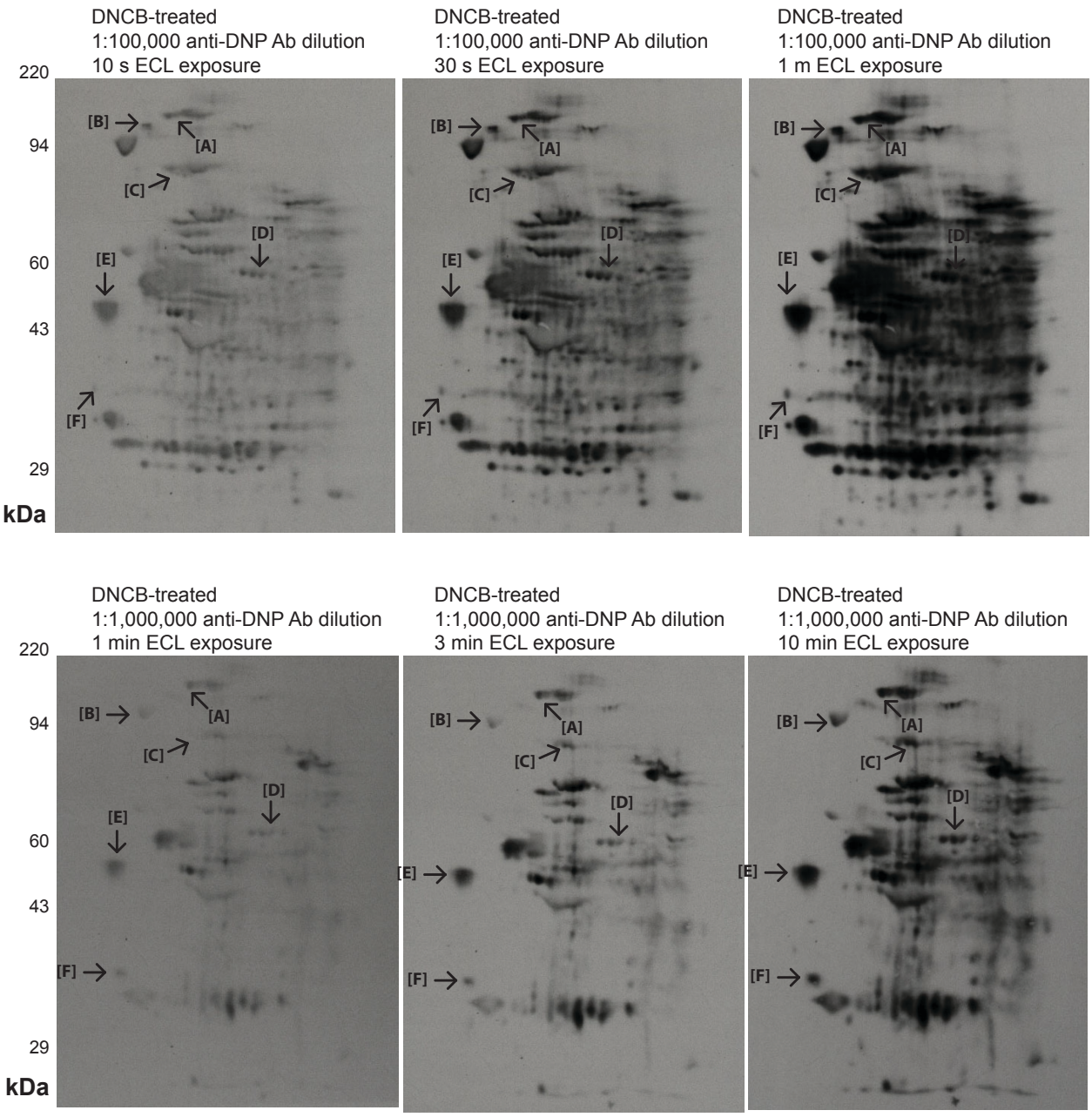

Figure A8. Development of excised spots (labeled from [A] to [F] with arrows) probed with anti-DNP antibody and ECL. All the images show the same cellular lysate sample – that is, DNCB-modified. PVDF membrane was stained with anti-DNP antibody diluted 1:100,000 and developed over 1 min **(top)** or 1:1,000,000 **(bottom)** and developed over 10 min. Looking at spot trend overall, I chose the spots that were well distinct and grew darker.

7. Supplementary Data for Chapter 3: Mass Spectrometry Results

Table A1. Complete List of Identified Proteins Including Unmodified Proteins

	Name	Gene ID	Molecular Weight (kDa)
1	4F2 cell-surface antigen heavy chain	SLC3A2	68
2	6-phosphofructo-2-kinase/fructose-2,6-biphosphatase 4	PFKFB4	54
3	14-3-3 protein epsilon	YWHAE	29
4	14-3-3 protein theta	YWHAQ	28
5	14-3-3 protein zeta/delta	YWHAZ	28
6	26 S protease regulatory subunit 4	PSMC1	49
7	26 S protease regulatory subunit 7	PSMC2	49
8	26 S proteasome non-ATPase regulatory subunit	PSMD1	106
9	60 kDa heat shock protein, mitochondrial	HSPD1	61
10	60S ribosomal protein L23a	RPL23A	18
11	116 kDa U5 small nuclear ribonucleoprotein component	EFTUD2	109
12	A-kinase anchor protein 8-like	AKAP8L	72
13	A-kinase anchor protein 9	AKAP9	454
14	ADP-ribosylation factor 3	ARF3	21
15	ADP-ribosylation factor-binding protein GGA1	GGA1	70
16	ATP-dependent RNA helicase DDX19A	DDX19A	54
17	ATP-dependent RNA helicase DDX19B	DDX19B	54
18	ATP-dependent RNA helicase DDX39A	DDX39A	49
19	Abl interactor 1	ABI1	55
20	Acidic leucine-rich nuclear phosphoprotein 32 family member B	ANP32B	29
21	Actin, alpha cardiac muscle 1	ACTC1	42
22	Actin, cytoplasmic 1	ACTB	42
23	Actin-related protein 3	ACTR3	47
24	Adenylyl cyclase-associated protein 1	CAP1	52
25	Adenylyl cyclase-associated protein 2	CAP2	53
26	Alanine--tRNA ligase, cytoplasmic	AARS	107
27	Aldehyde dehydrogenase, mitochondrial	ALDH2	56
28	Alpha-N-acetylgalactosaminidase	NAGA	47
29	Alpha-actinin-1	ACTN1	103
30	Alpha-actinin-4	ACTN4	105
31	Angiotensinogen	AGT	53
32	Ankyrin repeat domain-containing protein 13A	ANKRD13A	68
33	Ankyrin repeat domain-containing protein 17	ANKRD17	274
34	Annexin A5	ANXA5	36
35	Annexin A6	ANXA6	76
36	Apoptosis inhibitor 5	API5	59
37	Atlastin-3	ATL3	61

Table A1, continued

38	Bcl-2-like protein 13	BCL2L13	53
39	Beta-arrestin-1	ARRB1	47
40	Beta-hexosaminidase subunit beta	HEXB	63
41	Bridging integrator 2	BIN2	62
42	CAAX prenyl protease 1 homolog	ZMPSTE24	55
43	CD276 antigen	CD276	57
44	COP9 signalosome complex subunit 1	GPS1	56
45	Calcium-binding and coiled-coil domain-containing protein 1	CALCOCO1	77
46	Caprin-1	CAPRIN1	78
47	Carboxypeptidase Q	CPQ	52
48	Cathepsin L1	CTSL	38
49	Chloride intracellular channel protein 1	CLIC1	27
50	Cleft lip and palate transmembrane protein 1-like protein	CLPTM1L	62
51	Coatomer subunit delta	ARCN1	57
52	Coiled-coil domain-containing protein 43	CCDC43	25
53	Condensin-2 complex subunit H2	NCAPH2	68
54	Copine-1	CPNE1	59
55	Copine-2	CPNE2	61
56	Coronin-1A	CORO1A	51
57	Coronin-1B	CORO1B	54
58	Coronin-7	CORO7	101
59	Cytosolic non-specific dipeptidase	CNDP2	53
60	D-3-phosphoglycerate dehydrogenase	PHGDH	57
61	DCC-interacting protein 13-alpha	APPL1	80
62	DNA replication licensing factor MCM6	MCM6	93
63	Deoxyhypusine hydroxylase	DOHH	33
64	Desmoplakin	DSP	332
65	Diacylglycerol kinase zeta	DGKZ	124
66	Dihydrolipoyllysine-residue succinyltransferase component of 2-oxoglutarate dehydrogenase complex, mitochondrial	DLST	49
67	Dipeptidyl peptidase 2	DPP7	54
68	Disintegrin and metalloproteinase domain-containing protein 15	ADAM15	93
69	Docking protein 2	DOK2	45
70	E3 ubiquitin-protein ligase KCMF1	KCMF1	42
71	E3 ubiquitin-protein ligase RING1	RING1	42
72	E3 ubiquitin-protein ligase RNF146	RNF146	39
73	Elongation factor 1-alpha 1	EEF1A1	50
74	Elongation factor 1-beta	EEF1B2	25
75	Endoplasmin	HSP90B1	92

Table A1, continued

76	Enolase-phosphatase E1	ENOPH1	29
77	Epidermal growth factor receptor substrate 15-like 1	EPS15L1	94
78	Eukaryotic initiation factor 4A-II	EIF4A2	46
79	Eukaryotic peptide chain release factor GTP-binding subunit ERF3A	GSPT1	56
80	Eukaryotic translation initiation factor 5	EIF5	49
81	Extended synaptotagmin-1	ESYT1	123
82	F-BAR and double SH3 domains protein 1	FCHSD1	77
83	F-box-like/WD repeat-containing protein TBL1X	TBL1X	62
84	FAD synthase	FLAD1	65
85	FAS-associated factor 1	FAF1	74
86	FAS-associated factor 2	FAF2	53
87	FERM domain-containing protein 8	FRMD8	51
88	FGGY carbohydrate kinase domain-containing protein	FGGY	60
89	Filaggrin-2	FLG2	248
90	G patch domain and KOW motifs-containing protein	GPKOW	52
91	Gelsolin	GSN	86
92	General vesicular transport factor p115	USO1	108
93	Glucose-6-phosphate isomerase	GPI	63
94	Glucosidase 2 subunit beta	PRKCSH	59
95	Glycine--tRNA ligase	GARS	83
96	Golgi-associated PDZ and coiled-coil motif-containing protein	GOPC	51
97	Guanine nucleotide-binding protein G(k) subunit alpha	GNAI3	41
98	HLA class I histocompatibility antigen, B-15 alpha chain	HLA-B	40
99	Heat shock 70 kDa protein 1A	HSPA1A	70
100	Heat shock 70 kDa protein 4	HSPA4	94
101	Heat shock 70 kDa protein 13	HSPA13	52
102	Heat shock cognate 71 kDa protein	HSPA8	71
103	Heat shock protein 105 kDa	HSPH1	97
104	Heat shock protein HSP 90-alpha A2	HSP90AA2P	39
105	Heat shock protein HSP 90-alpha	HSP90AA1	85
106	Heat shock protein HSP 90-beta	HSP90AB1	83
107	Hematopoietic lineage cell-specific protein	HCLS1	54
108	Hemoglobin subunit alpha	HBA1	15
109	Hemoglobin subunit beta	HBB	16
110	Hemoglobin subunit gamma-2	HBG2	16
111	Heterogeneous nuclear ribonucleoprotein H	HNRNPH1	49
112	Heterogeneous nuclear ribonucleoprotein K	HNRNPK	51
113	Heterogeneous nuclear ribonucleoprotein Q	SYNCRIP	70
114	Heterogeneous nuclear ribonucleoprotein R	HNRNPR	71
115	Heterogeneous nuclear ribonucleoprotein U	HNRNPU	91

Table A1, continued

116	Hexokinase-3	HK3	99
117	Histone H2B type 1-A	HIST1H2BA	14
118	Histone H4	HIST1H4A	11
119	Hornerin	HRNR	282
120	Hsc70-interacting protein	ST13	41
121	Hsp90 co-chaperone Cdc37	CDC37	44
122	Hypoxia up-regulated protein 1	HYOU1	111
123	Immunoglobulin kappa variable 2-28	IGKV2-28	13
124	Importin subunit alpha-1	KPNA2	58
125	Importin subunit beta-1	KPNB1	97
126	Inhibitor of growth protein 3	ING3	47
127	Integrin alpha-4	ITGA4	115
128	Integrin beta-2	ITGB2	85
129	Interferon regulatory factor 5	IRF5	56
130	Interleukin enhancer-binding factor 2	ILF2	43
131	Junction plakoglobin	JUP	82
132	Keratin, type I cuticular Ha3-II	KRT33B	46
133	Keratin, type I cytoskeletal 9	KRT9	62
134	Keratin, type I cytoskeletal 10	KRT10	59
135	Keratin, type I cytoskeletal 14	KRT14	52
136	Keratin, type I cytoskeletal 16	KRT16	51
137	Keratin, type II cuticular Hb5	KRT85	56
138	Keratin, type II cuticular Hb6	KRT86	53
139	Keratin, type II cytoskeletal 1	KRT1	66
140	Keratin, type II cytoskeletal 2 epidermal	KRT2	65
141	Keratin, type II cytoskeletal 4	KRT4	57
142	Keratin, type II cytoskeletal 5	KRT5	62
143	Keratin, type II cytoskeletal 6A	KRT6A	60
144	Keratin, type II cytoskeletal 6B	KRT6B	60
145	Keratin, type II cytoskeletal 6C	KRT6C	60
146	L-lactate dehydrogenase B chain	LDHB	37
147	Lamin-B2	LMNB2	70
148	Leucine-rich PPR motif-containing protein, mitochondrial	LRPPRC	158
149	Lon protease homolog, mitochondrial	LONP1	106
150	Lupus La protein	SSB	47
151	Lysophosphatidylcholine acyltransferase 1	LPCAT1	59
152	Lysosomal Pro-X carboxypeptidase	PRCP	56
153	Lysosomal alpha-glucosidase	GAA	105
154	Major vault protein	MVP	99
155	Matrix metalloproteinase-14	MMP14	66
156	Myosin-9	MYH9	227

Table A1, continued

157	NAD-dependent malic enzyme, mitochondrial	ME2	65
158	Neutral amino acid transporter A	SLC1A4	56
159	Neutral amino acid transporter B(0)	SLC1A5	57
160	Nicotinate phosphoribosyltransferase	NAPRT	58
161	Nuclease-sensitive element-binding protein 1	YBX1	36
162	Nucleolin	NCL	77
163	Nucleosome assembly protein 1-like 1	NAP1L1	45
164	015457-DECOY	015457-DECOY	?
165	Opioid growth factor receptor	OGFR	73
166	Oxysterol-binding protein-related protein 2	OSBPL2	55
167	PRAME family member 12	PRAMEF12	55
168	Peptidyl-prolyl cis-trans isomerase FKBP4	FKBP4	52
169	Peptidyl-prolyl cis-trans isomerase FKBP5	FKBP5	51
170	Phosphate carrier protein, mitochondrial	SLC25A3	40
171	Phosphatidylinositol 4-phosphate 5-kinase type-1 gamma	PIP5K1C	73
172	Phosphoglucomutase-2	PGM2	68
173	Phospholipase D3	PLD3	55
174	Plastin-2	LCP1	70
175	Prenylcysteine oxidase 1	PCYOX1	57
176	Probable Xaa-Pro aminopeptidase 3	XPNPEP3	57
177	Proliferating cell nuclear antigen	PCNA	29
178	Prolyl 3-hydroxylase 1	P3H1	83
179	Protein ERGIC-53	LMAN1	58
180	Protein Hook homolog 3	HOOK3	83
181	Protein LYRIC	MTDH	64
182	Protein OS-9	OS9	76
183	Protein PRRC1	PRRC1	47
184	Protein RCC2	RCC2	56
185	Protein Shroom3	SHROOM3	217
186	Protein disulfide-isomerase A3	PDIA3	57
187	Protein disulfide-isomerase A4	PDIA4	73
188	Protein disulfide-isomerase A6	PDIA6	48
189	Protein disulfide-isomerase	P4HB	57
190	Protein misato homolog 1	MSTO1	62
191	Protein phosphatase Slingshot homolog 3	SSH3	73
192	Protein scribble homolog	SCRIB	175
193	Putative heat shock protein HSP 90-alpha A4	HSP90AA4P	48
194	Putative heat shock protein HSP 90-beta 4	HSP90AB4P	58
195	Pyridoxal-dependent decarboxylase domain-containing protein 1	PDXDC1	87

Table A1, continued

196	Q5HYW3-DECOY	Q5HYW3-DECOY	?
197	Rab proteins geranylgeranyltransferase component A 2	CHML	74
198	Ran GTPase-activating protein 1	RANGAP1	64
199	RanBP-type and C3HC4-type zinc finger-containing protein 1 OS	RBCK1	58
200	Rap1 GTPase-GDP dissociation stimulator 1	RAP1GDS1	66
201	Ras GTPase-activating-like protein IQGAP1	IQGAP1	189
202	Ras-related protein Rab-7a	RAB7A	23
203	Ras-related protein Rab-10	RAB10	23
204	Reticulocalbin-1	RCN1	39
205	Reticulon-4	RTN4	130
206	Rho GTPase-activating protein 27	ARHGAP27	98
207	Ribonuclease inhibitor	RNH1	50
208	SHC SH2 domain-binding protein 1	SHCBP1	76
209	SUMO-activating enzyme subunit 2	UBA2	71
210	SWI/SNF complex subunit SMARCC2	SMARCC2	133
211	SWI/SNF-related matrix-associated actin-dependent regulator of chromatin subfamily E member 1	SMARCE1	47
212	Serine/threonine-protein phosphatase 2A 55 kDa regulatory subunit B alpha isoform	PPP2R2A	52
213	Serine/threonine-protein phosphatase 2A 56 kDa regulatory subunit gamma isoform	PPP2R5C	61
214	Serine/threonine-protein phosphatase 2A 65 kDa regulatory subunit A alpha isoform	PPP2R1A	65
215	Serine/threonine-protein phosphatase 2B catalytic subunit alpha isoform	PPP3CA	59
216	Serine/threonine-protein phosphatase 5	PPP5C	57
217	Serum albumin	ALB	69
218	Shootin-1	SHTN1	72
219	Sodium/potassium-transporting ATPase subunit alpha-1	ATP1A1	113
220	Sorting nexin-4	SNX4	52
221	Splicing factor 3A subunit 3	SF3A3	59
222	Stress-70 protein, mitochondrial	HSPA9	74
223	Striatin	STRN	86
224	Structural maintenance of chromosomes protein 2	SMC2	136
225	Succinyl-CoA:3-ketoacid coenzyme A transferase 1, mitochondrial	OXCT1	56
226	Synaptophysin-like protein 1	SYPL1	29
227	T-complex protein 1 subunit alpha	TCP1	60
228	T-complex protein 1 subunit beta	CCT2	57
229	T-complex protein 1 subunit epsilon	CCT5	60

Table A1, continued

230	T-complex protein 1 subunit theta	CCT8	60
231	TELO2-interacting protein 2	TTI2	57
232	TRAF-type zinc finger domain-containing protein 1	TRAFD1	65
233	Thiamine-triphosphatase	THTPA	26
234	Torsin-1A-interacting protein 1	TOR1AIP1	66
235	Transcription initiation factor TFIID subunit 7	TAF7	40
236	Transcription intermediary factor 1-beta	TRIM28	89
237	Transforming protein RhoA	RHOA	22
238	Transitional endoplasmic reticulum ATPase	VCP	89
239	Tropomyosin alpha-1 chain	TPM1	33
240	Tropomyosin alpha-3 chain	TPM3	33
241	Tropomyosin alpha-4 chain	TPM4	29
242	Trypsin-1	PRSS1	27
243	Trypsin-3	PRSS3	33
244	Tryptophan--tRNA ligase, cytoplasmic	WARS	53
245	Tubulin alpha-1A chain	TUBA1A	50
246	Tubulin alpha-1B chain	TUBA1B	50
247	Tubulin alpha-1C chain	TUBA1C	50
248	Tubulin beta chain	TUBB	50
249	Tubulin beta-2A chain	TUBB2A	50
250	Tubulin beta-4B chain	TUBB4B	50
251	U4/U6.U5 tri-snRNP-associated protein 1	SART1	90
252	UDP-N-acetylhexosamine pyrophosphorylase	UAP1	59
253	Ubiquitin carboxyl-terminal hydrolase 5	USP5	96
254	Ubiquitin carboxyl-terminal hydrolase 11	USP11	110
255	Ubiquitin carboxyl-terminal hydrolase 13	USP13	97
256	Ubiquitin-60S ribosomal protein L40	UBA52	15
257	Ubiquitin-like modifier-activating enzyme 1	UBA1	118
258	Unconventional prefoldin RPB5 interactor 1	URI1	60
259	V-type proton ATPase subunit B, brain isoform	ATP6V1B2	57
260	V-type proton ATPase subunit B, kidney isoform	ATP6V1B1	57
261	V-type proton ATPase subunit H	ATP6V1H	56
262	Vimentin	VIM	54
263	WW domain-binding protein 4	WBP4	43
264	Wiskott-Aldrich syndrome protein family member 2	WASF2	54
265	X-ray repair cross-complementing protein 5	XRCC5	83
266	Xaa-Pro dipeptidase	PEPD	55
267	Xylulose kinase	XYLB	58
268	Zinc finger protein 131	ZNF131	71
269	[F-actin]-methionine sulfoxide oxidase MICAL1	MICAL1	118
270	[Pyruvate dehydrogenase [acetyl-transferring]]-phosphatase 1, mitochondrial	PDP1	61

Table A2. List of DNCB-Modified Peptides and Mass Spectrum

60S ribosomal protein L13
Peptide sequence: RNKSTESLQANVQRLK*

Seq	#	B	Y	#
R	1	157.10843	2204.04102	16
N	2	271.15136	2047.93991	15
K	3	565.24632	1933.89699	14
S	4	652.27835	1639.80202	13
T	5	753.32603	1552.76999	12
E	6	882.36862	1451.72232	11
S	7	969.40065	1322.67972	10
L	8	1082.48471	1235.64770	9
Q	9	1210.54329	1122.56363	8
A	10	1281.58040	994.50505	7
N	11	1395.62333	923.46794	6
V	12	1494.69174	809.42501	5
Q	13	1622.75032	710.35660	4
R	14	1778.85143	582.29802	3
L	15	1891.93550	426.19691	2
K*	16	2186.03046	313.1128	1

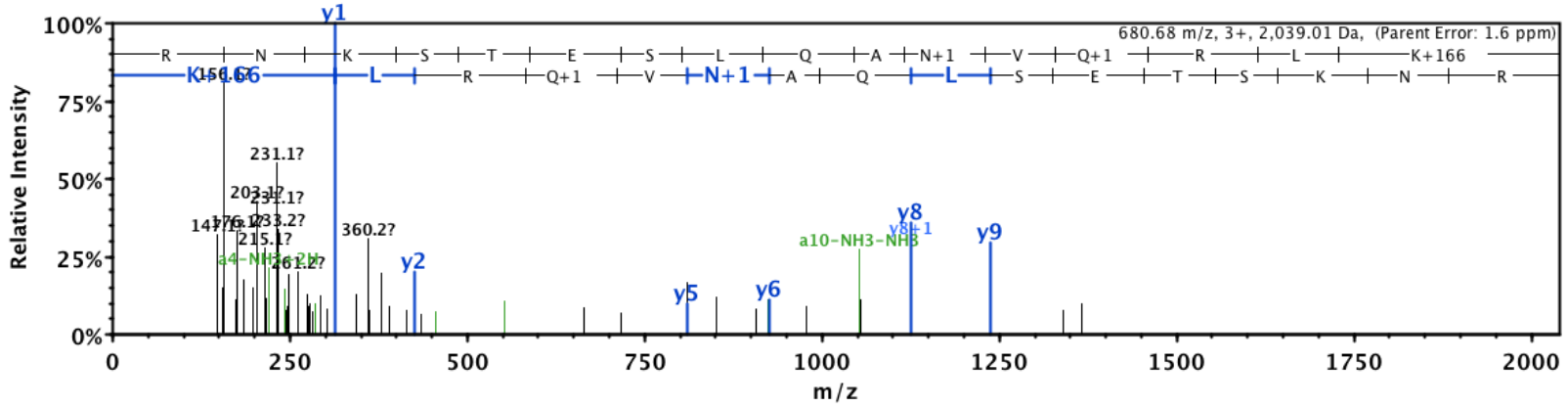

DnaJ homolog superfamily B member 11

Peptide sequence: QLLK*QGSVQK

Seq	#	B	Y	#
Q	1	129.06590	1294.67358	10
L	2	242.14996	1166.61500	9
L	3	355.23403	1053.53093	8
K*	4	649.32899	940.44687	7
Q	5	777.38757	646.3519	6
G	6	834.40903	518.2933	5
S	7	921.44106	461.27187	4
V	8	1020.50947	374.23984	3
Q	9	1148.56805	275.17143	2
K	10	1276.66301	147.11285	1

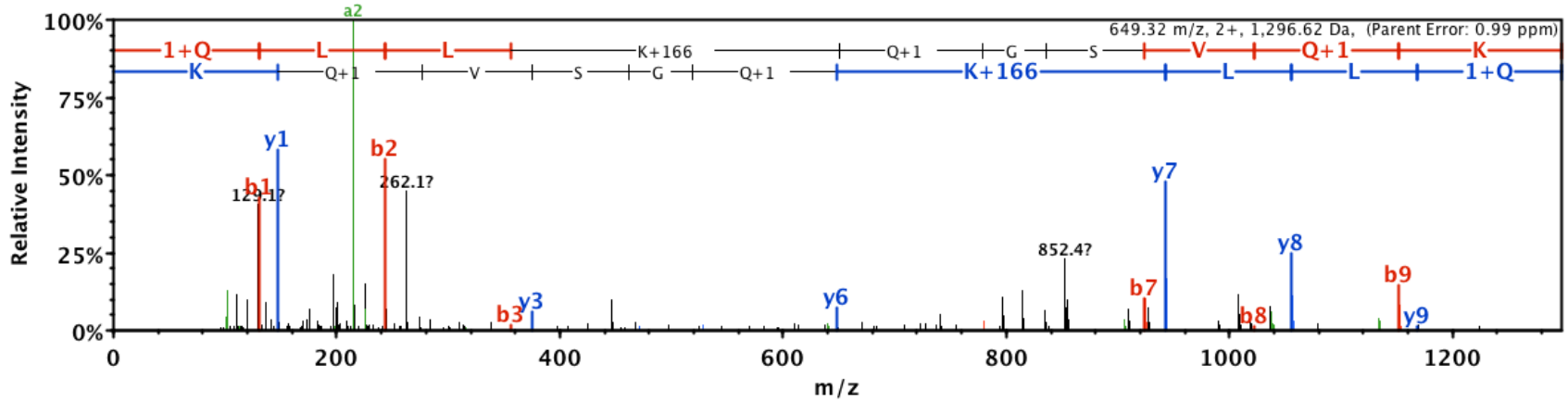

Endoplasmin

Peptide sequence: ELISNASDALK*IR

Seq	#	B	Y	#
E	1	130.04991	1595.80096	13
L	2	243.13398	1466.75837	12
I	3	356.21804	1353.67430	11
S	4	443.25007	1240.59024	10
N	5	557.29300	1153.55821	9
A	6	628.33011	1039.51528	8
S	7	715.36214	968.47817	7
D	8	830.38908	881.44614	6
A	9	901.42620	766.41920	5
L	10	1014.51026	695.38209	4
K*	11	1308.60522	582.29802	3
I	12	1421.68928	288.20306	2
R	13	1577.79040	175.11900	1

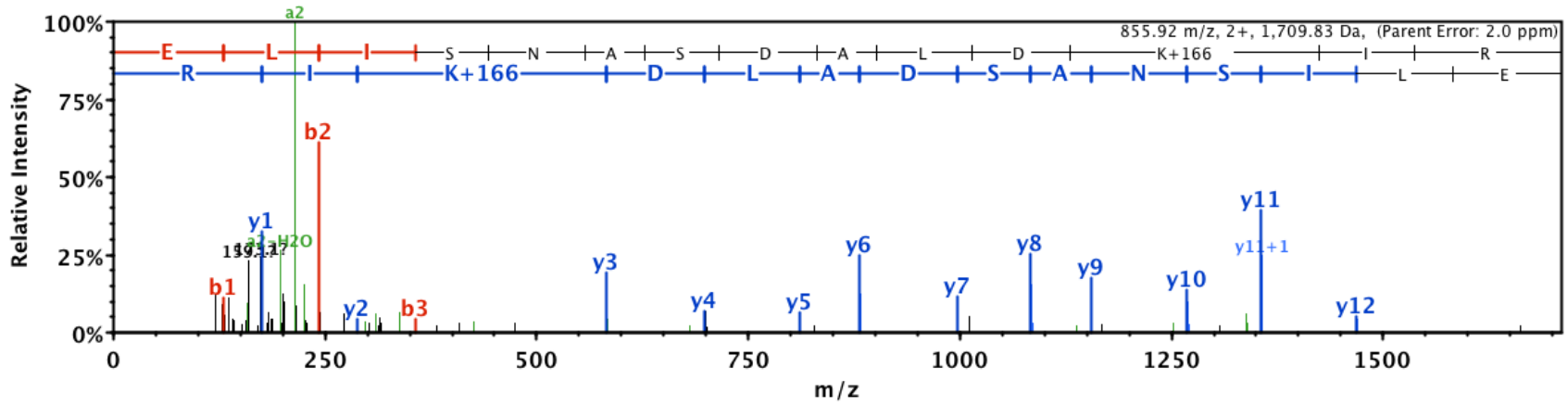

Peptide sequence: NLGTIAK*SGTSEFLNK

Seq	#	B	Y	#
N	1	115.05025	1845.89632	16
L	2	228.13431	1731.85339	15
G	3	285.15578	1618.76933	14
T	4	386.20345	1561.74786	13
I	5	499.28752	1460.70018	12
A	6	570.32463	1347.61612	11
K*	7	864.41959	1276.57901	10
S	8	951.45162	982.48404	9
G	9	1008.47309	895.45202	8
T	10	1109.52076	838.43055	7
S	11	1196.55279	737.38287	6
E	12	1325.59538	650.35085	5
F	13	1472.66380	521.30825	4
L	14	1585.74786	374.23984	3
N	15	1699.79079	261.15578	2
K	16	1827.88575	147.11285	1

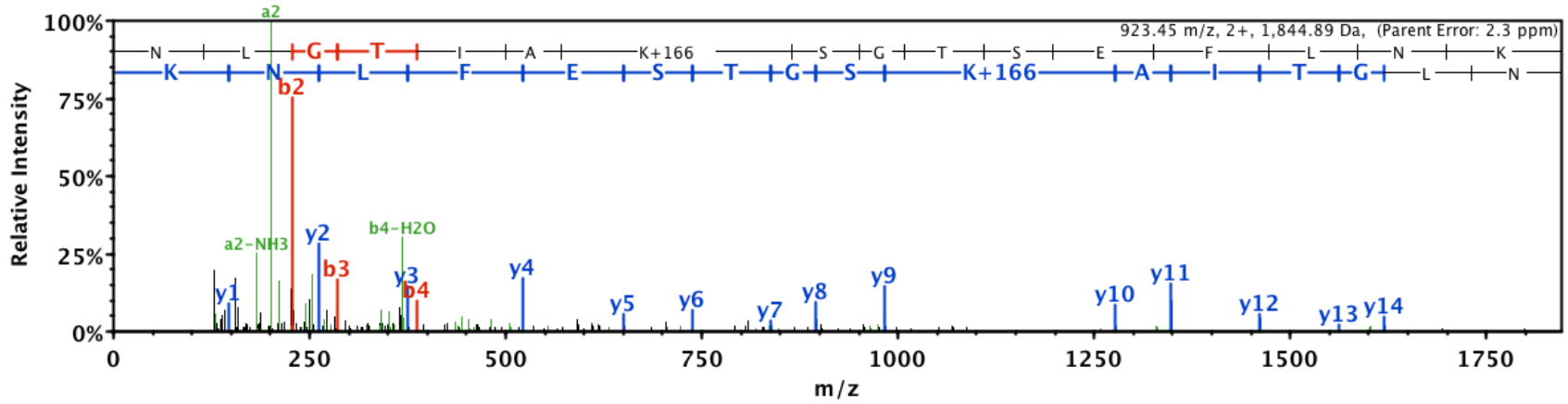

Peptide sequence: EFEPLLNWMK*DK

Seq	#	B	Y	#
E	1	130.04991	1715.77197	12
F	2	277.11833	1586.72938	11
E	3	406.16092	1439.66096	10
P	4	503.21368	1310.61837	9
L	5	616.29775	1213.56561	8
L	6	729.38181	1100.48154	7
N	7	843.42474	987.39748	6
W	8	1029.50405	873.35455	5
M	9	1160.54454	687.27524	4
K*	10	1454.63950	556.23475	3
D	11	1569.66644	262.13979	2
K	12	1697.76140	147.11285	1

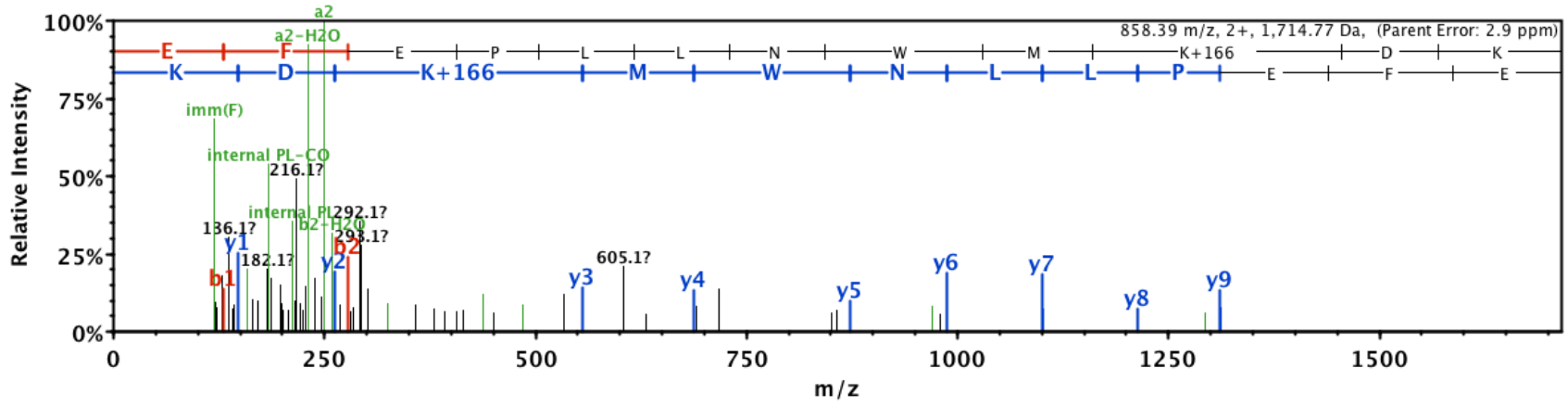

Peptide sequence: LTESPC*ALVASQYGWSGNMER

Seq	#	B	Y	#	Seq	#	B	Y	#
L	1	114.09139	2465.04822	21	Q	12	1366.59294	1227.52118	10
T	2	215.13906	2351.96416	20	Y	13	1529.65627	1099.46260	9
E	3	344.18166	2250.91648	19	G	14	1586.67773	936.39927	8
S	4	431.21368	2121.87389	18	W	15	1772.75705	879.37781	7
P	5	528.26645	2034.84186	17	S	16	1859.78908	693.29849	6
C*	6	797.27563	1937.78909	16	G	17	1916.81054	606.26647	5
A	7	868.31275	1668.77991	15	N	18	2030.85347	549.24500	4
L	8	981.39681	1597.74279	14	M	19	2161.89395	435.20207	3
V	9	1080.46522	1484.65873	13	E	20	2290.93654	304.16159	2
A	10	1151.50234	1385.59032	12	R	21	2447.03766	175.11900	1
S	11	1238.53437	1314.55320	11					

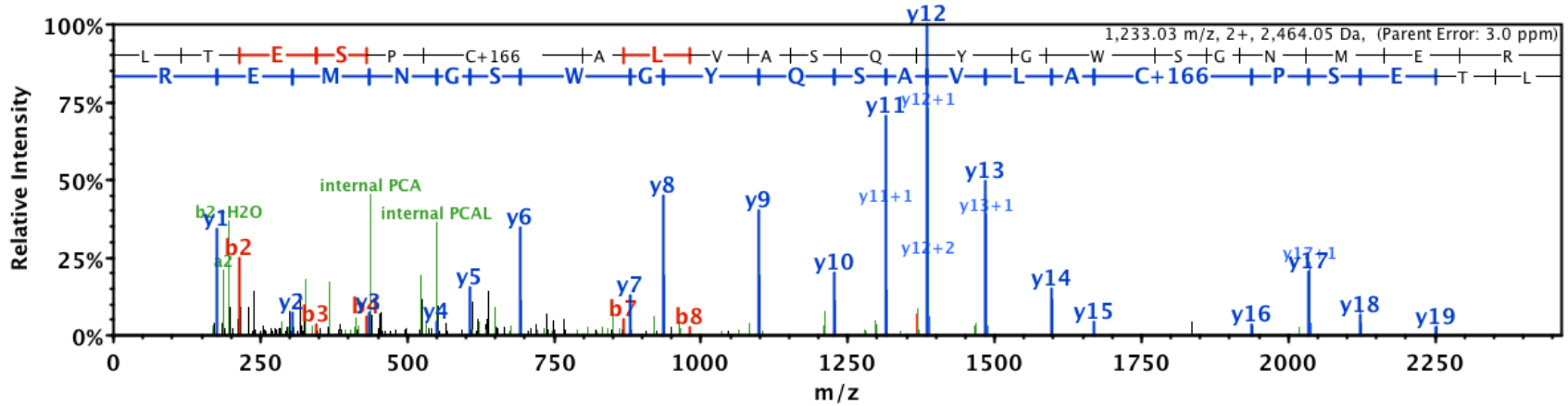

Peptide sequence: IMK*AQAYQTGK

Seq	#	B	Y	#
I	1	114.09139	1404.65621	11
M	2	245.13187	1291.57215	10
K*	3	539.22683	1160.53166	9
A	4	610.26395	866.43670	8
Q	5	738.32252	795.39959	7
A	6	809.35964	667.34101	6
Y	7	972.42297	596.30390	5
Q	8	1100.48154	433.24057	4
T	9	1201.52922	305.18199	3
G	10	1258.55068	204.13431	2
K	11	1386.64565	147.11285	1

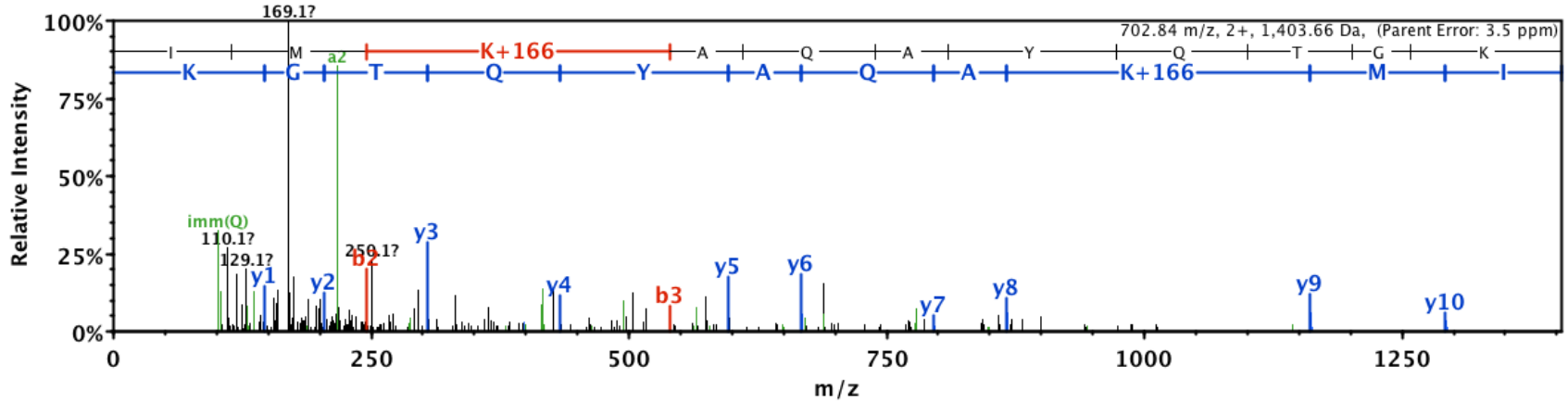

Heat shock protein HSP90-alpha

Peptide sequence: TKFENLC*K

Seq	#	B	Y	#
T	1	102.05500	1148.50267	8
K	2	230.14996	1047.45499	7
F	3	377.21838	919.36003	6
E	4	506.26097	772.29162	5
N	5	620.30390	643.24902	4
L	6	733.38796	529.20610	3
C*	7	1002.39714	416.12203	2
K	8	1130.49211	147.11285	1

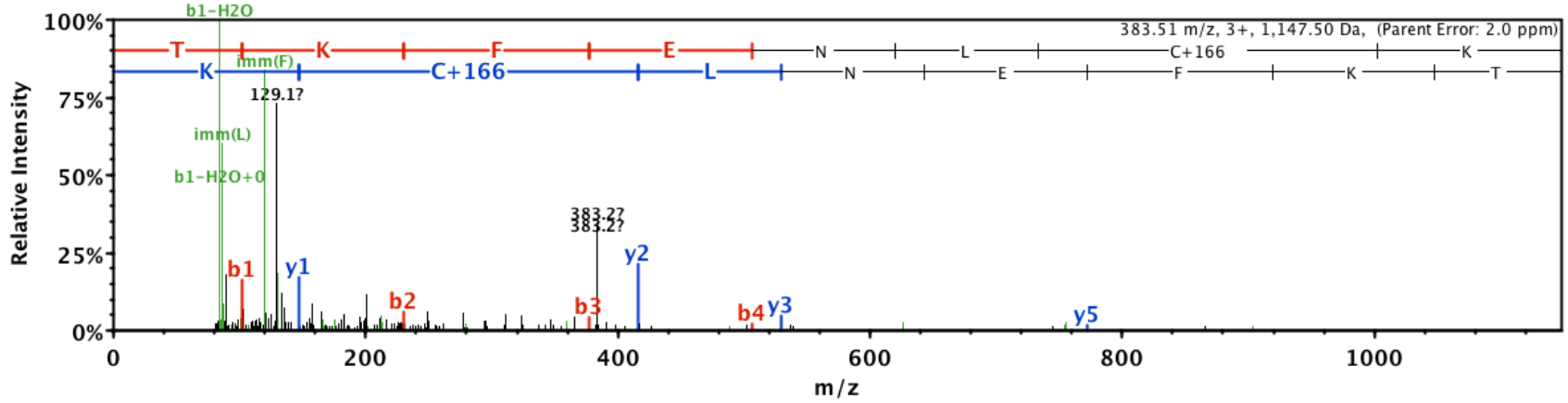

Peptide sequence: LVTSPCC*IVTSTYGWTANMER

Seq	#	B	Y	#	Seq	#	B	Y	#
L	1	114.09139	2498.07708	21	T	12	1371.59050	1228.54158	10
V	2	213.15980	2384.99301	20	Y	13	1534.65383	1127.49390	9
T	3	314.20748	2285.92460	19	G	14	1591.67529	964.43057	8
S	4	401.23951	2184.87692	18	W	15	1777.75461	907.40911	7
P	5	498.29227	2097.84489	17	T	16	1878.80228	721.32979	6
C	6	601.30145	2000.79213	16	A	17	1949.83940	620.28212	5
C*	7	870.31064	1897.78295	15	N	18	2063.88232	549.24500	4
I	8	983.39470	1628.77376	14	M	19	2194.92281	435.20207	3
V	9	1082.46312	1515.68970	13	E	20	2323.96540	304.16159	2
T	10	1183.51079	1416.62128	12	R	21	2480.06651	175.11900	1
S	11	1270.54282	1315.57360	11					

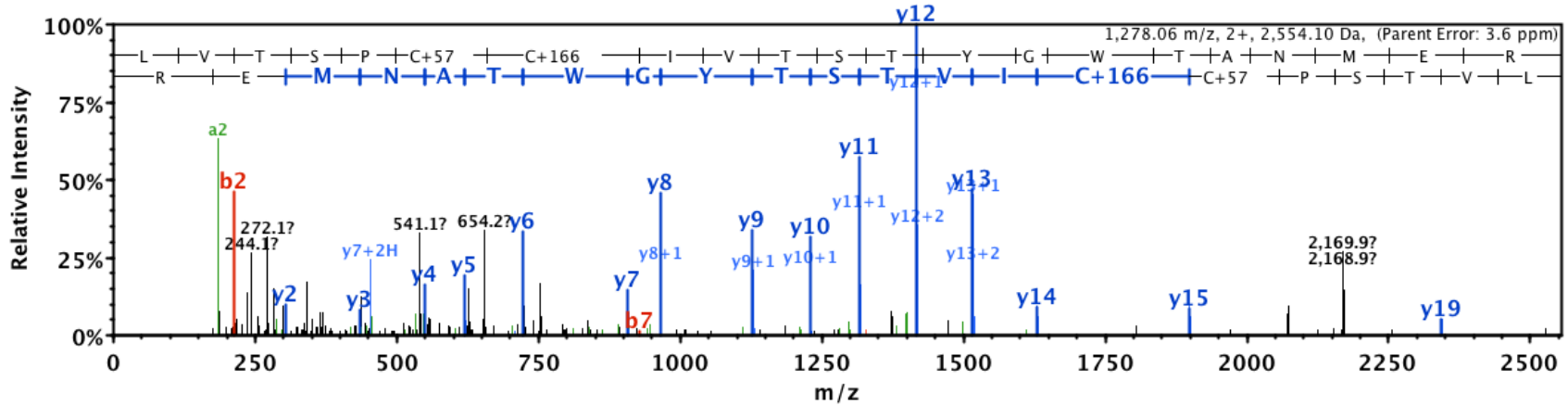

Heat shock protein HSP90-beta

Peptide sequence: ADLINNLGTIAK*SGTK

Seq	#	B	Y	#
A	1	72.04444	1781.90140	16
D	2	187.07138	1710.86429	15
L	3	300.15544	1595.83735	14
I	4	413.23951	1482.75328	13
N	5	527.28243	1369.66922	12
N	6	641.32536	1255.62629	11
L	7	754.40942	1141.58336	10
G	8	811.43089	1028.49930	9
T	9	912.47856	971.47784	8
I	10	1025.56263	870.43016	7
A	11	1096.59974	757.34609	6
K*	12	1390.69470	686.30898	5
S	13	1477.72673	392.21402	4
G	14	1534.74820	305.18199	3
T	15	1635.79587	248.16053	2
K	16	1763.89084	147.11285	1

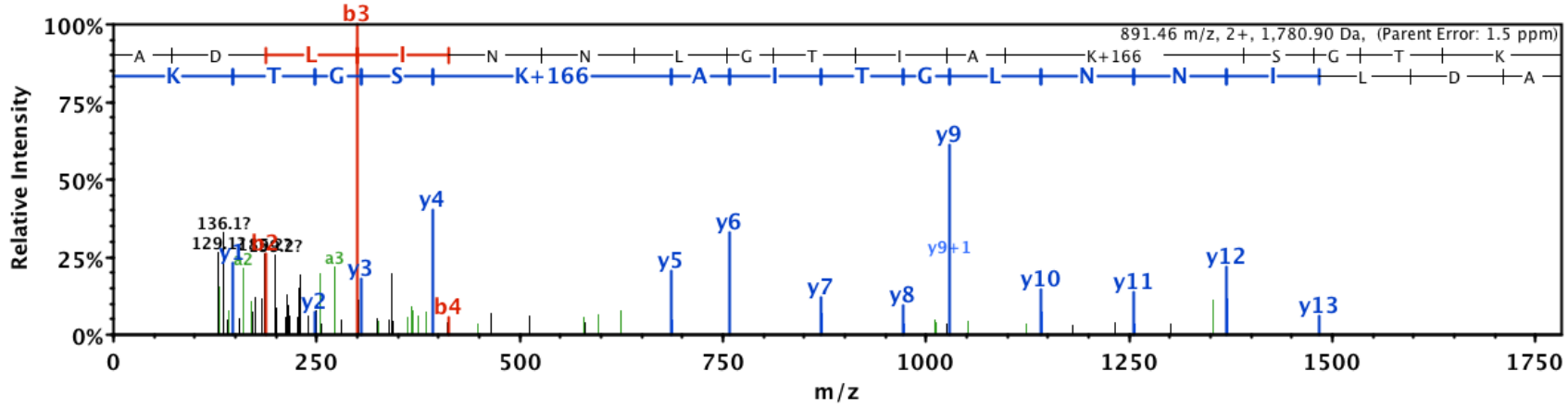

Peptide sequence: VILHLK*EDQTEYLEER

Seq	#	B	Y	#
V	1	100.07574	2181.04444	16
I	2	213.15980	2081.97602	15
L	3	326.24386	1968.89196	14
H	4	463.30277	1855.80790	13
L	5	576.38684	1718.74898	12
K*	6	870.48180	1605.66492	11
E	7	999.52439	1311.56996	10
D	8	1114.55134	1182.52737	9
Q	9	1242.60991	1067.50042	8
T	10	1343.65759	939.44185	7
E	11	1472.70018	838.39417	6
Y	12	1635.76351	709.35157	5
L	13	1748.84758	546.28825	4
E	14	1877.89017	433.20418	3
E	15	2006.93276	304.16159	2
R	16	2163.03387	175.11900	1

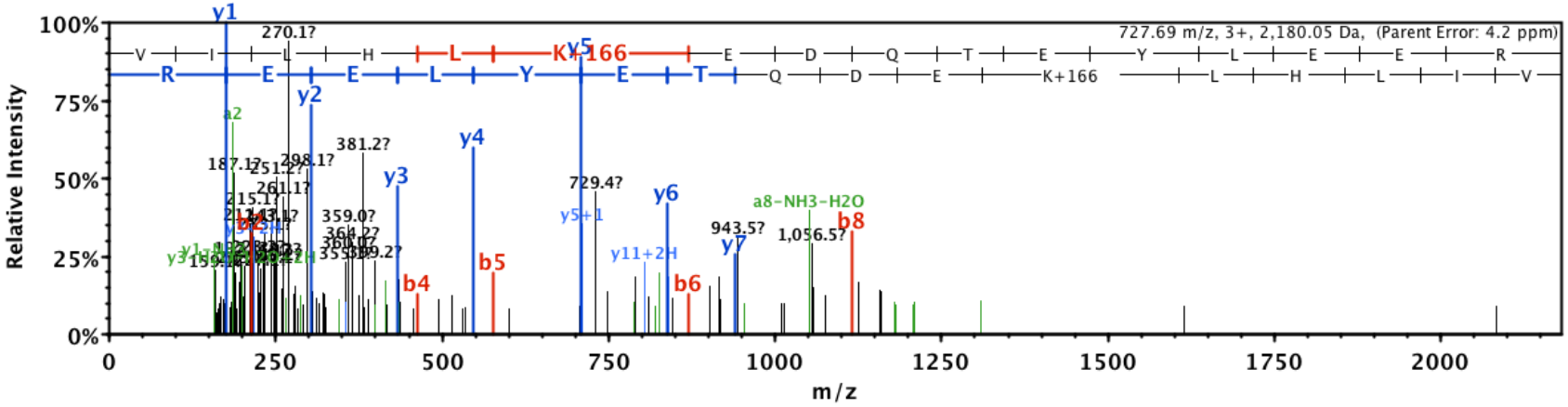

Peptide sequence: VFIMDSC*DELIPEYLNFIR

Seq	#	B	Y	#	Seq	#	B	Y	#
V	1	100.07574	2483.12434	19	I	11	1432.57452	1164.64121	9
F	2	247.14415	2384.05593	18	P	12	1529.62728	1051.55715	8
I	3	360.22821	2236.98752	17	E	13	1658.66987	954.50439	7
M	4	491.26870	2123.90345	16	Y	14	1821.73320	825.46179	6
D	5	606.29564	1992.86297	15	L	15	1934.81727	662.39846	5
S	6	693.32767	1877.83603	14	N	16	2048.86019	549.31440	4
C*	7	962.33685	1790.80400	13	F	17	2195.92861	435.27147	3
D	8	1077.36380	1521.79481	12	I	18	2309.01267	288.20306	2
E	9	1206.40639	1406.76787	11	R	19	2465.11378	175.11900	1
L	10	1319.49045	1277.72528	10					

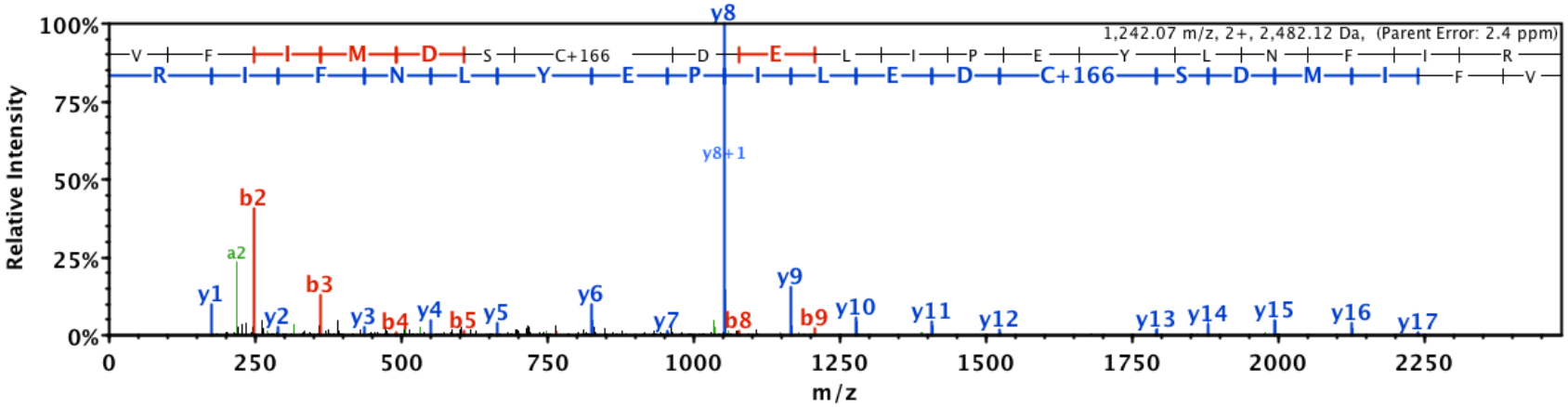

Peptide sequence: LVSSPC*CIVTSTYGWTANMER

Seq	#	B	Y	#	Seq	#	B	Y	#
L	1	114.09139	2484.06143	21	T	12	1357.57485	1228.54158	10
V	2	213.15980	2370.97736	20	Y	13	1520.63818	1127.49390	9
S	3	300.19183	2271.90895	19	G	14	1577.65964	964.43057	8
S	4	387.22386	2184.87692	18	W	15	1763.73896	907.40911	7
P	5	484.27662	2097.84489	17	T	16	1864.78663	721.32979	6
C*	6	753.28580	2000.79213	16	A	17	1935.82375	620.28212	5
C	7	856.29499	1731.78295	15	N	18	2049.86667	549.24500	4
I	8	969.37905	1628.77376	14	M	19	2180.90716	435.20207	3
V	9	1068.44747	1515.68970	13	E	20	2309.94975	304.16159	2
T	10	1169.49514	1416.62128	12	R	21	2466.05086	175.11900	1
S	11	1256.52717	1315.57360	11					

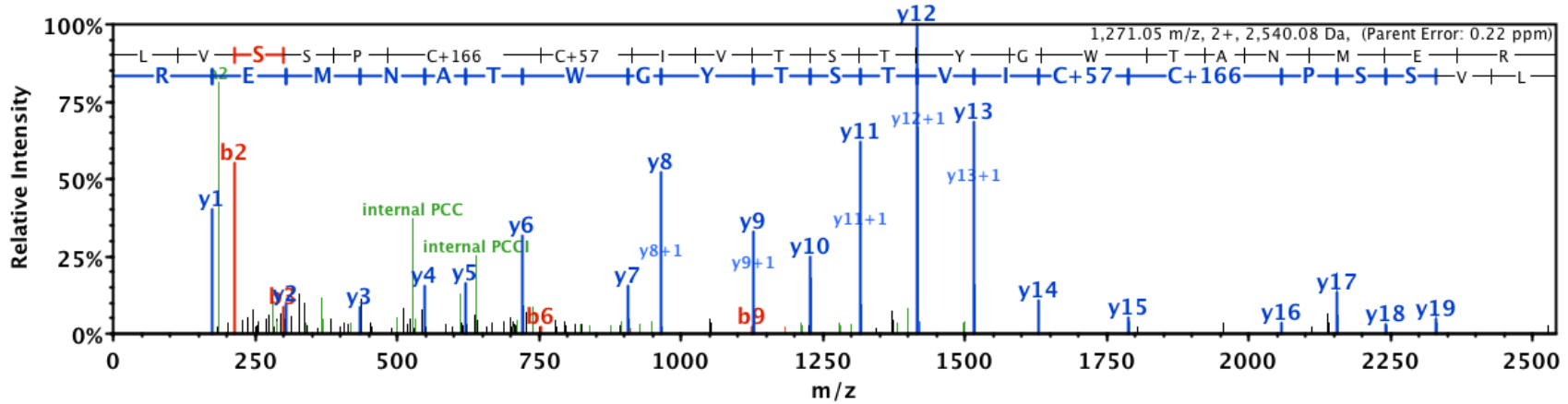

Peptide sequence: QK*AEADKNDK

Seq	#	B	Y	#
Q	1	129.06590	1312.57498	10
K*	2	423.16086	1184.51641	9
A	3	494.19797	890.42144	8
E	4	623.24057	819.38433	7
A	5	694.27768	690.34174	6
D	6	809.30462	619.30462	5
K	7	937.39959	504.27768	4
N	8	1051.44251	376.18272	3
D	9	1166.46946	262.13979	2
K	10	1294.56442	147.11285	1

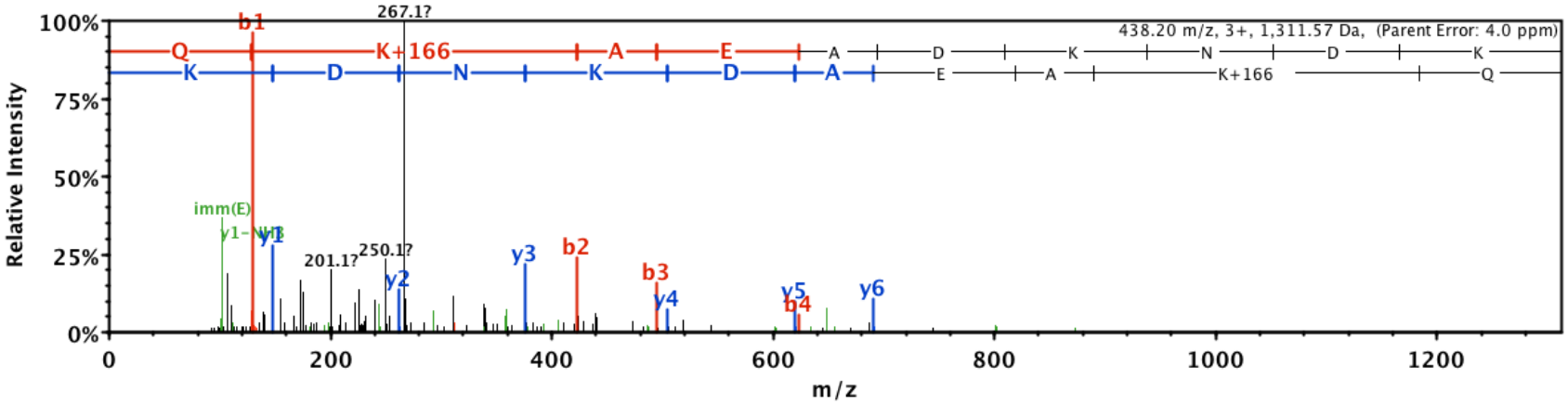

Protein disulfide-isomerase A3

Protein sequence: VDC*TANTNTCNK

Seq	#	B	Y	#
V	1	100.07574	1449.53551	12
D	2	215.10268	1350.46709	11
C*	3	484.11186	1235.44015	10
T	4	585.15954	966.43096	9
A	5	656.19666	865.38329	8
N	6	770.23958	794.34617	7
T	7	871.28726	680.30324	6
N	8	985.33019	579.25557	5
T	9	1086.37787	465.21264	4
C	10	1189.38705	364.16496	3
N	11	1303.42998	261.15578	2
K	12	1431.52494	147.11285	1

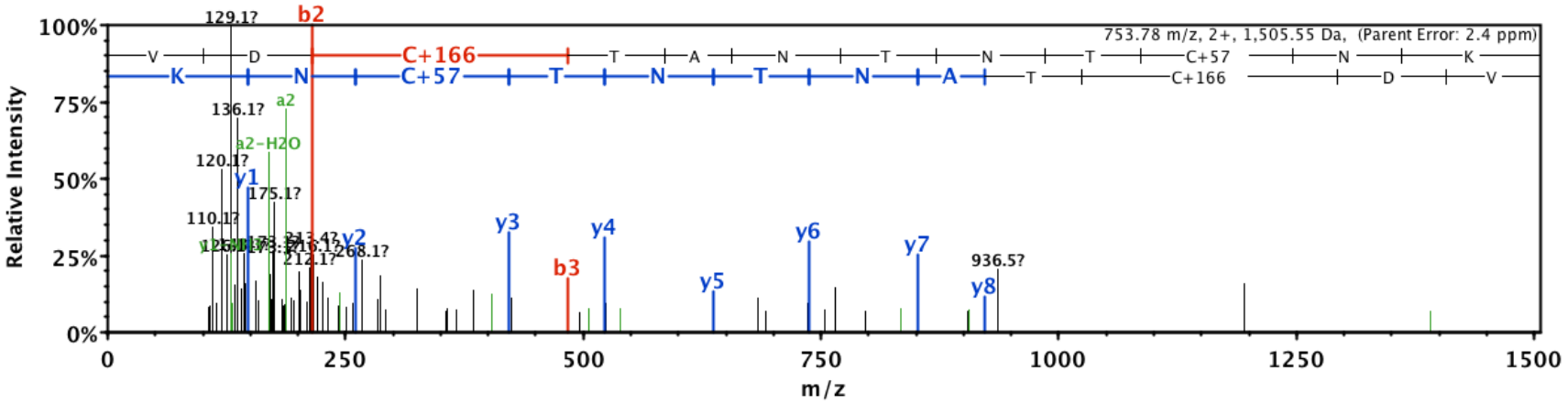

Peptide sequence: FIQENIFGIC*PHMTEDNK

Seq	#	B	Y	#	Seq	#	B	Y	#
F	1	148.07574	2301.98891	18	C*	10	1331.57109	1240.43434	9
I	2	261.15980	2154.92050	17	P	11	1428.62385	971.42515	8
Q	3	389.21838	2041.83644	16	H	12	1565.68276	874.37239	7
E	4	518.26097	1913.77786	15	M	13	1696.72325	737.31348	6
N	5	632.30390	1784.73527	14	T	14	1797.77092	606.27299	5
I	6	745.38796	1670.69234	13	E	15	1926.81352	505.22531	4
F	7	892.45637	1557.60828	12	D	16	2041.84046	376.18272	3
G	8	949.47784	1410.53986	11	N	17	2155.88339	261.15578	2
I	9	1062.56190	1353.51840	10	K	18	2283.97835	147.11285	1

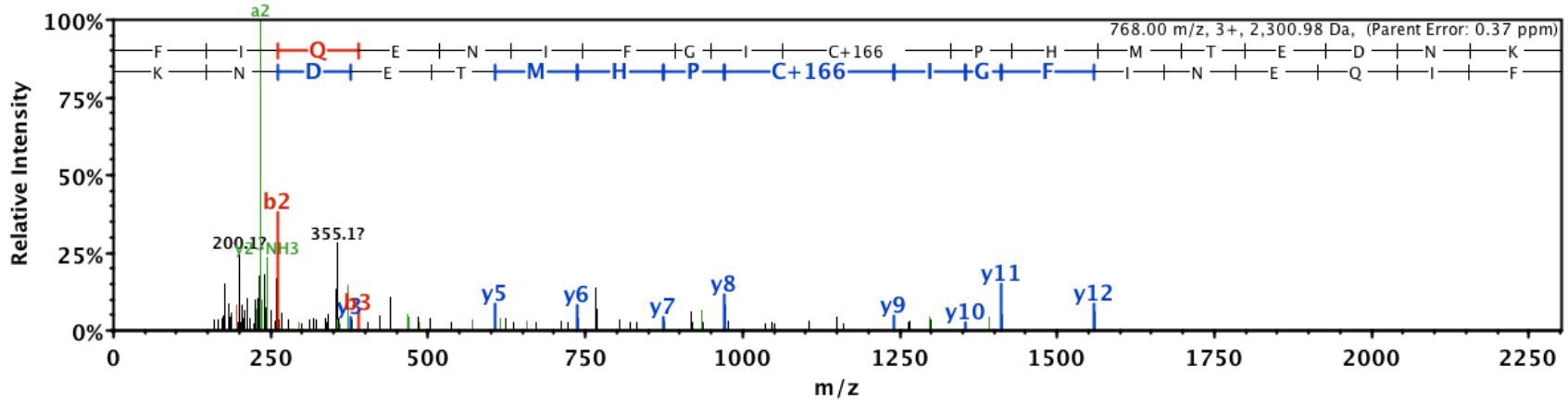

Ribonuclease inhibitor

Protein sequence: DSPC*QLEALK

Seq	#	B	Y	#
D	1	116.03426	1269.54018	10
S	2	203.06629	1154.51324	9
P	3	300.11906	1067.48121	8
C*	4	569.12824	970.42844	7
Q	5	697.18682	701.41926	6
L	6	810.27088	573.36068	5
E	7	939.31348	460.27662	4
A	8	1010.35059	331.23403	3
L	9	1123.43465	260.19691	2
K	10	1251.52961	147.11285	1

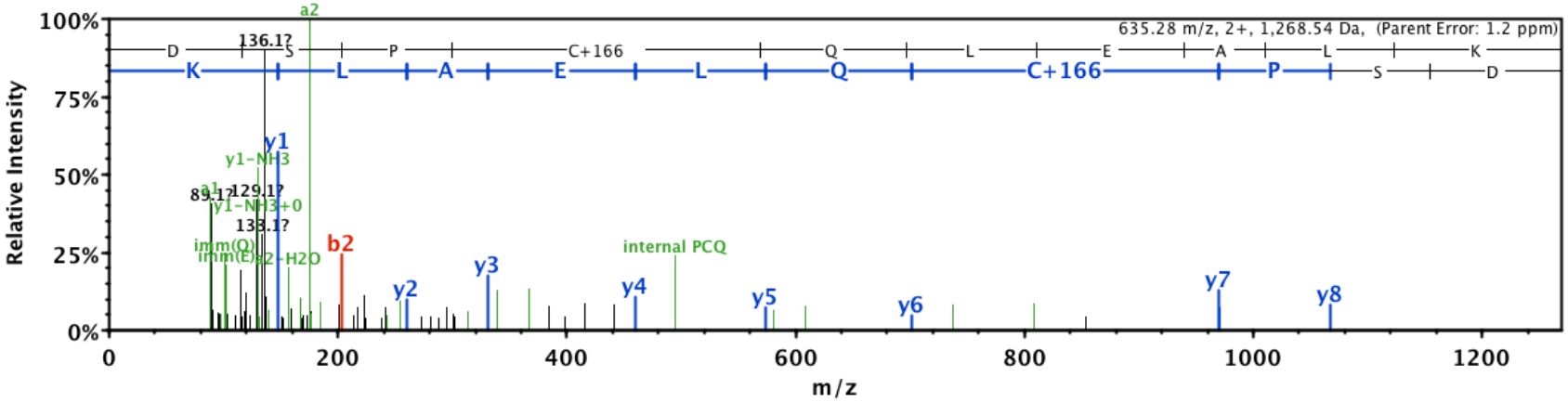

Peptide sequence: LGDVGMAELC*PGLLHPSSR

Seq	#	B	Y	#	Seq	#	B	Y	#
L	1	114.09139	2117.97287	19	P	11	1252.49587	963.53708	9
G	2	171.11285	2004.88881	18	G	12	1309.51734	866.48432	8
D	3	286.13979	1947.86734	17	L	13	1422.60140	809.46286	7
V	4	385.20821	1832.84040	16	L	14	1535.68546	696.37879	6
G	5	442.22967	1733.77199	15	H	15	1672.74438	583.29473	5
M	6	573.27015	1676.75052	14	P	16	1769.79714	446.23582	4
A	7	644.30727	1545.71004	13	S	17	1856.82917	349.18305	3
E	8	773.34986	1474.67292	12	S	18	1943.86120	262.15102	2
L	9	886.43392	1345.63033	11	R	19	2099.96231	175.11900	1
C*	10	1155.44311	1232.54627	10					

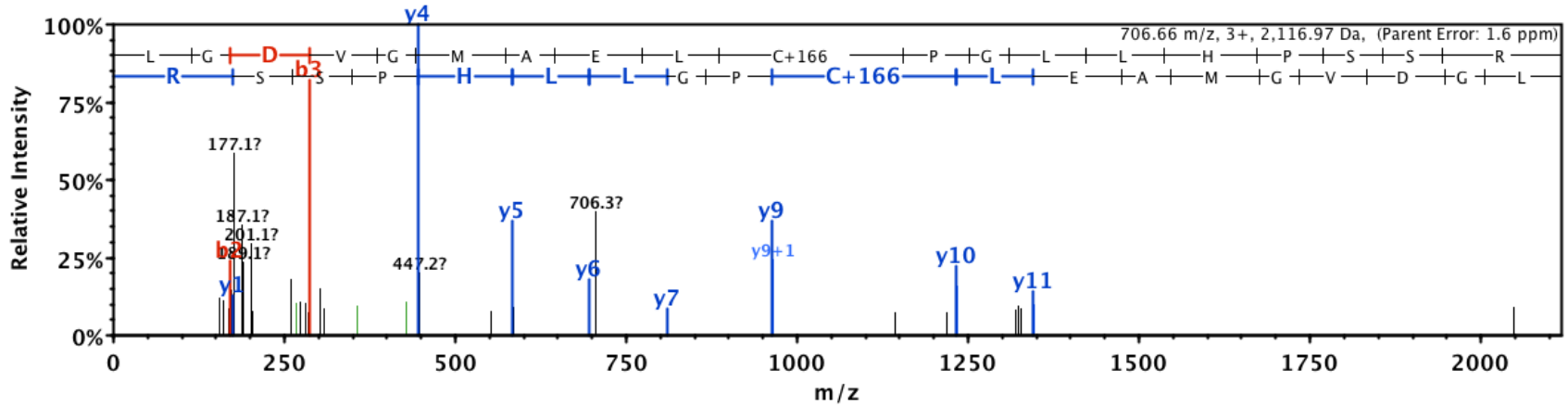

Spectrin, beta chain, non-erythrocytic 1

Peptide sequence: K*QQMLENQMEVR

Seq	#	B	Y	#
K*	1	295.10228	1699.75125	12
Q	2	423.16086	1405.65629	11
Q	3	551.21944	1277.59771	10
M	4	682.25992	1149.53913	9
L	5	795.34399	1018.49865	8
E	6	924.38658	905.41459	7
N	7	1038.42951	776.37199	6
Q	8	1166.48808	662.32907	5
M	9	1297.52857	534.27049	4
E	10	1426.57116	403.23000	3
V	11	1525.63958	274.18741	2
R	12	1681.74069	175.11900	1

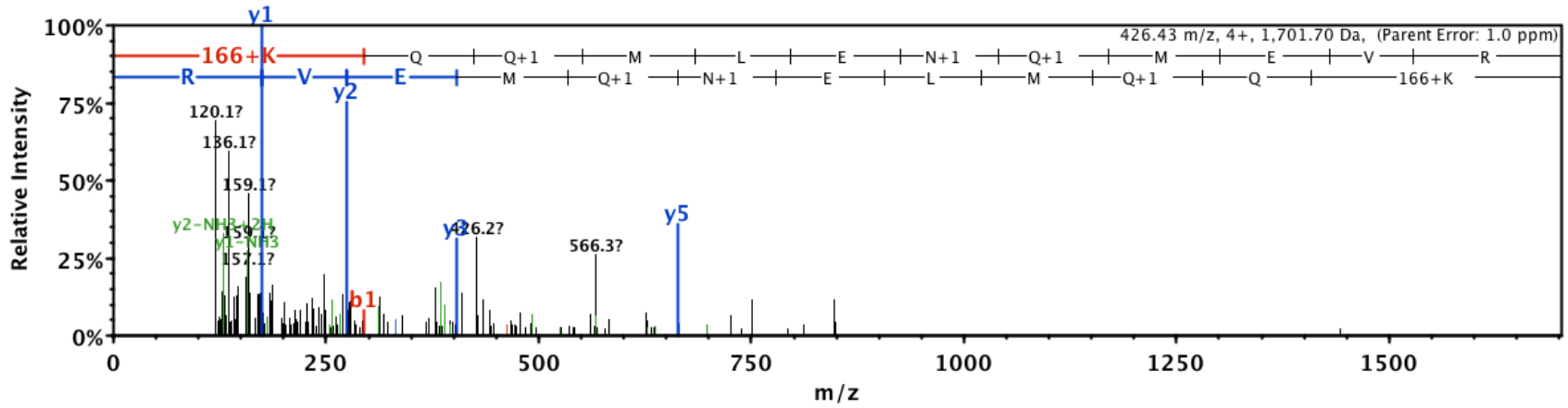

Tubulin alpha-1C

Peptide sequence: TIQFVDWC*PTGFK

Seq	#	B	Y	#
T	1	102.05500	1707.74575	13
I	2	215.13906	1606.69808	12
Q	3	343.19764	1493.61401	11
F	4	490.26605	1365.55544	10
V	5	589.33447	1218.48702	9
D	6	704.36141	1119.41861	8
W	7	890.44072	1004.39167	7
C*	8	1159.44991	818.31235	6
P	9	1256.50267	549.30317	5
T	10	1357.55035	452.25040	4
G	11	1414.57181	351.20273	3
F	12	1561.64023	294.18126	2
K	13	1689.73519	147.11285	1

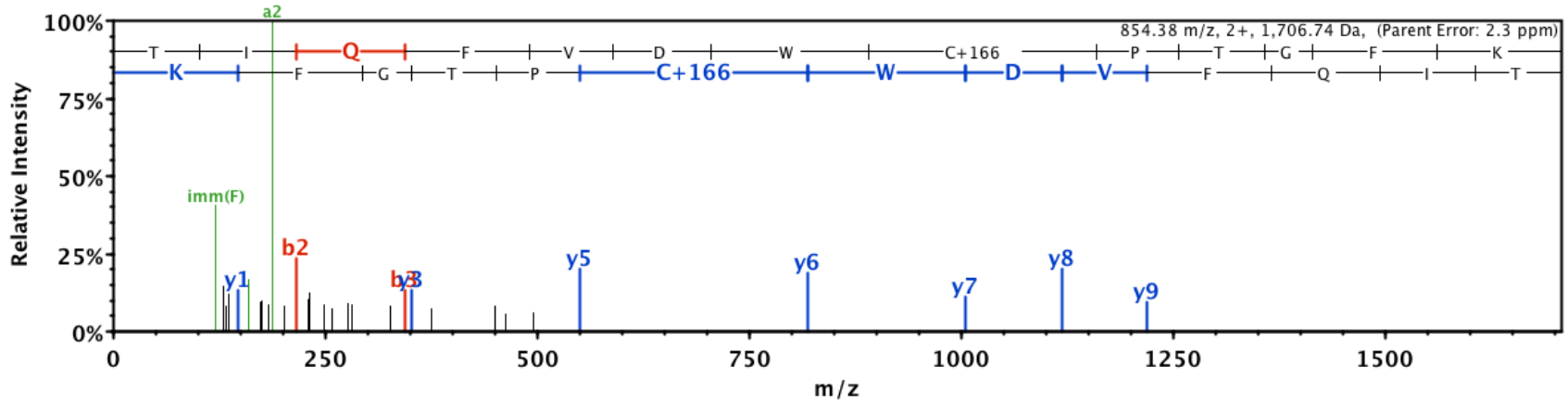

8. Gene-Suppression Using Lentivirus-Packaged shRNA

Primers were purchased from Integrative DNA Technology. They were suspended in Nuclease-Free Water (Promega, Madison, WI) upon receipt and stored in -20 ^{O}C. The following list is the primer sequences that I used for knockdown validation and evaluation of IL-8 mRNA expression.

Table A3 Forward and Reverse Sequence of Primers for qPCR

Gene	Primer Sequence
DNAJB11	Forward 5'-CCTCGTCAGCAAGACGAAATA-3' Reverse 5'-GAGGCTCACCTTCTCCAATAAA-3'
HSP90AA1	Forward 5'-GAAGATGACC CTACTGCTGATG-3' Reverse 5'-CACAAGACTGGGTCTGAGTTATT-3'
HSP90AB1	Forward 5'-GGATGACAGCGGTAAGGATAAG-3' Reverse 5'-GAGCCCGACGAGGAATAAATAG-3'
PDIA3	Forward 5'-AACCTGGAGCCCAAGTATAAAG-3' Reverse 5'-TCGGCCCGACGAGGAATAAATAG-3'
RNH1	Forward 5'-GCTGGTCCTGTACGACATTA-3' Reverse 5'-CGGATCTGAGCGTTTCTCTT-3'
SPTBN1	Forward 5'-AAGAGGAAGAGGAGAGGAAGAG-3' Reverse 5'-GAGGAACATTAGGCACAGAGAG-3'
ACTB	Forward 5'-TTGGCAATGAGCGGTTCC-3' Reverse 5'-GTTGAAGGTAGTTTCGTGGATG-3'
IL-8	Forward 5'-ATACTCCAAACCTTTCCACCC-3' Reverse 5'-TCTGCACCCAGTTTTCCTTG-3'

9. Detection of Knockdown by qPCR

Detailed experimental: Transduction was performed according to the manufacturer's recommended protocol. About 12,000 THP-1 cells were seeded in a 96-well plate with 105 µl cell culture medium containing 8 µg/ml transduction reagent, hexadimethrine bromide (Day 1). Then, 15 µl of lentiviral particles were added to reach 120 µl total volume. About 16 h later, the cells were replenished with fresh cell culture medium (Day 2). Because THP-1 cells are non-adherent cells, they had to be centrifuged to remove supernatant. But instead of centrifuging, I placed the

culture plate on a flat surface for 5 minutes for the cells to sit on the bottom of the plate, then gently removed 100 µl of supernatant from the top. After adding 120 µl of fresh medium was added to each well, the plate was gently tapped to mix and further cultured. From Day 4, the cells were transferred to T25 flask and cultured with 5 µg/ml puromycin to positively select the cells that were expressing knockdown. When the cells reached over 90 % confluency, they were collected and counted. Approximately 3 x 10^6 cells for each knockdown were collected for RNA isolation, reverse-transcription, and qPCR for the target gene. Because the lentivirus itself can change the cell's internal functions, an empty vector was used as a transduction control. The entire process was repeated 3 times to generate error bars and statistical significance.

There were three major experimental groups in this assay: 1) the knockdown, which was expected to show suppression of the target gene, 2) empty vector, which was transduced with empty vector and thus was not expected to show huge suppression of the target gene, and 3) the wild type, which was the cells that normally express the target genes. The knockdown data were normalized to the gene expression of the normal cells. In addition to experimental groups, there was an endogenous control gene, whose gene expression should not differ between knockdown and normal samples. Actin-beta (ACTB) is a housekeeping gene that serves as an endogenous control in many cell types including THP-1s.

Data Analysis Workflow: The entire experiment was performed in triplicate to generate error bars and statistical significance. Real-time PCR yields data in the threshold cycle (Ct) value, which is the number of polymerase reaction cycles required to produce a detectable amount of fluorescent level. As the first step to data analysis, delta Ct (dCt) values were calculated by taking the

difference between Ct value for knockdown, empty vector, and wild type (Ct_{KO}, Ct_{EV}, and Ct_{WT} respectively) and Ct value for ACTB.

$$dCt_{KO} = Ct_{KO,gene} - Ct_{KO,ACTB}$$

Here, $Ct_{KO,gene}$ expresses Ct value for the gene of interest in knockdown cDNA sample and $Ct_{KO,ACTB}$ expresses Ct value for ACTB in knockdown cDNA sample. Delta Ct value calculates for the difference between the expression of the target gene and the housekeeping gene. This serves as the measurement of change in internal gene expression. The same equation was used to calculate dCt_{EV} and dCt_{WT}. For the rest of replicates, the same equation was used to calculate three dCt values for each ($dCt_{KO,1}$, $dCt_{KO,2}$, $dCt_{KO,3}$ and so on). Then, three dCt values were averaged and the standard deviation was obtained. In this appendix, the average dCt values were denoted as dCt_{KO}, dCt_{EV}, dCt_{WT} and the standard deviations were denoted as SD_{KO}, SD_{EV}, and SD_{WT}

To compare the gene expression of knockdown or empty vector samples to wild type, double delta threshold cycle (ddCt) values were calculated by taking the difference between dCt values for knockdown and wild type:

$$ddCt_{KO} = dCt_{KO} - dCt_{WT}$$

The same formula was used to calculate $ddCt_{EV}$ and $ddCt_{WT}$. The standard error for each ddCt values were obtained by taking the standard error.

$$SE_{KO} = \sqrt{{SD_{KO}}^2 + {SD_{WT}}^2}$$

The same formula was used to calculate SE_{EV} and SE_{WT}. Before converting ddCt values to fold change, the upper and lower limits of ddCt were calculated by adding or subtracting SE values. Replication of DNA occurs at an exponential rate, and thus change of Ct value by 1 means that

there are two-fold changes in the quantity of DNA. After the upper and lower limits ddCt values were obtained, they were converted to fold change by,

$$Fold\ Change = 2^{-ddCt}$$

The medium of the upper and lower limit of fold change was graphed, and the difference between the medium and upper limit was reported as the error bars.

Statistical significance was calculated using unpaired t-test on ddCt value and standard error from the mean.

Supplementary Data for qPCR

Table A4. DNAJB11 – Raw Data for Knockdown Detection qPCR and Calculation Table

		Run 1	Run 2	Run 3	Average	Error
Untreated	Target	29.838	29.159	30.253		
	ACTB	15.028	14.024	14.864		
	dCt	14.810	15.134	15.388	15.111	0.167
	ddCt				0.000	0.237
	Fold change	0.849	1.178		1.013	0.164
DNAJB11 KO	Target	39.379	40.000	39.628		
	ACTB	15.674	11.643	12.317		
	dCt	23.705	28.357	27.311	26.458	1.409
	ddCt				11.347	1.419
	Fold change	1.436×10^{-4}	1.027×10^{-3}		5.851×10^{-4}	4.415×10^{-4}

Table A5. HSP90AA1 – Raw Data for Knockdown Detection qPCR and Calculation Table

		Run 1	Run 2	Run 3	Average	Error
Untreated	Target	33.633	34.240	35.275		
	ACTB	15.028	14.024	14.864		
	dCt	18.605	20.216	20.410	19.744	0.572
	ddCt				0.000	0.809
	Fold change	0.571	1.752		1.161	0.590
HSP90AA1 KO	Target	40.000	40.000	34.165		
	ACTB	12.515	13.715	12.330		
	dCt	27.485	26.285	21.835	25.202	1.718
	ddCt				5.458	1.811
	Fold change	6.483×10^{-3}	0.0798		0.0432	0.0367

Table A6. HSP90AB1 – Raw Data for Knockdown Detection qPCR and Calculation Table

		Run 1	Run 2	Run 3	Average	Error
Untreated	Target	19.259	20.312	20.106		
	ACTB	15.028	14.024	14.864		
	dCt	4.231	6.287	5.241	5.253	0.594
	ddCt				0.000	0.839
	Fold change	0.559	1.789		1.174	0.615
HSP90AB1 KO	Target	40.000	40.000	36.636		
	ACTB	20.943	18.983	17.804		
	dCt	19.057	21.017	18.832	19.636	0.694
	ddCt				14.382	0.913
	Fold change	2.487×10^{-5}	8.817×10^{-5}		5.652×10^{-6}	3.165×10^{-5}

Table A7. PDIA3 – Raw Data for Knockdown Detection qPCR and Calculation Table

		Run 1	Run 2	Run 3	Average	Error
Untreated	Target	31.879	31.449	31.064		
	ACTB	15.028	14.024	14.864		
	dCt	16.851	17.424	16.199	16.825	0.354
	ddCt				0.000	0.501
	Fold change	0.707	1.415		1.061	0.354
PDIA3 KO	Target	40.000	40.000	38.743		
	ACTB	17.637	16.463	15.898		
	dCt	22.363	23.537	23.115	23.005	0.343
	ddCt				6.180	0.493
	Fold change	9.797×10^{-3}	0.0194		0.0146	4.806×10^{-3}

Table A8. RNH1 – Raw Data for Knockdown Detection qPCR and Calculation Table

		Run 1	Run 2	Run 3	Average	Error
Untreated	Target	16.639	17.236	16.662		
	ACTB	15.028	14.024	14.864		
	dCt	1.611	3.211	1.797	2.206	0.505
	ddCt				0.000	0.715
	Fold change	0.609	1.641		1.125	0.516
RNH1 KO	Target	35.744	37.490	40.000		
	ACTB	16.559	17.574	15.648		
	dCt	19.185	19.916	24.352	21.151	1.614
	ddCt				18.945	1.692
	Fold change	6.136×10^{-7}	6.402×10^{-6}		3.508×10^{-6}	2.894×10^{-6}

Table A9. SPTBN1 – Raw Data for Knockdown Detection qPCR and Calculation Table

		Run 1	Run 2	Run 3	Average	Error
Untreated	Target	35.461	38.022	36.172		
	ACTB	15.028	14.024	14.864		
	dCt	20.433	23.998	21.308	21.913	1.073
	ddCt				0.000	1.517
	Fold change	0.349	2.862		1.606	1.256
SPTBN1 KO	Target	40.000	38.975	40.000		
	ACTB	15.620	13.501	14.713		
	dCt	24.380	25.474	25.287	25.047	0.338
	ddCt				3.134	1.187
	Fold change	0.0500	0.259		0.155	0.105

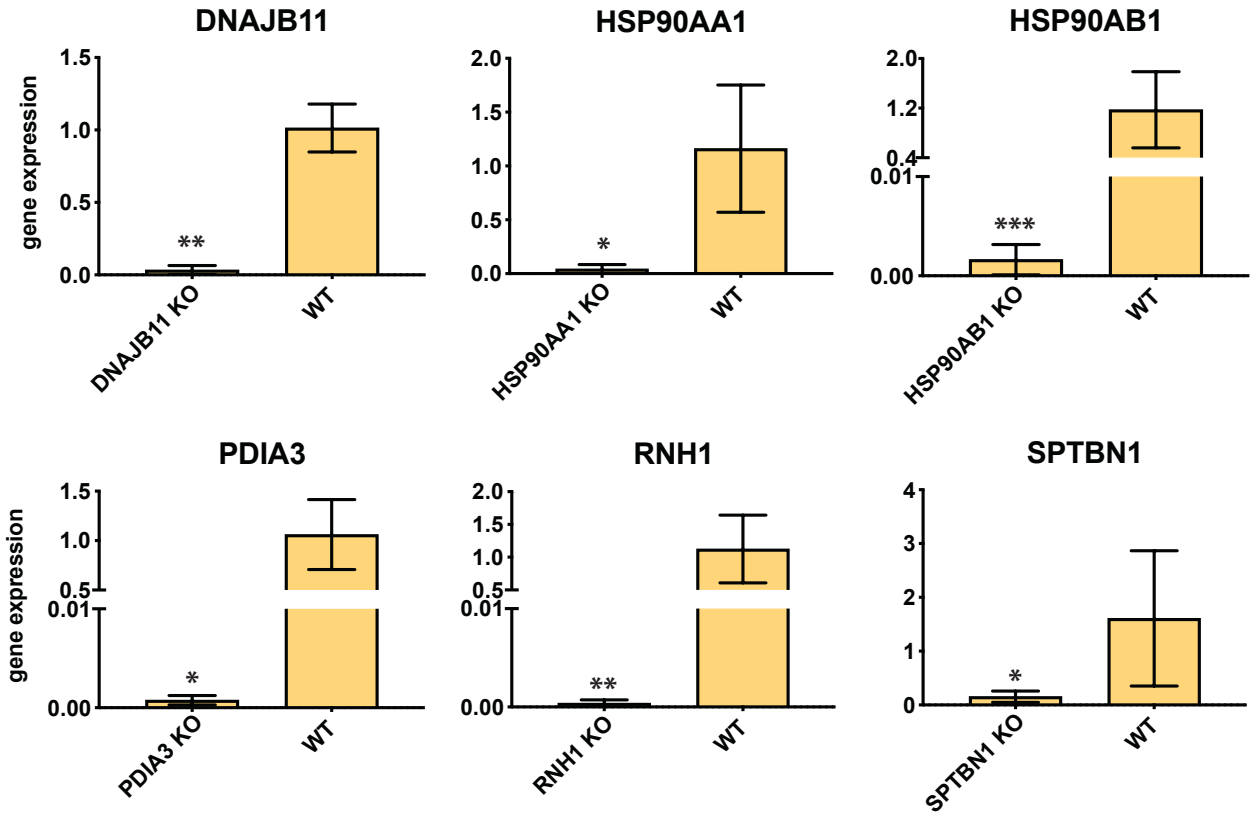

Figure A9. Transduced cells expressed the suppression of their target genes from the qPCR experiment amplifying the target genes. Gene expression of transduced cells (KO of each graph) was normalized to normal THP-1 cells (WT). This experiment confirms a successful generation of knockdown cells. * indicates significance in comparison to the WT. *$p < 0.05$, **$p < 0.005$, ***$p < 0.0005$

10. Time-Dependence DNCB-Protein Modification

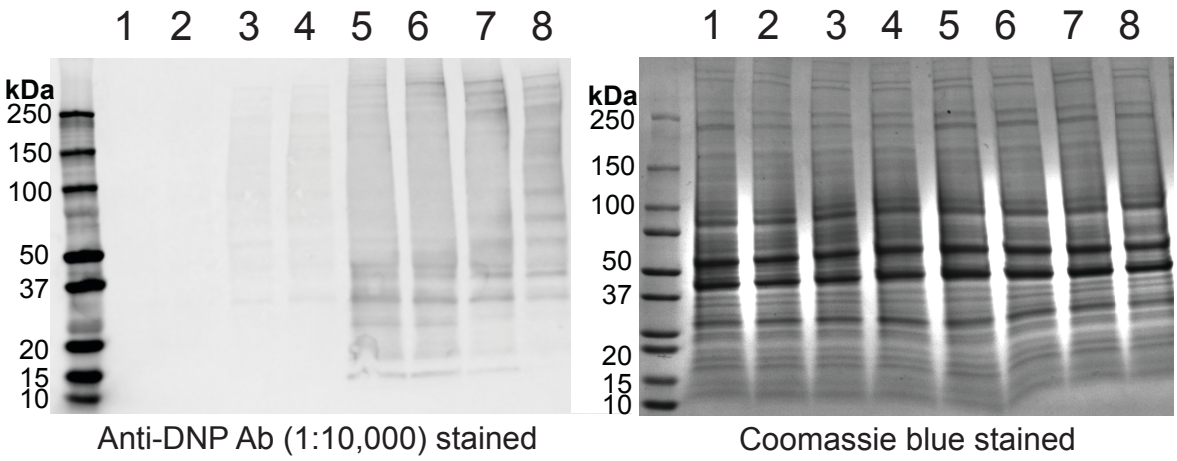

Figure A10. Western blot showing DNCB-protein modification process through time. THP-1 cells were incubated with DNCB for the following duration. Lane 1: Untreated, Lane 2-8: DNCB treated, Lane 2: less than 1 min, Lane 3: 10 min, Lane 4: 20 min, Lane 5: 30 min, Lane 6: 1 h, Lane 7: 4 h, and Lane 8: 8 h.

11. References

1. Crossland, R. K. & Servis, K. L. Facile synthesis of methanesulfonate esters. *J. Org. Chem.* **35**, 3195–3196 (1970).

2. Carballada, P. C. *et al.* Variation of the Viologen Electron Relay in Cyclodextrin-Based Self-Assembled Systems for Photoinduced Hydrogen Evolution from Water. *European Journal of Organic Chemistry* **2012**, 6729–6736 (2012).

3. Denehy, E., White, J. M. & Williams, S. J. Electronic Structure of the Sulfonyl and Phosphonyl Groups: A Computational and Crystallographic Study. *Inorg. Chem.* **46**, 8871–8886 (2007).

4. van der Aar, E. M. *et al.* Enzyme kinetics and substrate selectivities of rat glutathione S-transferase isoenzymes towards a series of new 2-substituted 1-chloro-4-nitrobenzenes. *Xenobiotica* **26**, 143–155 (1996).

5. Haydon, D. J. *et al.* Creating an Antibacterial with in Vivo Efficacy: Synthesis and Characterization of Potent Inhibitors of the Bacterial Cell Division Protein FtsZ with Improved Pharmaceutical Properties. *J. Med. Chem.* **53**, 3927–3936 (2010).

6. Al-Hiari, Y. M., Qaisi, A. M., El-Abadelah, M. M. & Voelter, W. Synthesis and Antibacterial Activity of Some Substituted 3-(Aryl)- and 3-(Heteroaryl)indoles. *Monatsh. Chem.* **137**, 243–248 (2006).

7. Shang, J. *et al.* Aromatic Triazole Foldamers Induced by C–H···X (X = F, Cl) Intramolecular Hydrogen Bonding. *J. Org. Chem.* **79**, 5134–5144 (2014).

8. O'Farrell, P. H. High resolution two-dimensional electrophoresis of proteins. *J. Biol. Chem.* **250**, 4007–4021 (1975).

9. Burgess-Cassler, A., Johansen, J. J., Santek, D. A., Ide, J. R. & Kendrick, N. C. Computerized quantitative analysis of coomassie-blue-stained serum proteins separated by two-dimensional electrophoresis. *Clin. Chem.* **35**, 2297–2304 (1989).